REPORT DOCUMENTATION PAGE

Form Approved OMB No. 0704-0188

1. REPORT DATE *(DD-MM-YYYY)*	2. REPORT TYPE	3. DATES COVERED *(From – To)*
21-09-2001	Final Report	26 April 2000 - 26-May-01

4. TITLE AND SUBTITLE

Nanoscale wear resistant ceramic materials with low friction

5a. CONTRACT NUMBER
F61775-00-WE009

5b. GRANT NUMBER

5c. PROGRAM ELEMENT NUMBER

6. AUTHOR(S)

Dr. Bas Kerkwijk, Professor Gyula Julius Vancso

5d. PROJECT NUMBER

5d. TASK NUMBER

5e. WORK UNIT NUMBER

7. PERFORMING ORGANIZATION NAME(S) AND ADDRESS(ES)

University of Twente
P.O. Box 217
Enschede NL-7500 AE
The Netherlands

8. PERFORMING ORGANIZATION REPORT NUMBER

N/A

9. SPONSORING/MONITORING AGENCY NAME(S) AND ADDRESS(ES)

EOARD
PSC 802 BOX 14
FPO 09499-0014

10. SPONSOR/MONITOR'S ACRONYM(S)

11. SPONSOR/MONITOR'S REPORT NUMBER(S)
SPC 00-4009

12. DISTRIBUTION/AVAILABILITY STATEMENT

Approved for public release; distribution is unlimited.

13. SUPPLEMENTARY NOTES

14. ABSTRACT

This report results from a contract tasking University of Twente as follows: The contractor will investigate the improvement of tribological properties of zirconia/alumina composites by optimizing their microstructure and by addition of solids with friction-reducing properties.

20020710 042

15. SUBJECT TERMS
EOARD, Composites, Ceramics, Friction and wear

16. SECURITY CLASSIFICATION OF:			17. LIMITATION OF ABSTRACT	18, NUMBER OF PAGES	19a. NAME OF RESPONSIBLE PERSON
a. REPORT	b. ABSTRACT	c. THIS PAGE			Charles H. Ward, Maj, USAF
UNCLAS	UNCLAS	UNCLAS	UL	120	19b. TELEPHONE NUMBER *(Include area code)* +44 (0)20 7514 3154

AQ F02-10-2171

Wear and friction of nanostructured zirconia and alumina ceramics and composites

Bas Kerkwijk

Kerkwijk, Bas

Reprinted from:

Wear and friction of nanostructured zirconia and alumina ceramics and composites.

ISBN: 90-36513340 (CD-ROM edition)

Financially supported by the Dutch Technology Foundation STW

Wear and friction of nanostructured zirconia and alumina ceramics and composites

Bas Kerkwijk

1 Tribology and ceramics

1.1 Introduction

Tribology relates to the study of wear, friction and lubrication of surfaces (of materials). In every day life, tribological processes always occur whenever two materials are in some way in moving contact with each other.

Examples of wear are generally accepted: people have to buy new clothes or shoes every now and then and in the case of chalking on a blackboard it is even necessary that wear takes place. Besides these examples we can think about normal polishing of stone tiles or sanding of wood or paint layers. For industrial applications wear is not wanted in all cases. Moving equipment parts, for example, should preferably last the lifetime of the equipment itself to minimise maintenance costs.

Besides wear prevention, it is also necessary to minimise friction between contacting surfaces. This creates a more efficient system, because friction always results in the formation of heat. Both wear and friction of materials can be generally controlled in any of two ways: by choosing proper materials or by using lubricants. The latter choice simply changes the influence of parameters such as contact pressure, temperature, velocity and roughness on the tribological behaviour. The right choice of materials depends on the application demands. Engineering polymers, for instance, can only be used for moving parts of applications working under mild conditions (e.g. low contact pressure, moderate temperatures, etc.). At somewhat higher temperatures or loads metals may be needed. In moving equipment parts, metals always need lubrication: greases and oils are used to minimise the contact between two materials in moving parts. However, the use of these lubricants may be undesirable for environmental reasons, but the absence of lubricants implies that the materials used must be extremely wear resistant, since the intensity of the contact becomes more severe, because the asperities of the rough surfaces are no longer or only partly separated by a (thick) lubricating layer.

Besides the problem of the lubrication needed for the application, metals have disadvantages when working in a corrosive environment, at temperatures higher than 600°C, at extremely high loads or without the presence of a lubricant. In those cases, it is necessary to work with ceramics or ceramic coatings, since various properties of ceramics are considered to be superior to those of metals. Some of these properties, e.g. hardness, ability to withstand high temperatures, corrosion resistance and shape firmness, are important properties to obtain wear-resistant materials, specifically under dry sliding conditions.

Structural ceramics have been part of an ever increasing field of research over the last 25 years. Starting from the goal of developing the "all ceramic" car engine for higher efficiencies that has still not been reached, spin-offs from this research resulted in a broad

range of applications that showed the merits of using ceramic materials because of their specific properties. Research on ceramics showed that they could be suitable for wear-resistant applications, but practice showed that they were still not wear-resistant enough.

At present we can find applications of ceramics in a broad variety of situations, as mentioned by Sibold [1]. Sibold describes that most applications of wear-resistant structural ceramics are based on their extra-ordinary hardness and high corrosion resistance. Applications mentioned mainly involve pump components, all types of valves and seals, and components of wire drawing machines and metal extrusion dies. Developments in ceramic engineering have resulted in solving the major problems of practical use.

Oxide ceramics find increased application as head and joint components of total hip replacements. Willmann [2] showed that various combinations of either alumina or zirconia with another material can be used in such applications. Especially the combination of alumina against alumina shows low wear in clinical tests.

As far as the commercialisation of ceramics is concerned, Savitz [3] showed that advanced structural ceramics have a relatively long way to go from development to practical implementation, compared to for instance the implementation of advanced materials and their developments in semi-conductor industry. Savitz states that advanced ceramics are mainly implemented as high-temperature materials, long-life materials and low-weight materials. Still some other barriers, besides long development time, must be overcome for suppliers and developers: cost price, process variability and dimensional capability. On the other hand, users of ceramics have some other barriers to cross, like design reliability, availability of materials, design guidelines and familiarity with ceramics. Savitz also clearly states that the material's properties are no longer a barrier for current applications.

The research described in this thesis is focused on the tribological behaviour of ceramic materials by studying dry sliding wear with pin-on-disc measurements. For wear measurements various set-ups can be used. The use of pin-on-disc tests eliminates lining problems and provides a rather easy set-up for wear measurements.

Special attention is paid to consolidation of the ceramic microstructure for the preparation of dense, homogeneous ceramics, both composites and single-phase materials. For composites it may include a hard, tough or lubricating second phase. A homogeneous green ceramic microstructure is created by suspension/colloidal processing, resulting in a dense homogeneous ceramic after sintering. By using these processes, ceramics can be made with a controlled homogeneous microstructure that have a positive influence on the wear resistance. Major goals of the research in this thesis are the development of better wear-resistant materials and a better understanding of the relation between microstructure (intrinsic material properties) and wear behaviour.

The ceramics are also tested in practical situations to translate the test results to real-life measurements and vice versa. The aim is translated into three specific objectives that can be used for the test results. The major objectives can be partly formulated from generally recognised criteria for materials suitable for unlubricated applications:

- Prepare wear-resistant ceramics ($k_w << 10^{-6}$ mm^3/(N·m) [4,5], see equation (1.1)).

- Obtain low friction ($f < 0.2$ [4] , see equation (1.2)).
- Relate ceramic microstructure to tribological properties.

Additionally, both the specific wear rate and the coefficient of friction should not depend on the operating conditions, especially velocity and temperature [4].

1.2 Definitions

1.2.1 Wear and wear mechanisms

Wear resistance is not a property that can just be described for a material specifically. It is influenced by many parameters determined by both the system and the material that are used. Since wear is primarily a system property (also depending on load, velocity, temperature), it is usually described in terms of a specific wear rate, k_w:

$$k_w = \frac{V_w}{F \cdot s}\left[\frac{\mathrm{m}^3}{\mathrm{N} \cdot \mathrm{m}}\right] \tag{1.1}$$

Here, V_w is the wear volume of the examined sample [mm^3], F is the applied load on the configuration [N] and s is the sliding distance [m]. All materials that are tested on their tribological behaviour are characterised by this parameter. This parameter represents wear as function of system conditions only.

A schematic picture of the development of the wear volume as function of sliding distance is given in Figure 1.1, where the slope of the graph (if divided by the applied normal force and with a linear increase in wear volume) is a representation of the specific wear rate. In case of a non-linear increase in wear volume, the specific wear rate would be defined by $k_w = (1/F)*(dV/ds)$.

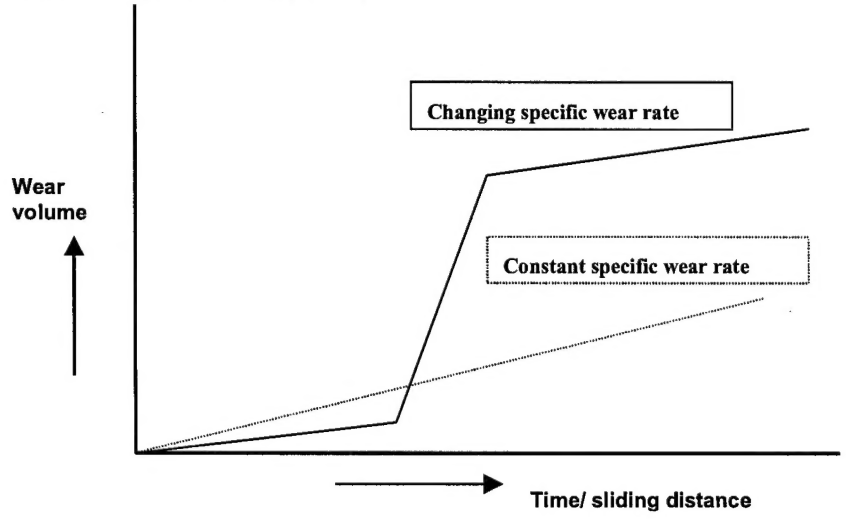

Figure 1.1: Development of wear volume in time at a given applied normal force; the slope of the curve (divided by the applied normal force) represents the specific wear rate.

For wear in general it is important to know the main mechanisms that cause wear. In general, there are four mechanisms of wear that can take place in any kind of material.

Abrasive wear is defined as the removal or the displacement of material caused by the presence of hard asperities on a counterface. Depending on the properties of the wear surface, these hard asperities may result in scratching, grooving or ploughing. It is a mechanism that also becomes important when during the wear process material is pulled out of the original polished surface and is captured between the two contacting surfaces. When hard particles are pulled out, they can act as an additional abrasive material, causing wear of the softer contacting surface. Further wear causes more material loss and this causes severely deformed surfaces. Hardness of a material is a very important parameter for this wear mechanism, especially the difference in hardness between the two contacting materials.

Adhesive wear occurs during the sliding process when solids in contact adhere and the binding forces in the junction become stronger than those within one of the solids. Hardness of the materials also influences the type of adhered layer that is formed (mainly thickness), but in general any of three types are formed:

- a thin continuous film adhered to both contacting surfaces
- a thick continuous film adhered to both contacting surfaces or to one of them
- a thick discontinuous film adhered to both contacting surfaces.

Delamination wear (Figure 1.2) in ceramics is mainly related to the nucleation of subsurface cracks and their propagation parallel to the surface. The process can occur by the following steps, taking place individually or sequentially:

- smoothening of the softer surface due to deformation and/or removal of asperities,
- induction of plastic deformation on the softer surface by the presence of harder asperities,
- nucleation of cracks below the surface due to increasing subsurface deformation,
- delamination of long and thin wear sheets at places where the cracks are able to propagate to the surface.

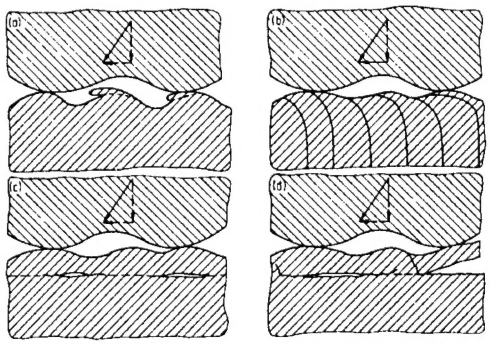

Figure 1.2: Example of stages in delamination wear: (a) plastic deformation at local asperities, (b) formation of cracks in the bulk, (c) propagation of cracks parallel to the surface, (d) delamination of cracked layer.

Corrosive or tribochemical wear is mainly caused by environmental effects that can be divided into three types [6,7]:

- formation of adsorbed layers
- change of surface properties, followed by adsorption

- formation of tribochemical products.

Under dry sliding conditions the influence of the environment on tribochemical wear processes is mainly related to the presence of water in the air (relative humidity) or elevated temperatures. Under lubricated conditions the presence of the lubricating phase in the contact (e.g. water, oil, paraffin) can influence the tribochemistry of the wear process. All this means that corrosive or tribochemical wear results from the formation and removal of chemical reaction products at the contact surfaces. It is clear that the wear processes that are influenced by corrosion, occur even faster at elevated temperatures.

The four mechanisms described, can cause either mild or severe wear, depending on system parameters like load, velocity and humidity and material's properties like hardness, toughness and thermal conductivity.

1.2.2 Wear in ceramics

For ceramics there are a couple of specific wear phenomena by which material removal takes place during the previously described mechanisms. Ceramics show fracture processes during wear that are typical for brittle materials. Microcracking is the largest cause of wear in ceramics, but plastic deformation can occur in fine-grained materials (on a scale < 1 μm) or when locally temperatures become extremely high. Zum Gahr [8] and He [9] have given good summaries of the mechanisms and the accompanying wear phenomena for ceramics.

Another important feature in wear of ceramics is the transition from mild to severe wear at certain loads or velocities. In general, this transition is usually noticed by a change in the way wear takes place; the wear phenomenon changes from plastic deformation to brittle fracture and microcracking. In Figure 1.1, a schematic representation is already given of how such a wear process develops during wear testing. The transition point is found where the measured wear volume shows a sudden increase in time.

The main reason for this transition to occur, is the increased material pull-out at higher loads or velocities (microcracking and delamination) or during prolonged sliding. This material pull-out causes a larger contribution of abrasion to the wear process. The application of ceramics under extreme loading or velocity conditions suffers from this transition, but under unlubricated conditions the value for the transition load for ceramics is lower than for metals. Therefore, it is necessary to develop ceramic materials with higher transition load. The transition phenomena for ceramics are well reported by researchers of NIST [10,11] and other groups [12].

The wear (transition) mechanisms that occur are predominantly dependent on the tribological contact stress in the material (mainly resulting from the applied load). Low contact stresses usually result in wear induced by plastic deformation. With increasing contact stress cracks are formed and at a critical point these cracks develop to create severe wear processes. This transition point is related to the point where the tribological stress exceeds the critical crack or fracture stress. This can happen at both a local, microscopic and macroscopic scale. Wang and Hsu [10,11] demonstrated the feasibility of various models for wear volume predictions that were found in literature from 1962-1993. Most of these models are based on the fact that when the maximum tensile strength, σ_{max}, ex-

ceeds the value for the critical stress, σ_D, in a material, cracks appear on the surface. For wear volume predictions, the normalised threshold stress, (σ_{max}/σ_D), is of particular interest. Theoretically this value should equal 1, but due to surface cracks present before wear the value for σ_D is usually significantly lower in polycrystalline ceramics. Woydt *et al.* [12] reported transition phenomena for the self-mating wear of MgO-stabilised zirconia. These transitions were defined as stress-induced surface fatigue transitions (inter-granular microcracking), humidity-dependent protective physical and chemically induced layer film formation, pressure-dependent phase transformations and tribo-oxidation-induced wear-reducing or wear-accelerating transitions, mainly indicating the extreme difficulty of tribological research in relation to material properties and operating conditions.

Looking at the influence of system parameters, several authors have developed wear maps over the last years. These maps are based on experimental results and describe the influence of load, sliding velocity and temperature on the wear rate of materials. Based on these wear maps it is also easy to predict wear transitions [5,13,14,15,16]. More recently new attempts were made to describe wear of ceramics by means of a new parameter [17]. The authors describe a non-dimensional parameter to capture the influence of pressure, fracture toughness, crack length and coefficient of friction and the wear rate is then expressed as a function of this parameter using different constants for different materials .

1.2.3 Friction

The other important issue in tribological studies of materials, is friction. Friction, occurring between two surfaces in contact with each other, can be the cause of several other features influencing wear of materials. The coefficient of friction, f, is defined as the ratio between the measured friction force, F_F, and the applied normal force, F_N:

$$f = \frac{F_F}{F_N} \tag{1.2}$$

Frictional heating is usually the most important feature influencing wear. Due to the relatively low thermal conductivity of most oxide ceramics, the contacting materials will be heated. The thermal aspects influence the performance or efficiency of the system. For instance, the presence of temperature gradients, may propagate crack formation in the contacting surfaces, which can cause severe wear. These thermal aspects in tribology are important for the determination of [18]:

- magnitude and location of the maximum temperature
- effects of thermal gradients on the geometry of the contact, and
- heat flow to and from components of the system.

Ashby *et al.* [19] developed temperature maps for frictional heating during dry sliding. These maps are applicable to all kinds of materials and can be used to predict temperature developments and wear mechanisms in ceramics during sliding. The model can also predict local flash temperatures in the surfaces due to roughness asperities on the surface, which is especially important for ceramics due to their relatively low thermal con-

ductivity. This model was adjusted by Bos [18], whose corrections concern the description of the actual shape of the heat source (contact). Using his description, it is possible to create a model, describing the severity of the thermal influences on the tribological contact. Most of this work will be dealt with in chapter 5 where a general description of the modelling of the wear tests is described.

1.2.4 Solid state lubrication

Friction reduction for ceramic couples is an important issue in ceramic engineering. For the widest range of possible applications of ceramics, the ceramics must have low friction at high temperatures and preferably under unlubricated conditions. Normally lubrication can be performed using water, oils, greases and solids. Lubricated sliding processes are numerously reported in literature, but it is clear that during lubricated processes, the properties of the materials used are far less important than for unlubricated ones. The intensity of the surface contact is lower when a lubricating layer is present.

If lubrication is necessary at high temperatures, the possibilities of available materials are rapidly limited to solid state lubricants. Peterson *et al.* [20] already showed some 40 years ago that there is a wide variety of materials available for lubrication at temperatures above 700°C. Lubricants are then applied as a third material to the tribosystem. This makes that the lubricant has finite lifetime as a functional material, since it is consumed during the process. When one is able to incorporate the lubricants in a ceramic matrix material that is used in a tribosystem, one can possibly create a self-supplying lubricating phase. Only little wear in the material then results in the presence of a small amount of lubricant in the contact. This creates a system that is constantly lubricated. In this thesis, lubrication issues will not be treated with the exception of the case of self-lubricating ceramics, which is referred to as solid state lubrication.

An example of the use of solid state lubricants is given by Wang *et al.* [21]. They describe friction and wear of PSZ ceramics lubricated by copper or copper oxide. They succeed in lowering the friction from 0.4 to 0.14 under varying loads (18-80 N) and velocities (0.01-0.1 m/s). The accompanying wear they measure becomes significant only at loads above 40 N. Below this load the lubricated couples show no wear. They describe how the coefficient of friction depends on the properties of the solid lubricating film. The coefficient of friction is then defined as the ratio between the shear strength of the lubricant film, the true contact area and the normal contact load. Thus low friction means that the contact area at a given load should be small and the lubricant film must have low shear strength (soft films, material with low melting point). The small contact area can be achieved by creating thin films on hard substrates. The contact load is then largely supported by the substrate, since the thin film reduces the roughness of the surface only by a small extent. The best results were obtained using a CuO film, where friction was in steady-state at 0.14 and wear was negligible at a load of 37 N.

1.3 Wear resistant materials

1.3.1 Introduction

Materials related aspects can influence the tribological behaviour significantly. Czichos *et al.* [4] describe the use of "advanced materials" for tribological applications. They make a general distinction between polymers, metals and ceramics. Table 1.1 shows the tribological characteristics in relation to the material's properties of these three classes. Combining the important properties of each material specifically, provides a beneficial material for a broad variety of applications, though in practice metals are the most widely used. The use of ceramics may be most suitable when compared to metals because of their lower mass forces, better abrasion resistance, better temperature resistance and better corrosion resistance. Problems encountered when using ceramics contacts are [4]:

Table 1.1: Tribological characteristics in relation to material types [4].

Tribological characteristic	Qualitative order
Mass forces	$F_{polymer} < F_{ceramics} < F_{metal}$
Hertzian pressures	$P_{polymer} < P_{metal} < P_{ceramics}$
Frictional heating	$T_{metal} < T_{polymer} < T_{ceramics}$
Adhesion energy (surface tension)	$Ad_{polymer} < Ad_{metal} < Ad_{ceramics}$
Abrasion	$Ab_{ceramics} < Ab_{metal} < Ab_{polymer}$
Tribochemical activity	$R_{polymer}$, $R_{ceramics} < R_{metal}$

- the high contact pressures resulting from their high Young's modulus
- the shift of the shear stress maximum from bulk to the surface, and
- the large frictional heating.

Besides that, the lower fracture toughness may impose specific problems under impulse loading.

Polymeric materials may be beneficial in use compared to metals with respect to their low interfacial adhesion energy, leading to low friction. The limitation in operating temperature is of course a major drawback in the use of polymers. Their large deformation at already relatively low loads is also a disadvantage, since this seriously decreases the maximum applicable contact pressures. Erdemir [22] describes wear and friction of the broad variety of materials that is available for engineering applications.

1.3.2 State-of-the-art wear-resistant ceramics

1.3.2.1 General

Important ceramics materials for all kind of structural applications are ZrO_2 (for instance Y_2O_3-stabilised), Al_2O_3, SiC, Si_3N_4 and SiAlON. Their use has been studied extensively over the past few decades. Furthermore, there is a more specific class of borides and nitrides like B_4C, TiC, TiN, AlN and BN that are used for their extremely high hardness.

These materials also receive a lot of attention, but have their high cost price and their complicated tribochemistry as major drawbacks.

Nearly all single-phase ceramics have one or more specific beneficial properties, but usually these are accompanied by one or more drawbacks. These drawbacks may be overcome by the incorporation of a second ceramic phase with advantages in that respect, while trying to retain the matrix properties as much as possible. Composites of all kinds can be made in this way and their application seems unlimited. It is a separate class of materials that received a lot of attention in research over the last 15 years.

As already mentioned, in practice several ceramic/ceramic couples for wear testing exist. The most frequently applied ceramics are Al_2O_3, ZrO_2-Y_2O_3, SiC, and Si_3N_4. The choice for a specific couple primarily depends on the application in mind. Hardness, chemical and thermal properties vary between the mentioned ceramics. Testing under practical conditions for an application results in a choice for a specific material, as described by Jahanmir [23]. The author gives general information on the basic principles of friction and wear of all kind ceramic materials.

Hsu and Shen [16] give an overview of ceramic wear maps, studying the influence of operating parameters. They study the four most important structural ceramics, Al_2O_3, ZrO_2-Y_2O_3, SiC, and Si_3N_4. Wear maps are given for all four ceramics after self-mated sliding under dry air, in paraffin oil or water. The wear maps are used to create wear transition diagrams depending on load and velocity. They show that under dry sliding conditions alumina is the most easily used material, showing the broadest variety in velocity and load where wear is mild. Based on the wear maps, Hsu and Shen [16] treated a wear model, in which fracture mechanics were used. The wear volume calculated from the model is expressed by:

$$V_w = C \cdot \frac{\sigma_{max}}{\sigma_D} \cdot \frac{F \cdot s}{H_v} \tag{1.3}$$

H_v is the temperature dependent Vickers hardness and C is a constant. The authors use the definition of Hamilton for the maximum tensile stress at the surface:

$$\sigma_{max} = \left(\frac{1-2\nu}{3} + \frac{4+\nu}{8} \cdot \pi f \right) \cdot P_0 \tag{1.4}$$

where ν is Poisson's ratio and P_0 is the maximum Hertzian pressure. They relate the critical stress, σ_D, to the grain size and, using these equations, they could correlate the experimental data for Si_3N_4 well for the severe wear regime, where wear is dominated by fracture processes. For mild wear the theory overestimated the wear data. The limitations of the wear map concept are related to the amount and variety of wear experiments performed and to the coexistence of various wear mechanisms during a single experiment. Microstructural parameters as grain size and grain size distribution also have a noticeable effect on the tribological behaviour. Besides that, no attention was paid to thermal or tribochemical effects. Furthermore, there are many possible ways of lubricating tribosystems. They all bring their unique tribochemistry to the materials couples used creating many more problems to the wear map concept and their related models.

1.3.2.2 Y-TZP and Y-TZP based composites

In recent years several wear tests have been performed on zirconia-based materials. The wear behaviour of Y-TZP (yttria-stabilised tetragonal zirconia polycrystals) is strongly dependent on the nature of the counterface. Usually self-mating wear tests are performed, but the largest problem that is encountered is the low thermal conductivity of Y-TZP, often causing extremely high contact temperatures. This means that it is difficult to compare results of tests using this tribosystem with others including a ceramic with a higher thermal conductivity like SiC or Al_2O_3, because temperature effects (i.e. local melting) can not be excluded in the case of Y-TZP. One has to take the thermal effects into account to be able to make a meaningful comparison.

Breznak *et al.* [24] and Breval *et al.* [25] presented a full analysis of the wear behaviour and wear debris life-cycle of Y-TZP and SiC at room temperature. They found steady-state coefficients of friction of 0.4 for self-mating Y-TZP tests, which are app. 50% lower than previously reported values. The wear they measured is extremely high compared to wear measured for SiC couples [25]. Their general conclusion is that none of the examined material combinations would be suitable for application in a working engine without lubrication [24]. They state that higher toughness of Y-TZP compared to SiC results in wear dominated by intergranular fracture for Y-TZP and intragranular fracture for SiC.

The work of Libsch *et al.* [26] presents a strong sliding velocity dependence of the wear behaviour of various stabilised zirconias. This was not found for alumina-based ceramics. Libsch also presents results on a zirconia-alumina composite ceramics with a coarse grain size and undefined microstructure. Wear of these composites was large due to macroscale structural damage, which was not found for Y-TZP. Based on the experiments, Libsch proposes a wear equation relating the wear rate (k_w) to the normal load (F), sliding velocity (v) and sliding time (t):

$$k_w = C \cdot F^a \cdot v^b \cdot t^c \tag{1.5}$$

This model does not show a good relation with experimental data. The values for the constants C, a, b, and c, show a large variation compared to the constants reported by others [27]. Stachowiak *et al.* [28] tested a large quantity of partially stabilised zirconias (PSZ) and Y-TZP samples under varying conditions. They measured coefficients of friction of 0.6 under dry sliding in air and wear rates in the order of 10^{-5} $mm^3/(N \cdot m)$ and concluded that the wear behaviour is strongly dependent on the operating and environmental conditions. Wang *et al.* [29] studied the specific abrasive wear resistance of Y-TZP ceramics. Some were composites with a small addition of alumina to the Y-TZP matrix. The transformation toughening mechanism in Y-TZP caused an increased abrasive wear resistance. Various Mg-PSZ and Y-TZP ceramics were tested together with a composite of Y-TZP and 20 wt% alumina by Medevielle *et al.* [30]. They found that the composite showed the lowest wear loss compared to the zirconias.

Not only intrinsic mechanical properties can explain the differences between various materials, but phenomena like dielectricity, polarisation energy and contact charges have to be considered as well. Woydt *et al.* [31] show that Y-TZP ceramics already show severe wear at sliding velocities between 0.04 and 0.14 m/s at loads of 10 N. The magnitude of wear depends on tribological stress and the possible reactions related to these

stresses, e.g. point and cycling-contact-pressure, cyclic and thermal dilatation and phase transitions. Woydt concludes that the transition from mild to severe wear can be shifted to higher velocities by using materials with higher thermal conductivities. This may also imply the use of counterfaces with higher thermal conductivity in all tribological cases. Kong *et al.* [32] report steady-state coefficients of friction of 0.4-0.55 for dry sliding. Under low loads Y-TZP shows a good wear behaviour, but the wear transition load is low indicated by an abrupt increase of the wear rate (2 orders of magnitude). Lee *et al.* [15] have prepared wear maps for Y-TZP ceramic (grain size ≈ 1 μm) under various conditions. An example of such a wear map is given in Figure 1.3. Lee showed that for self-mating couples wear rates varied between 10^{-6} and 10^{-4} $mm^3 \cdot m^{-1}$ depending on speed and load condition combinations. Low wear rates were measured under low speed and load, while the load was varied between 2 and 380 N and the velocities ranged between 10^{-3} and 0.5 $m \cdot s^{-1}$. The transition from mild to severe wear is attributed to the change in wear mechanism from plastic deformation to brittle fracture. Coefficients of friction vary between 0.45 and 0.7. Again, these values may be too high for practical applications. They can only be lowered by application of a lubricant (either water or a solid state film), on the condition that the roughness of the sliding surfaces is low (typically < 0.1 μm).

Tse *et al.* [33] reported on the influence of aging in water of Y-TZP on wear. Samples which were aged 5 times longer in humid air (120°C) showed a 4 times larger dry wear rate due to the larger amount of monoclinic phase present before wear testing. Other authors also describe aging under the influence of environment [34,35].

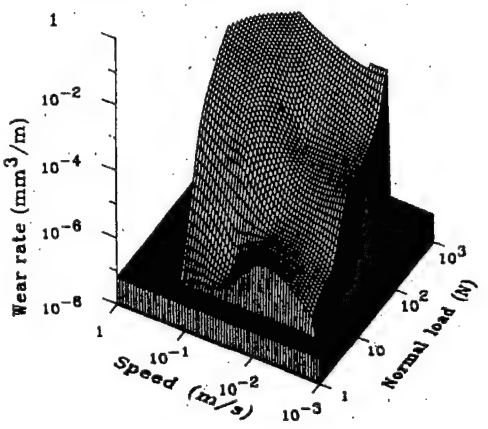

Figure 1.3: Ceramic wear map for Y-TZP in dry air conditions [15].

Wear tests performed by He *et al.* [9], using SiC balls or commercial Y-TZP material against Y-TZP show similar features as reported in other literature. Wear mechanisms are typically the same (plastic deformation under mild conditions and microcracking under more severe conditions). A major effect of the grain size of the Y-TZP material is found, resulting in a low wear rate, typically for fine-grained systems, of 10^{-6} $mm^3/(Nm)$ under mild conditions (see section 1.4.2). To the best of our knowledge no other examples are found about wear tests on Y-TZP materials with the same small grain size as this material.

An example of combining the favourable properties of single-phase materials in composites is the addition of a certain amount of a harder phase like alumina to a Y-TZP matrix for improvement of the wear resistance of the relatively soft Y-TZP material, so-called alumina-dispersed zirconia (ADZ). This gives improved hardness to the composite and when the added amount is large enough, an increased thermal conductivity may be

reached as well. There is not much information at hand about wear behaviour of this type of composite.

Sornakumar *et al.* [36] have studied steel cutting performance of various Y-TZP and composite ceramics. They reported that an addition of 20% alumina causes improved toughness, enhanced thermal shock resistance and hardness of partially stabilised zirconia (Y-TZP). This was also reported by Shi *et al.* [37]. Because of these improved properties, the ADZ ceramic exhibits a better cutting performance than Y-TZP. Li *et al.* [38] have reported that an increasing amount of Al_2O_3 in PSZ results in a material with an increased fracture toughness compared to monolithic PSZ, but still the values are lower than for tetragonal Y-TZP, as expected. They also show that the fracture toughness is more improved when larger alumina grains are dispersed in the Y-TZP matrix, but they do not give a good explanation for this. The improved fracture toughness can be beneficial, because the wear resistance is positively influenced by the toughness in case of abrasive wear. The overall influence of toughness on wear resistance is not exactly known. He *et al.* [9] show that ADZ composites have a better wear resistance compared to pure Y-TZP ceramic, but no difference is found for the transition load. The enhanced wear resistance is due to the higher hardness of the α-alumina phase.

1.3.2.3 Alumina and alumina-based composites

Considering the combination of cost and properties, alumina is *the* ceramic material to use. Of most structural ceramics it is by far the cheapest. Its hardness is 9 on Moh's scale which ranks the hardness of diamond at 10 as the hardest existing material [39]. Alumina-based ceramics in general show better wear resistance than zirconia due to their higher hardness. Also the larger thermal conductivity of alumina-based ceramics contributes to better tribological properties. There are of course specific applications in which zirconia-based ceramics show better behaviour. Especially in the area of cutting tools, the better mechanical properties of zirconia are of major importance for practical use. The main disadvantage of pure alumina is its lower toughness compared to zirconia, resulting in brittle fracture occurring faster. One way to increase the toughness of alumina is by addition of a certain amount of zirconia (ZTA composite). This gives a significant increase of the fracture toughness and bending strength. Especially the abrasive wear resistance of alumina is very good, but alumina is very susceptible to wear transitions due to increasing load and sliding velocity. The load at which transition from mild to severe wear occurs is higher for ZTA [9].

Dong *et al.* [40] describe the tribological characteristics of alumina at various loads, and temperatures. Tests were performed at low sliding velocities to minimise the influence of thermal effects. Wear of alumina was found to be mild ($k_w < 10^{-6}$ mm^3/(N·m)) except in those cases where the load was larger than 20 N in the temperature range between 200 and 800°C. Coefficients of friction ranged between 0.4 and 0.6 for mild wear and were 0.85 in cases of severe wear. The results are translated into a wear transition diagram, shown in Figure 1.4. Four separate wear regions are indicated. At low temperatures tribochemical reactions between the alumina surfaces and water vapour control the tribological performance (region I). The contact load has the largest influence at intermediate

temperatures (regions II and IV) and at high temperatures impurities influence the surface properties of the alumina resulting in a protective layer (region III).

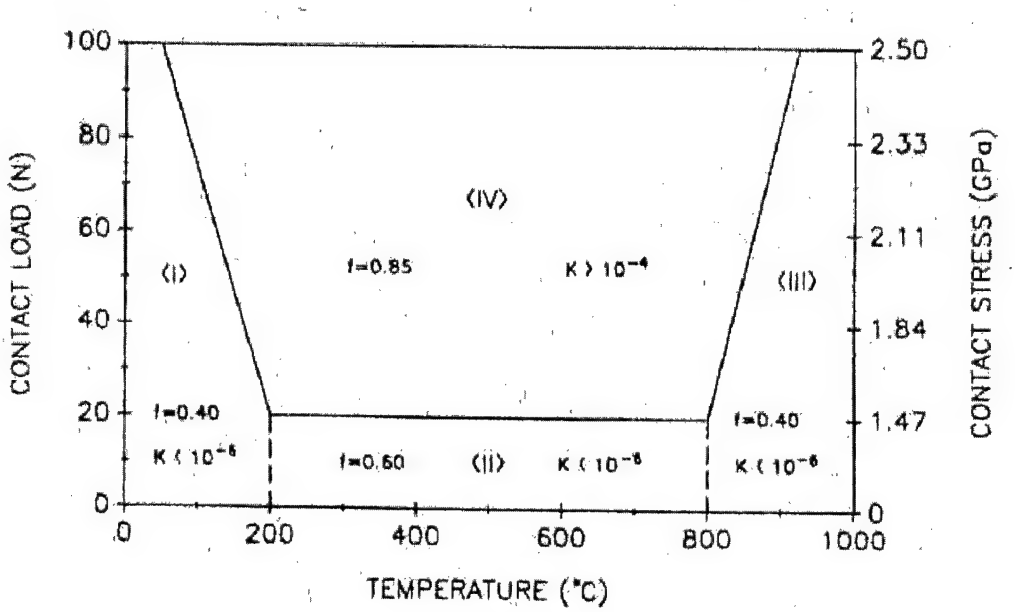

Figure 1.4: Wear transition diagram for alumina (self-mating tests), showing four distinct regions. The friction coefficient, *f*, and the wear coefficient, denoted here as *K*, for each region are indicated in the figure [40].

Zum Gahr *et al.* [41] showed that alumina compared to Y-TZP and SiC has the lowest wear in self-mating tests. Under more severe test conditions wear of alumina increased because of its brittleness. Wang and Hsu [42] studied the influence of operating parameters and environment on the wear transition of alumina. They showed that transition phenomena in alumina are inevitable and can be demonstrated in practically all cases by a sudden increase in coefficient of friction. All the phenomena depend on environment, operating parameters (load, velocity, temperature, lubrication) and microstructure of the alumina used.

Blomberg *et al.* [44] stated that alumina sliding against itself shows a mild wear regime with wear rates as low as 10^{-9} $mm^3/(Nm)$ and a severe wear regime with wear rates several orders of magnitude higher. Friction coefficients were below and above 0.6, respectively. The dominating wear mechanism changed from microfracture (polishing by plastic deformation and weak abrasion) in the mild wear regime to macrofracture (strong abrasion by microcracking) in the severe wear regime. A similar description of wear in alumina is given by Cho *et al.* [45]. They described the wear of alumina in two stages. Initially, there is mild wear involving "ductile" grooving (plastic deformation) of the surface, followed by severe wear involving grain boundary cracking and grain pull-out after a critical time. They consider the wear transition to be a ductile to brittle transition (Figure 1.5).

Wang *et al.* [43] demonstrate the occurrence of wear transition phenomena in alumina and various ZTA ceramics. After the transition, wear is dominated by microfracture and grain pull-out. Besides that, the wear transition load of ZTA ceramics is much higher than for monolithic alumina. It was also found that the transition load increased with higher zirconia content, which was attributed to small and uniform grains in the composite together with phase transformation induced surface compression stress and the lower elastic modulus which results in larger Hertzian contact and hence lower tensile stress. Modelling work showed that optimisation of the wear transition resistance needs refinement of the grain size and avoidance of the introduction of internal stresses.

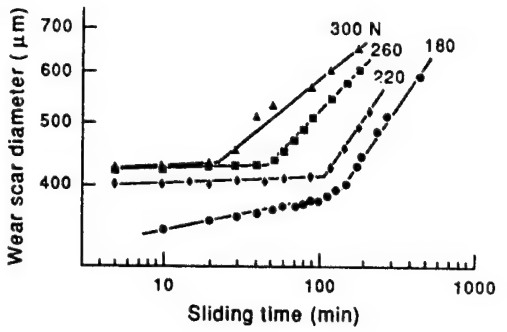

Figure 1.5: Wear vs. sliding time showing the abrupt change in functional dependence for each load, indicative of two stage wear behaviour [45].

In the work of Cherif *et al.* [46] the main wear mechanisms in alumina and ZTA were identified as abrasion and chipping by inter- and transgranular cracking. They achieved the best possible wear resistance at the optimum amount of zirconia in alumina of 16 wt%. The presence of wear debris was found to be beneficial since it acted as a lubricant by changing the load distribution over the surface and consuming energy when the particles of the debris were ground and plastically deformed. The beneficial influence of the presence of the debris was confirmed by studying the life cycle of the debris for ZTA. In other work, Cherif [47] showed that debris is predominantly formed when contacting asperities cause microcracking. The debris is ground to the point where cleaving requires more energy then plastic deformation. Zirconia debris is more easily deformed while alumina debris shows more chemical affinity with water from the air to form hydroxides. When deformation is no longer possible, the debris is removed and new debris is formed that undergoes the same life-cycle.

Esposito *et al.* [48] reported low coefficients of friction for alumina self-mating couples. Values are as low as 0.2. This value increases somewhat with increasing sliding distance. Esposito ascribes this behaviour to the presence of a very fine compacted layer of wear debris that acts as a solid lubricant. In other work [49] the author reports similar measurements on zirconia-alumina composite ceramics. Again, coefficients of friction are very low (0.15), but they are connected to high wear rates for all materials of at least 10^{-6} $mm^3/(N \cdot m)$. The low friction is again explained by the presence of a large amount of debris acting as a bearing. The tribochemical film formed from the debris consists of aluminium hydroxide.

Trabelsi *et al.* [50] tried to relate the wear behaviour of ZTA ceramics to its mechanical properties. They found that the wear resistance of ZTA is decreased compared to pure alumina, but the fracture toughness and strength are improved. They showed that the influence of the contact temperature is predominant, because of the strong temperature dependence of toughening mechanisms. Tests performed under oil lubricated conditions

by C. He *et al.* [51], clearly showed that the wear transition load is raised with increasing zirconia content. The transition from mild to severe wear is typically accompanied by a change of the wear mechanism from plastic deformation with some grain pull-out to a fracture-dominated wear process. They state that the presence of zirconia can have at least three possible effects, either positive or negative: refinement of alumina grain size (smaller size and narrower size distribution), reduction in hardness and formation of a compressive zone in the wear track.

1.4 Relation between ceramic properties and tribological behaviour

1.4.1 Influence of material properties

The previous section made clear that material (bulk) properties are strongly related to the tribological behaviour of a material. Their influence on the various wear mechanisms is different, so the absolute influence of a material property on the wear behaviour is difficult to establish. In the various models that are described, relations are given between wear volumes and some important mechanical and thermal properties. The most widely used properties in modelling are hardness (H), fracture toughness (K_{1C}), bending strength (σ_b), Young's modulus (E), thermal conductivity (K) and thermal shock resistance (ΔT_{shock}). These properties all have a distinct influence on the various possible wear mechanisms.

An example of the influence of the differences in hardness of two materials on the abrasive wear resistance is given in Figure 1.6. Here, the abrasive wear rate (in arbitrary units) is plotted as a function of the ratio of hardness of the abrasive and hardness of the wear surface. The figure clearly shows that, when the hardness of the abrasive is larger than the hardness of the worn surface, wear of the surface will be severe. The influence of intrinsic material properties like grain size, porosity and composition on wear resistance in general, is not as well documented in literature as the extrinsic ones (mechanical and thermal properties). This is caused by the dominance of the properties of the tribosystem over the properties of the materials used. The hardness of a material has a large influence on wear behaviour. As shown in Figure 1.6, the wear rate of a material increases with increasing hardness of abrasive particles. In general it is clear that materials possessing a combination of high hardness and fracture toughness, will be the most wear resistant.

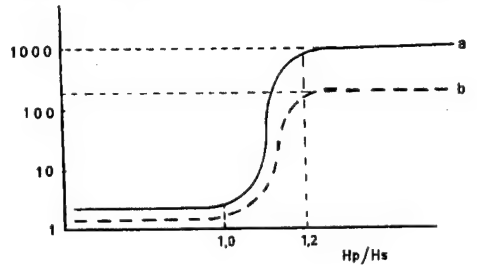

Figure 1.6: Abrasive wear as a function of the ratio of hardness of the abrasive, *Hp*, and hardness of the wear surface, *Hs* (a: sharp abrasive particles; b: rounded abrasive particles). Numbers along the *y*-axis give an impression of the ratio of wear rates in various wear regimes [52].

The influence of the hardness can, however, be considered both positive and negative. Materials with a high hardness are more wear resistant, but an increasing hardness lowers the threshold value for transition from mild to severe wear. The fracture toughness

has a positive influence on the resistance against lateral crack propagation (if the toughness is large), but its overall effect (considering all wear mechanisms) is not very clear yet. In Figure 1.7 the influence of transition loads (threshold values) and hardness on wear rate is shown as a function of the normal force. From this figure it is obvious that a high hardness can be beneficial for an enhanced wear resistance, but that the accompanying decrease of the threshold force has a bad influence on wear performance.

Evans *et al.* [27] developed a model for combining hardness and wear rate. For this model it is assumed that wear of a material occurs by lateral fracture. This means that cracks in the material propagate perpendicular to the moving direction of the abrading particle. They derived the following equation for the wear volume at high loads, assuming that lateral fracture occurs when the abrading or sliding particle exceeds the fracture threshold force:

$$V_w = \alpha \frac{F^{9/8}}{\sqrt{K_{1c} \cdot H}} \cdot E^{4/5} \cdot s \qquad (1.6)$$

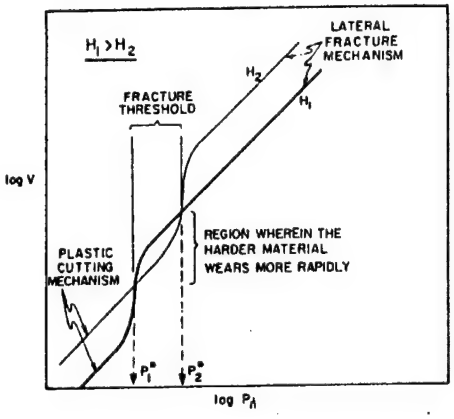

Figure 1.7: Schematic indicating the wear rate as function of normal force in two materials with a different hardness, H, but similar levels of toughness, K_c, and of E/H [27].

Here, α is a material-dependent constant, F is the applied normal force, K_{1c} is the fracture toughness, H is the hardness, E is Young's modulus and s is the sliding distance. The authors state that the depth of the lateral cracks defines the potential material removal zone. Beyond the lateral fracture threshold, at lower loads, material is removed by another mechanism: plastic cutting. Here, the material removal rate is predominantly related to the hardness, the normal force and the particle geometry:

$$V_w \propto \frac{F \cdot s}{H} \cdot \cot\left(\frac{\Psi}{2}\right) \qquad (1.7)$$

Here, Ψ is the incoming angle of the penetrating particle. The predicted wear volume for this mechanism is one order of magnitude smaller than for the lateral fracture mechanism. It was found that the model corresponds reasonably well for a fracture-dominated wear process, which usually occurs in brittle solids like ceramics.

The work of Trabelsi *et al.* [50] showed that for a wide variety of alumina-based composites with Y-TZP, the fracture toughness significantly improved with increasing Y-TZP content, but that hardness values decreased. On the whole, the wear volume increased as well, showing that the hardness has a larger influence on the wear behaviour than the toughness. According to Trabelsi this is related to the fact that frictional heating during dry sliding diminishes the increased toughening behaviour by the addition of Y-TZP. Thermal properties become important in situations with high sliding velocities and the absence of a lubricant. The lubricant normally consumes a lot of the heat released by friction in the contact. The severity of the effect of thermal processes is usually related to the thermal conductivity and thermal shock resistance of the materials.

1.4.2 Influence of microstructure

The ceramic microstructure influences the material's properties, and with that, indirectly the tribological properties as well. The grain size (and distribution) and porosity of a sintered ceramic body directly influence some of the material properties like thermal shock resistance and bending strength.

Hah *et al.* [53] showed that the relationship between hardness and alumina grain size (pure alumina) follows a Hall-Petch-type equation, which implies an increasing hardness with decreasing grain size. Alumina with the smallest grain size shows the lowest wear rate, as expected. They also reported that, even under the mild conditions used, formation of relatively soft aluminium hydroxide in the wear debris occurs (measured by infrared spectrometry). This decreases the abrasive influence of the debris and therefore the wear rate decreases. As reported by Wang *et al.* [42] a smaller grain size of alumina causes lower wear at moderate loads and it shifts the wear transition load to a higher level. This can be attributed to the presence of smaller grain boundaries and defects that require higher stress to propagate the existing cracks and defects. Cho *et al.* [45] show that an increased grain size in alumina results in a shorter time before wear transition takes place. This suggests that the critical stress for grain boundary cracking decreases with increasing grain size. The influence of the grain boundaries on tribological behaviour is not quite clear.

The importance of grain boundary strength was shown by Krefetz and Fischer [54]. They showed that the weakening of grain boundaries of alumina by doping with yttria, leads to a wear rate that is 10 times larger than for undoped alumina. This process is more pronounced in the intermediate wear regime where wear occurs by grain boundary fatigue. This is in conflict with the work of Terheci [55] and others [56] who state that coarser grained alumina exhibits better wear behaviour because the relative influence of grain boundaries is less. Krell and Klaffke [57] showed that fine-grained aluminas (grain size 0.4 μm) have a fretting wear rate of at least one order of magnitude lower than for coarse-grained alumina (grain size 3 μm). The coefficient of friction was not influenced by the microstructure. The influence of grain size on wear was not found for zirconia.

The work of Liang *et al.* [58] showed that for zirconia, the properties of the grain material have a much larger influence on the mechanical and tribological properties than the grain boundary purity and processing. This means that high purity and strong grain boundaries do not necessary translate into superior tribological properties. Using low loads, for instance, results mainly in transgranular wear while grain boundary effects are negligible. Davidge and Riley [59] also showed that the wear rate of alumina increased in wet erosive wear with grain size increasing from 1 to 13 μm. These results were translated to a variety of other tests like ball-on-plate, sawing, dry erosion and grinding and they all showed the same trend.

Zum Gahr *et al.* [60] showed an important dependence of the wear performance on the grain size. They showed that the value of the transition load, indicating the start of severe wear, increased significantly with decreasing grain size. Similar relations between grain size and wear resistance were found by He [9], who found a Hall-Petch-type relation for

the wear resistance as function of grain size for Y-TZP ceramics with grain size varying between 0.15 and 0.9 μm (see section 1.3.2 as well).

1.5 Important aspects of ceramic processing

The main route to influence the ceramic microstructures is by controlling the ceramic processing methods. Most of the issues that are important for these processes are extensively treated in several books [61,62,63].

In general, ceramics are prepared by using the following steps and the important parameters for ceramic processing are all discussed in relation to these steps:

- powder synthesis,
- consolidation,
- sintering,
- finishing.

Ceramic powder preparation can, for instance, be realised by using wet-chemical processes, involving the co-precipitation of metal salts that are washed with water and alcohol. Powder preparation is not much described in this thesis. Where possible, commercially available powders were used.

The starting powders for ceramic processing have special demands, for especially particle size and morphology. These demands depend on the chosen consolidation route. A distinction can be made between various consolidation routes:

- dry powder pressing
- suspension processing
  - ◊ colloidal pressure filtration
  - ◊ slip casting
  - ◊ centrifugal casting
  - ◊ tape casting
  - ◊ gel casting
- paste processing
  - ◊ extrusion
  - ◊ injection moulding

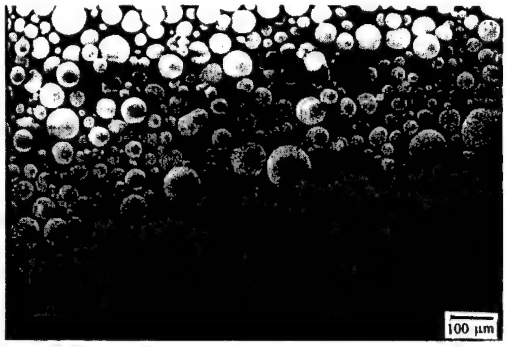

Figure 1.8: Typical example of a ceramic powder with spherical granules (controlled agglomeration by spray-drying) [64].

These are not all the possibilities, but the most important ones are listed. Consolidation by dry pressing is the most well-known method used for preparing ceramic pieces. For this method the particle morphology is of extreme importance. Irregularly shaped particles cause a lot of internal friction during pressing and they may result in high internal stresses or crack formation. Besides that the irregular shape may also be a cause of bad

stacking of the powder during filling of the pressing mould. Using powder particles with a good morphology (preferably spherical and soft agglomerates) results in a good stacking process for dry pressing and a good compaction during pressing. An example of such a powder is given in Figure 1.8. The chance of creating defects by stacking faults or remainders of hard agglomerates is significantly reduced. This is of course valid for composite ceramics as well. The presence of defects and inhomogeneities has a large negative effect on the properties of the ceramics in general. Examples are the final sintered density and mechanical properties such as hardness, toughness and strength.

For suspension processing the particle shape is of less importance, since in most of these processes the powder particles are de-agglomerated before the consolidation step. Usually suspensions are made based on water and powder with some kind of stabiliser. Examples are electrostatic stabilisation and steric hindrance. The resulting suspensions are stable in the sense that they show limited or very slow sedimentation. These suspensions can be consolidated in various ways. The technique most frequently used in this thesis is pressure filtration. Other possibilities are slip casting and centrifugal casting.

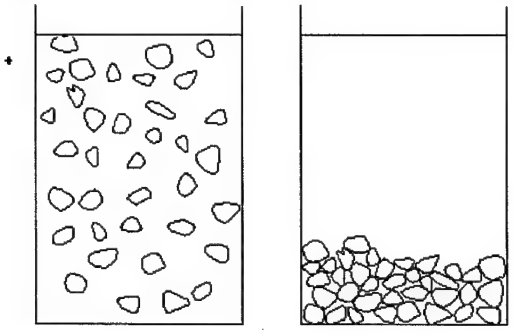

Figure 1.9: Schematic representation of suspension processing, where particles in a fluid are stacked by some means of either fluid removal or sedimentation.

Paste processing methods are not described in this thesis. Usually they involve not only stabilisers, but organic binders as well. The chosen consolidation route is of major importance for the homogeneity of the ceramic microstructure. In the case of composite materials (two or more separate ceramic phases in one matrix), the suspension preparation is the suitable step to create a homogeneous system. Dispersing and stabilising the system well means that the two phases are mixed properly and can be stacked in a very homogeneous way during the consolidation step. For both composites and single-phase ceramics the entire process can be used to control the presence of defects or large voids (Figure 1.9).

Sintering is used for strengthening and densification of the ceramic bodies. During sintering usually three stages are identified. After consolidation, the powder particles are bonded by neck growth to give the ceramic body strength. This is followed by densification where all large voids are removed and finally the grain will grow. Usually, the preference is for the lowest sintering temperature possible. This is done for cost effective reasons and to keep the ceramic grain size as small as possible. Typical grain sizes for single-phase alumina and Y-TZP are 2 and 0.4 μm, respectively. Sintered ceramics are usually finished by machining and polishing to give them their finial surface properties. By choosing a consolidation route that offers the possibility of near-net-shaping, it is possible to minimise the costs of the expensive post-treatments.

1.6 Outline of the thesis

The work described in this thesis deals with tribological properties of alumina, zirconia and composites of both materials. These tribological properties can be influenced by the homogeneity of the microstructure. Preparation of ceramic composites with a homogeneous microstructure is described in *chapter 2*. The influence of the second phase of the composites on the tribological properties is dealt with in *chapter 3*. The results of measurements on some exceptionally wear-resistant materials are given in *chapter 4*. Modelling of the tribological results is described in *chapter 5*. *Chapter 6* deals with friction reduction and in *chapter 7*, the relation between ceramic wear in practice and laboratory results is described.

Chapter 2 ***Homogeneous zirconia-toughened alumina ceramics with high dry-sliding wear-resistance*** (taken from a paper accepted for publication in *Journal American Ceramic Society*). This chapter deals with preparation of homogeneous composite ceramics. The tribological results are compared with those for inhomogeneous composites.

Chapter 3 ***Tribological properties of nanoscale zirconia-alumina composites*** (taken from *Wear*, **225-229** (1999) 1293-1302). This chapter deals with the general influence of a second phase on the tribological properties of alumina and zirconia. Microstructural issues that are addressed here mainly concern the improvement of density and the control of grain growth.

Chapter 4 ***Dry sliding wear of self-mated couples of zirconia, alumina and zirconia-alumina composites*** (taken from a paper accepted for publication in *Advanced Engineering Materials*). Self-mating tests on ZTA reveal an exceptionally low wear rate for a self-mating couple which usually shows a very bad wear performance due to the large cohesion and adhesion effects. The results are compared with those for other oxide ceramics.

Chapter 5 ***Wear of ceramics due to thermal stress: a new thermal severity parameter*** (submitted for publication). The model of Adachi *et al.* [5] is adjusted by implementing the work on frictional heating of Bos [17] as the thermal severity of a tribological contact (TS), whereas the same mechanical severity (MS), as described by Adachi, of the tribological contact is used. The developed model is verified by experiments and they show for most materials combinations a unified transition from mild to severe wear.

Chapter 6 ***Self-lubrication of alumina and zirconia ceramics by use of soft oxide additives*** (taken from a paper to be submitted for publication). Besides the work on manufacturing extremely wear resistant components, attention is paid to the reduction of friction. Frictional heating is largely reduced by lubrication, resulting in even lower wear. To avoid practical problems such as finite lifetime, low maximum applicable temperature, ceramic composites with a self-supplying content of solid state lubricant are prepared. Their frictional properties are compared to those for dry sliding unlubricated ceramic-ceramic tribosystems.

Chapter 7 ***Wear-resistant ceramics: two practical cases verified by tribological tests*** (taken from a paper submitted for publication). The translation of laboratory tests to practical results is an issue for this chapter. Mainly results for mechanical seals in a cogwheel pump are described. Not only tribological issues are addressed, but manufacturing and engineering issues as well. Since practice showed that actual operating conditions can vary a lot, it is necessary to make the connection back to dedicated laboratory tests again.

Chapter 8 ***Evaluation and perspectives***. Conclusions from the presented work and recommendations for future research, development and production are made.

1.7 References

1. J.D. Sibold, *Wear applications*, Engineered Materials Handbook, (1990), 973-977.
2. G. Willmann, *Oxide ceramics for articulating components of total hip replacements*, Bioceramics: Proceedings of the 10th international symposium on ceramics in medicine, Paris, France, 10 (1997) 123-126.
3. M. Savitz, *Commercialization of advanced structural ceramics: patience is a necessity*, Am. Ceram. Soc. Bull., 1 (1999) 53-56.
4. H. Czichos, D. Klaffke, E. Santner and M. Woydt, *Advances in tribology: the materials point of view*, Wear 190 (1995) 155-161.
5. K. Adachi, K. Kato and N. Chen, *Wear map of ceramics*, Wear, 203-204 (1997) 291-301.
6. S. Sasaki, *Tribochemistry in friction and wear of ceramics*, Jap. J. Tribol., 36 [7] (1991) 699-707.
7. S. Sasaki, *Effects of environment on friction and wear of ceramics*, Bull. Mech. Eng. Lab., 58 (1992) Japan.
8. K-H. Zum Gahr, *Microstructure and wear of materials*, Tribology Series Vol. 10, Elsevier Science Publishers BV, 1987.
9. Y. J. He, *Tribological and mechanical properties of fine-grained zirconia and zirconia-alumina ceramics*, Ph. D. thesis, University of Twente, The Netherlands, 1995.
10. Y. Wang and S.M. Hsu, *Wear and wear transition modelling of ceramics*, Wear 195 (1996) 35-46.
11. Y. Wang and S.M. Hsu, *Wear and wear transition mechanisms of ceramics*, Wear 195 (1996) 112-122.
12. M. Woydt, D. Klaffke, K.-H. Habig and H. Czichos, *Tribological transition phenomena of ceramic materials*, Wear, 136 (1990) 373-381.
13. S.M. Hsu, D.S. Lim, Y.S. Wang and R.G. Munro, *Ceramic wear maps: concept and method development*, Lubr. Eng., [47] 1 (1989) 49-54.
14. Y. S. Wang, S.M. Hsu and R.G. Munro, *Ceramics wear maps: alumina*, Lubr. Eng., 47 [1] (1991) 63-69.
15. S. W. Lee, S.M. Hsu and M.C. Shen, *Ceramic wear maps: zirconia*, J. Am. Ceram. Soc., 76 [8] (1993) 1937-1947.
16. S.M. Hsu and M.C. Shen, *Ceramic wear maps*, Wear, 200 (1996) 154-175.
17. S-S. Kim, S-W. Kim and S.M. Hsu, *A new parameter for assessment of ceramic wear*, Wear, 179 (1994) 69-73.
18. J. Bos, *Frictional heating of tribological contacts*, Ph. D. Thesis, University of Twente, 1995.
19. M. F. Ashby, Abulawi and Kong, *Temperature maps for frictional heating in dry sliding*, Tribol. Trans., 34 (1991) [4] 577-587.
20. M.B. Peterson, S.F. Murray and J.J. Florek, *Considerations of lubricants for temperatures above 1000°C*, ASLE Trans. 2 (1960) 225-230.
21. Y. Wang, F.J. Worzala and A.R. Lefkow, *Friction and wear properties of partially stabilized zirconia with solid lubricant*, Wear, 167 (1993) 23-31.
22. A. Erdemir, *Tribology: Friction and wear of engineering materials*, ed. I. M. Hutchings, Edward Arnold, London, 1992.
23. S. Jahanmir, *Friction and wear of ceramics*, Marcel Dekker, 1994.

24. J. Breznak, E. Breval and N.H. MacMillan, *Sliding friction and wear of structural ceramics, Part 1: Room temperature behaviour*, J. Mat. Sci., 20 (1985) 4657-4680.
25. E. Breval, J. Breznak and N.H. MacMillan, *Sliding friction and wear of structural ceramics, Part 2: Analysis of room-temperature wear debris*, J. Mat. Sci., 21 (1986) 931-935.
26. T.A. Libsch, P.C. Becker and S.K. Rhee, *Dry friction and wear of toughened zirconias and toughened aluminas against steel*, Wear, 110 (1986) 263-283.
27. A. G. Evans and D. B. Marshall, *Wear Mechanisms in ceramics*, Fundamentals on friction and wear of materials, ed. by D. A. Rigney, ASM International, (1981) 439-452.
28. G. W. Stachowiak and G.B. Stachowiak, *Unlubricated wear and friction of toughened zirconia ceramics at elevated temperatures*, Wear, 143 (1991) 277-295.
29. D. Wang, J. Li and Z. Mao, *Study of abrasive wear resistance of transformation toughened ceramics*, Wear, 165 (1993) 159-167.
30. A. Medevielle, F. Thévenot and D. Tréheux, *Wear resistance of stabilized zirconias*, J. Eur. Ceram. Soc., 15 (1995) 1193-1199.
31. M. Woydt, J. Kadoori, K.-H. Habig and H. Hausner, *Unlubricated sliding behaviour of various zirconia-based ceramics*, J. Eur. Ceram. Soc., 7 (1991) 135-145.
32. Y. Kong, Z. Yang, G. Zhang and Q. Yuan, *Friction and wear characteristics of mullite, ZTA and TZP ceramics*, Wear, 218 (1998) 159-166.
33. A. W. C. Tse, S. Lawson and C. Gill, *Low amplitude oscillatory wear of Y-TZP in various environments*, 8th CIMTEC, 1994.
34. I. Birkby, P. Harrison and R. Stevens, *The effect of surface transformation on the wear behaviour of zirconia TZP ceramics*, J. Eur. Ceram. Soc., 5 (1989) 37-45.
35. S. Lawson, *Environmental degradation of zirconia ceramics*, J. Eur. Ceram. Soc., 15 (1995) 485-502.
36. T. Sornakumar, R. Krishnamurthy and C.V. Gokularathnam, *Machining performance of phase transformation toughened alumina and partially stabilised zirconia composite cutting tools*, J. Eur. Ceram. Soc., **12** (1993) 455-460.
37. J. L. Shi, B.S. Li and T.S. Yen, *Mechanical properties of Al_2O_3 particle-Y-TZP matrix composite and its toughening mechanism*, J. Mat. Sci., 28 (1993) 4019-4022.
38. J.-F. Li and R. Watanabe, *Fracture toughness of Al_2O_3-particle-dispersed Y_2O_3-partially stabilized zirconia*, J. Am. Ceram. Soc., 78 [4] (1995) 1079-1082.
39. I. J. McColm, *Ceramic Hardness*, Plenum Press, New York, 1st edition, 1990.
40. X. Dong, S. Jahanmir and S.M. Hsu, *Tribological characteristics of α-alumina at elevated temperatures*, J. Am. Ceram. Soc., 74 [5] (1991) 1036-1044.
41. K-H. Zum Gahr, *Sliding wear of ceramic-ceramic, ceramic-steel and steel-steel pairs in lubricated and unlubricated contacts*, Wear, 133 (1989) 1-22.
42. Y. Wang and S.M. Hsu, *The effects of operating parameters and environment on the wear and wear transition of alumina*, Wear 195 (1996) 90-99.
43. Y.S. Wang, C. He, B.J. Hockey, P.I. Lacey and S.M. Hsu, *Wear transitions in monolithic alumina and zirconia-alumina composites*, Wear 181-183 (1995) 156-164.
44. A. Blomberg, M. Olsson and S. Hogmark, *Wear mechanisms and tribo mapping of Al_2O_3 and SiC in dry sliding*, Wear, 171 (1994) 77-89.
45. S-J. Cho, H. Moon, B.J. Hockey and S.M. Hsu, *The transition from mild to severe wear in alumina during sliding*, Acta Metall. Mater., [40] 1 (1992) 185-192.
46. K. Cherif, B. Gueroult and M. Rigaud, *Wear behaviour of alumina toughened zirconia materials*, Wear, 199 (1996) 133-121.
47. K. Cherif, B. Gueroult and M. Rigaud, *Al_2O_3-ZrO_2 debris life cycle during wear: effects of the third body on wear and friction*, Wear, 208 (1997) 161-168.
48. L. Esposito and A. Tucci, *Tribological behaviour of ceramic/ceramic and metal/ceramic couples*, Third Euro-Ceramics, V. 3, (1993) 301-306.
49. L. Esposito, R. Moreno, A.J. Sànchez Herencia and A, Tucci, *Sliding wear response of an alumina-zirconia system*, J. Eur. Ceram. Soc., 18 (1998) 15-22.
50. R. Trabelsi, D. Treheux, G. Orange, G. Fantozzi, P. Homerin and F. Thevenot, *Relationship between mechanical properties and wear resistance of alumina-zirconia ceramic composite*, Tribol. Trans., 32 (1989) [1] 77-84.

51. C. He, Y.S. Wang, J.S. Wallace and S.M. Hsu, *Effect of microstructure on the wear transition of zirconia toughened alumina*, Wear, 162-164 (1993) 314-321.
52. Reader *Tribologie: dynamische contact verschijnselen*, (in Dutch), University of Twente, (1990).
53. S.R. Hah, T.E. Fischer, P. Gruffel and C. Carry, *Effect of grain boundary dopants and mean grain size on tribomechanical behavior of highly purified α-alumina in the mild wear regime*, Wear, 181-183 (1995) 165-177.
54. S.B. Krefetz and T.E. Fischer, *Wear of yttria-doped α-alumina: effects of grain boundary composition and machine stiffness*, Wear, 211 (1997) 141-145.
55. M. Terheci, *Grain boundary and testing procedure: a new approach to the tribology of alumina materials*, Wear, 211 (1997) 289-301.
56. F. Xiong, R.R. Manory, L. Ward, M. Terheci and S. Lathabi, *Effects of grain size and test configuration on the wear bahviour of alumina*, J. Am. Ceram. Soc., 80 [5] (1997) 1310-1312.
57. A. Krell and D. Klaffke, *Effects of grain size and humidity on fretting wear in fine-grained alumina, Al_2O_3/TiC, and zirconia*, J. Am. Ceram. Soc., 79 [5] (1996) 1139-1146.
58. H. Liang, T.E. Fischer, M. Nauer and C. Carry, *Effect of grain boundary impurities on the mechanical and triboogical properties of zirconia surfaces*, J. Am. Ceram. Soc., 76 [2] (1993) 325-329.
59. R.W. Davidge and F.L. Riley, *Grain-size dependence of the wear of alumina*, Wear, 186-187 (1995) 45-49.
60. K.-H. Zum Gahr, W. Bundschuh and B. Zimmerlin, *Effect of grain size on friction and sliding wear of oxide ceramics*, Wear, 162-164 (1993) 269-279.
61. J.S. Reed, *Introduction to the principles of ceramic processing*, New York, Wiley, 1988.
62. D.W. Richerson, *Modern ceramic engineering*, Marcel Dekker, 1992.
63. T.A. Ring, *Fundamentals of ceramic powder processing and synthesis*, Academic Press, 1996.
64. G.S.A.M. Theunissen, *Microstructure, fracture toughness and strength of (ultra)fine-grained tetragonal zirconia ceramics*, Ph. D. Thesis, University of Twente, 1991.

2 Homogeneous zirconia-toughened alumina ceramics with high dry sliding wear resistance*

Abstract

The preparation of dense homogeneous zirconia-toughened alumina (ZTA) with high dry sliding wear resistance is described. These ZTA ceramics are obtained by sintering green compacts, made by colloidal filtration of well-defined ZrO_2-Al_2O_3 particle suspensions, for 2 hours at 1400°C. The optimum solid and stabiliser concentrations for the filtration process were determined. The sintered ZTA microstructure consists of a homogeneous distribution of zirconia grains in an alumina matrix with grain sizes of 0.2 and 0.5 μm, respectively. In pin-on-disc tribological measurements at relatively high initial contact pressures (app. 1 GPa) and sliding speeds (0.5 m/s) a very low specific wear rate (app. 10^{-9} mm^3/Nm) and a coefficient of friction of 0.5 were found. It is shown that, in this case, wear is dominated by abrasion and polishing.

2.1 Introduction

At present, lubricants are often used to reduce wear and friction in sliding contacts of moving parts in equipment. The use of these lubricants, however, becomes more and more unwanted for environmental and other reasons. In practical unlubricated sliding contacts the touching materials must be carefully chosen such that the specific wear rate is well below 10^{-6} mm^3/Nm with a friction coefficient preferably lower than 0.2 [1,2]. The wear mechanism should in any case be mild, meaning that the contacting materials preferably polish each other, resulting in a very low specific wear rate. The unwanted opposite of mild wear is "severe" wear in which contact-surface roughening takes places due to break-out of large pieces of material. In many cases a transition takes place from mild to severe wear if the load is increased [3]. In addition, the occurrence of fatigue at a constant load may trigger a rapid transfer from mild wear to severe wear after a certain sliding time (or distance).

In literature it is suggested that for many cases, the "ideal" dry sliding couple has not yet been found [4]. This may be connected with the fact that the materials investigated until now did not fulfil the requirements mentioned above. One of the major problems is the fact that the homogeneity of the available ceramic materials is insufficient for the applications in mind [5]. The homogeneity may be expressed in terms of the occurrence of, for instance, processing defects, unwanted second phases, oversized grains [6] and spatially correlated porosity. Many investigators have given examples of tribological properties of oxide ceramics, but not all use microstructural observations to identify the possible differences in wear and friction.

---

* Taken from: B. Kerkwijk, A.J.A. Winnubst, E.J. Mulder, accepted for publication, J. Am. Ceram. Soc., 1999.

Hsu and Shen [7] reported mild wear for dense alumina with 5 μm grains at sliding speeds up to 0.2 m/s. This alumina has a mild-to-severe wear transition pressure of 700 MPa. Using a lower sliding speed of <0.01 m/s, mild wear was found at pressures up to 2 GPa. Since the large grain size and low toughness of pure dense alumina are less favourable for dry sliding applications, alternative materials compositions should be considered as well. Dense zirconia ceramics can be obtained with much smaller grains and higher toughness than alumina. SiC and Si_3N_4 (ceramics with covalent bonding) are much harder and SiC has a higher thermal conductivity than the oxides. However, wear studies [7] of yttria stabilised-tetragonal zirconia (Y-TZP), SiC and Si_3N_4 ceramics showed a transition from mild to severe wear at much lower sliding speed and at a lower contact pressure than for single-phase alumina. The most obvious disadvantages for the use of zirconia are the low hardness and low thermal conductivity. The ceramics with covalent bonding are more difficult to process, generally leading to less homogeneous microstructures. In addition, the non-oxides SiC and Si_3N_4 are easily oxidised and form soft SiO_2 films at the surface that rapidly degrade. This process leads to unacceptable high wear rates [5]. As a consequence, developing high wear-resistant materials by starting with dense alumina ceramics and reducing its less-favourable properties by proper non-soluble additives seems to be a good strategy. Hence for the present study, work was focused on preparation and properties of fine-grained composites with an alumina matrix in which isolated small zirconia grains are present. Such a composite is well known in literature as zirconia-toughened alumina (ZTA). In ZTA with 8-15 vol% zirconia the favourable properties of alumina can be maintained since ZTA is nearly as hard and as thermally conductive as pure alumina. The zirconia may introduce extra toughening [8-10] and lead to a smaller (sub-micron) grain size in the ceramics. The enhanced toughness of the alumina phase may be caused by a latent possibility of martensitic phase transformation of the zirconia phase, but toughening due to crack-deflection is also possible, especially because of the small grain sizes used in the present study. A homogeneous distribution of small zirconia particles also acts as an impediment for alumina grain growth during sintering [9,11].

C. He *et al.* [3] studied dry sliding wear of ZTA, amongst others. The authors showed that the value of the mild-to-severe wear-transition load depends on:

- *The zirconia content*: An increase to 12 vol% results in an increase in wear-transition load.
- *The alumina matrix grain size*: Increasing grain size results in a decreasing wear-transition load.

Y.J. He *et al.* [8] observed mild wear with a very low wear rate of $2 \cdot 10^{-8}$ mm^3/Nm for ZTA under reciprocal dry sliding against a stainless steel plate. Test conditions were an initial mean contact pressure of 300 MPa and an average sliding speed of 0.02 m/s. The wear mechanism observed was mainly adhesive material transfer of a metallic layer on the ceramic surface. An increase in wear resistance by the addition of zirconia to alumina has also been reported by others [12-14]. Trabelsi *et al.* [10] stated that the addition of zirconia to alumina results in a material with a lower wear resistance due to the decrease in hardness. Most investigators conclude however [3,9] that an optimum amount of zirconia of 10-12 vol% exists, that provides enough improvement in toughness and decreased grain size to compensate for the lower hardness. Kamiya *et al.* [15] performed collision tests (erosive wear) on alumina and ZTA ceramics with Al_2O_3 or SiC particles and showed that ZTA had the lowest wear rate.

Unfortunately, detailed systematic studies on the effect of ZTA microstructure on wear-resistance are not yet available, meaning that not much material for comparison is present.

To obtain fine-grained ZTA ceramics with optimum wear properties, it is important that:

- The green compact consists of a homogeneous, close packing of well-defined particles with a narrow size distribution in the sub-micron range.
- The zirconia phase is homogeneously distributed in the matrix in the sintered alumina.
- The sintered material is defect-poor (low amount of faults and cracks).

During the consolidation or green forming step, several defects can be introduced, which remain or can even grow during the sintering step. Especially dry pressing of powders is known as a technique where defects are easily introduced due to density variations and (remainders of) powder agglomerates. It is generally accepted [16-23] that consolidation techniques based on colloidal processing result in a more defect-poor green ceramic body. To achieve this, it is necessary to prepare a homogeneous, stable suspension of well-defined non-agglomerated particles with a narrow size distribution. Unstable suspensions are known to result in an inhomogeneous green phase distribution due to flocculation/segregation effects [17,18,23]. Colloidal consolidation techniques such as pressure filtration, slip casting, centrifugal casting or electrophoretic deposition may (easily) lead to homogeneous green compacts with a close-packed particle stacking. The use of such a high-density homogeneous stacking may also lower sintering temperatures needed to obtain dense ceramics [20].

In this chapter the colloidal consolidation and tribological properties of ZTA ceramics are described. The objective of the present study has been the investigation of possibilities for improvement of the tribological properties of ZTA materials by increasing the homogeneity of the phase distribution. Therefore the preparation of very well defined microstructures is necessary and hence colloidal processing is chosen as the consolidation method.

2.2 Experimental

2.2.1 Powder preparation

Undoped zirconia for colloidal processing was prepared by precipitation of a diluted $ZrCl_4$ (Merck, Darmstadt, Germany) solution in an excess of ammonia. Further details of this method can be found elsewhere [24]. After washing with water and ethanol and then drying, the zirconium hydroxide precipitate was calcined at 500°C for 2 hours. This results in a 100% tetragonal zirconia phase as confirmed by XRD, with an average crystallite size of about 10 nm, calculated from XRD line broadening using the (111) reflection at 30° 2θ. The BET surface area of this powder is 100 m^2/g. The crystallite size of the α-alumina powder (AKP-50, Sumitomo Chemical Co. Ltd, Osaka, Japan) was 0.1-0.3 μm as specified by the manufacturer. The BET surface area of this powder is 10 m^2/g.

2.2.2 Colloidal consolidation

Various single phase suspensions of alumina and zirconia were prepared by using HNO_3 as stabilising agent and ball milling these systems with zirconia balls (∅ = 2 mm) for at least 16 hours. Acid concentrations used were 0.05, 0.10 and 0.15 M, based on the pure water phase. Acid concentrations lower than 0.05 M gave unstable suspensions. The alumina solid concentration was varied between 33 and 75 wt%. The zirconia solid concentration was kept

constant at 33 wt%. Appropriate volumes of each single-phase suspensions were mixed for 1 hour to obtain a suspension in which 15 wt% of the solid phase consists of ZrO_2 using the above described milling equipment and then filtered over a membrane filter with a pore size of 0.45 mm (ME25, Schleicher & Schuell, Dassel, Germany). The suspension surface remained in contact with the atmosphere while the driving force for the filtration process was created by a vacuum at the other side of the membrane filter. The disc-shaped green compact (Ø = 42 mm) could easily be released from the membrane filter after ten hours of drying in stagnant air at room temperature. The green compacts were sintered for 2 hours at 1350, 1400 or 1450°C (with heating and cooling at 2 and 4°C/min, respectively). Microstructural investigation was performed using SEM on polished and thermally etched samples. Grain sizes were determined using the linear intercept technique [25]. Cross-sectional SEM pictures of the samples were used to study possible segregation effects during filtration.

2.2.3 [illegible]urposes

Results of the tribological measurements of the colloidally processed ceramics were compared with those for dense ceramics made with a commercially available, spray-dried 85 wt% alumina and 15 wt% zirconia powder mixture. This material, further indicated as ZTACOM (Zirconia Sales, Surrey, Great Britain), was made by conventional uniaxial pre-forming of 48 mm Ø pellets at 30 MPa and isostatic pressing at 400 MPa. Sintering was done using an initial heating rate of 1°C/min up to 400°C and 1 hour dwell for binder burn-out, followed by heating at 2°C/min to 1600°C and a 2 hours dwell followed by cooling down at 4°C/min.

2.3 Wearing

Dry-sliding wear tests on ceramic discs were performed at room temperature on pin-on-disc tribometer (CSEM, Neuchatel, Switzerland). Commercially available 10 mm alumina bearing balls (grade 10, Gimex Technical Ceramics BV, Geldermalsen, The Netherlands) were used as pin material. The geometry of the test set-up is shown in Figure 2.1.

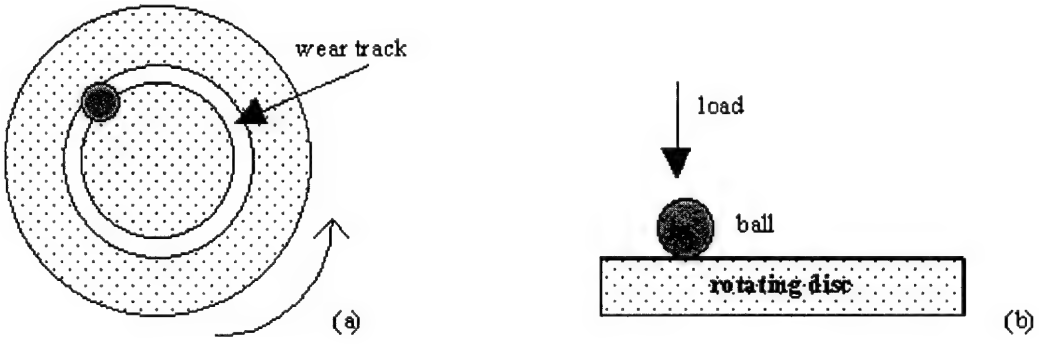

Figure 2.1: Tribological test set-up.

The sliding velocity in the contact was set at 0.5 m/s. A constant force, *F*, of 15.5 N was applied resulting in an initial mean Hertzian contact pressure of 1130 MPa. Dry sliding wear was measured in a controlled air atmosphere using a climate chamber (Heraeus HC4057, Balingen, Germany). The temperature was set at 23°C and the relative humidity at 40%. The

wear volume, V_w, was determined after a sliding distance, s, of 120 km. Wear is expressed in a specific wear rate k_w (in mm^3/Nm), using:

$$k_w = \frac{V_w}{F \cdot s} \tag{2.1}$$

The wear volume, V_w, was determined by measuring the weight loss of the sample or by determination of the wear volume from the wear track depth as measured by interference profiling (ATOS micromap, Pfungstadt, Germany). Both measurements gave values of the same order of magnitude. The friction force was measured continuously during the experiments and is expressed as a coefficient of friction. The coefficient of friction is defined as the ratio between the measured friction force and the applied normal force.

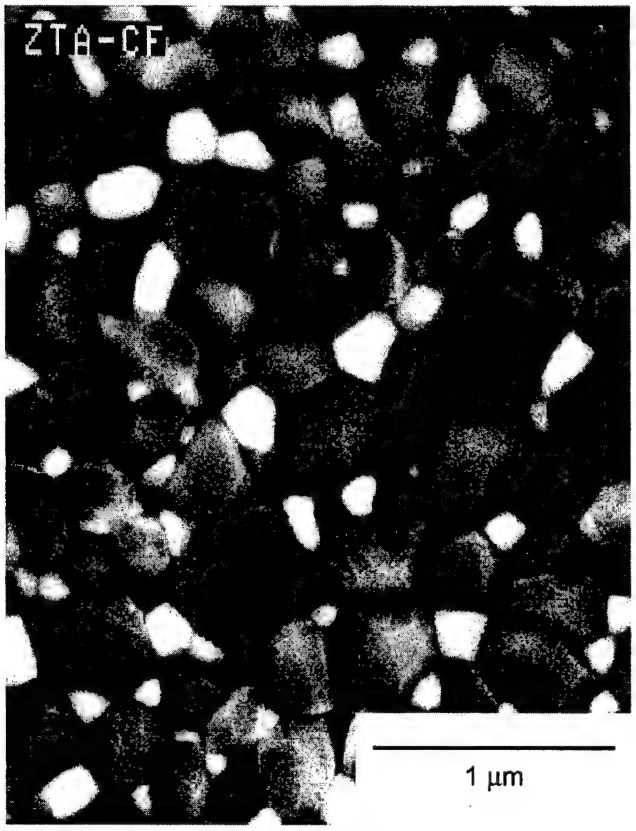

Figure 2.2: Microstructure of ZTA/5 after sintering at 1400°C; white phase represents zirconia and dark phase represents alumina .

2.4 Preparation of ZTA by colloidal filtration

2.4.1 Results

In Figure 2.2 the microstructure is shown of ZTA obtained by colloidal filtration and subsequent sintering at 1400°C for 2 hours. This sample is 99% dense and the grain size is 0.5 and 0.2 µm for alumina and zirconia, respectively. SEM pictures of several parts of a cross-section of this ceramic showed the same homogeneous microstructure with identical

alumina and zirconia phase concentrations. The height of the disc-shaped samples was up to 4 mm, depending on the solids loading during filtration.

Table 2.1: Compositions of the suspensions used for colloidal filtration of green compacts, their density in the green state and after sintering at 1450°C for 2 hours, total suspension solid loading, ϕ, and hindrance factor, h, calculated from equation 2.2 and the experimentally observed occurrence of collective particle movement and flocculation.

Suspension	$[HNO_3]$	Al_2O_3	ZrO_2	ρ_{green}	$\rho_{1450°C}$	ϕ	h	Collective	Flocculation
	$(mol \cdot l^{-1})$	(wt%)	(wt%)	(%)	(%)	(-)	(-)	particle movement	
ZTA/1	0.05	33	33	61	97	0.15	0.38	No	No
ZTA/2	0.15	33	33	61	92	0.15	0.38	No	Yes
ZTA/3	0.05	50	33	54	> 99	0.24	0.24	Yes	No
ZTA/4	0.10	50	33	59	98	0.24	0.24	Yes	Yes
ZTA/5	0.05	66	33	67	> 99	0.33	0.13	Yes	No
ZTA/6	0.05	75	33	59	97	0.38	0.09	Yes	No

The composition of the suspensions used, named ZTA/1-6, and the green and sintered densities of the consolidated compacts are given in Table 2.1. The ceramics made from the suspensions are indicated with the same designation code as the suspension. As can be seen in Table 2.1, the alumina solid and nitric acid concentrations affect the density of the ceramics after sintering at 1450°C. No consistent influence of both concentrations on the green densities of the consolidated cakes is found. However, ZTA/3 and ZTA/5 ceramics are the only ones that reach nearly full density.

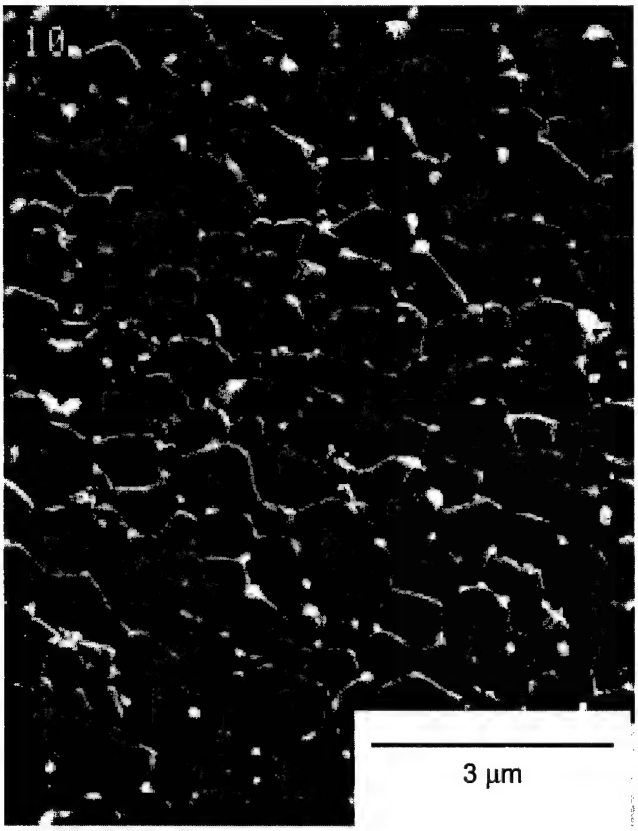

Figure 2.3: Microstructure of ZTA/1 (with low solid content during colloidal filtration) after sintering at 1450°C.

In Figure 2.3, a SEM picture is shown of the microstructure of the top part of the ZTA/1 ceramic disc. From this picture and in comparison with Figure 2.2 it is concluded that a low concentration of alumina in the starting suspension results in a significantly lower zirconia concentration in the top part of the ceramic disc; so no homogeneous distribution of the second phase is obtained. This implies that in ZTA/1 ceramics, there is an increase in zirconia content in the original filtration direction. Similar results were obtained with discs made with ZTA/2.

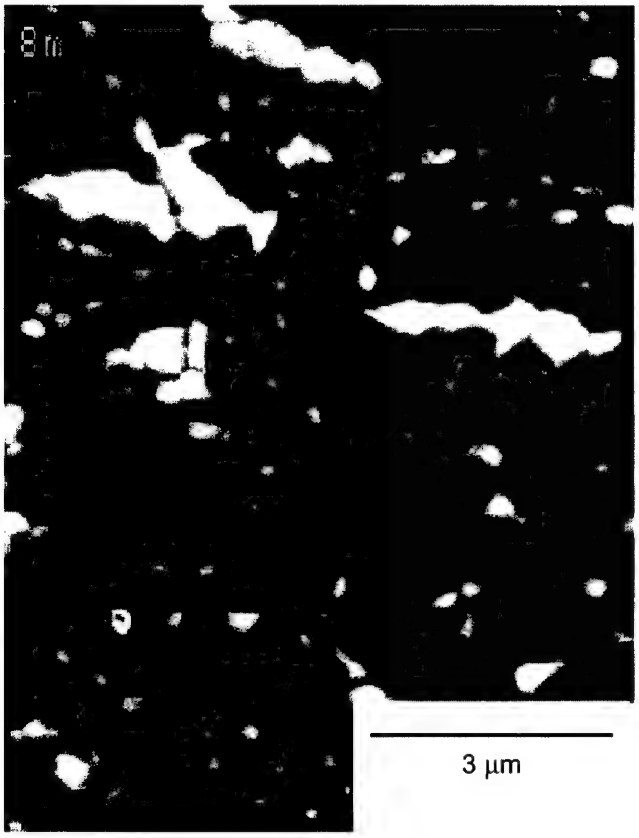

Figure 2.4: Microstructure of ZTA/4 (with high nitric acid concentration during colloidal filtration) after sintering at 1450°C.

Figure 2.4 shows that a high HNO_3 concentration (in ZTA/4) results in clustering (by flocculation) of the zirconia particles throughout the ceramic disc. In addition the top layer of the disc-shaped samples pealed off in most cases if a high acid concentration was used. Hence, the optimum solid and nitric acid concentration for obtaining a homogeneous ZTA compact, within the scope of the used materials and stabilisation route, is regarded to be the composition of ZTA/5, because of the higher solids loading and green density compared to ZTA/3. Details on ceramic microstructure (density, grain size) of ZTA/5 are given in Table 2.2.

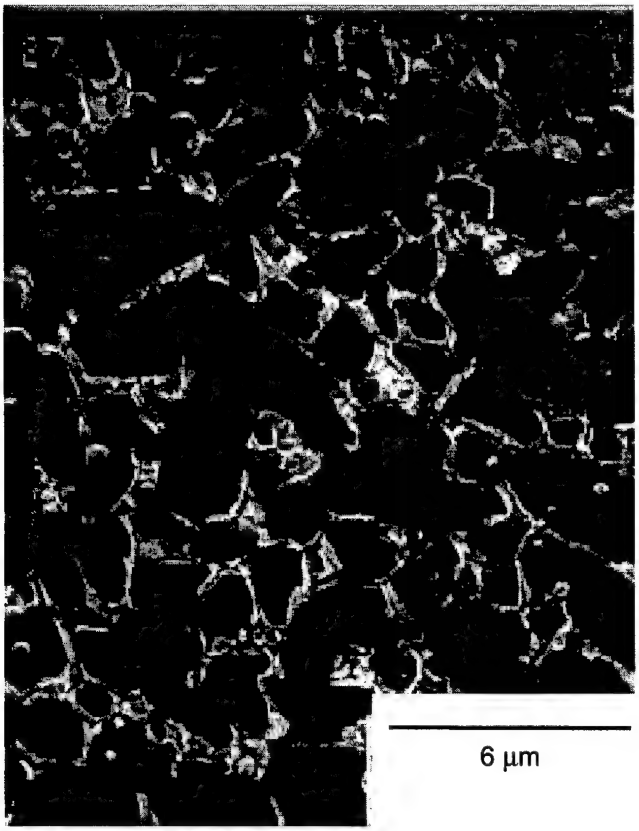

Figure 2.5: Microstructure of ZTACOM.

A SEM picture of ZTACOM is given in Figure 2.5 which shows a rather coarse structure while the homogeneity of the phase distribution is inferior to that of the colloidal-processed ceramic. Especially the grain boundaries of the ZTACOM are not well defined. When the material is sintered at 1450°C for 2 hours, a density of 90% is obtained, so a high sintering temperature is necessary. A density of 98% is reached only after sintering at 1600°C for 2 hours, resulting in grain sizes of 3.1 µm and 0.9 µm for alumina and zirconia, respectively.

Table 2.2: Microstructural characteristics of ZTA/5 after sintering at 1350, 1400 and 1450°C.

Sintering *T*(°C)	Density (%)	Grain size (and phase) Al_2O_3 (µm)	Grain size (and phase) ZrO_2 (µm)
1350	91	* (corundum)	*
1400	>99	0.51 (corundum)	0.16 (tetragonal & monoclinic)
1450	>99	0.7 (corundum)	0.3 (tetragonal & monoclinic)

2.4.2 Discussion

The alumina powder concentration in the single-phase suspension and the nitric acid concentration prior to mixing influence the zirconia-alumina phase distribution after consolidation (Figure 2.2 to Figure 2.4). The influence of these concentrations can be explained by two phenomena: sedimentation (possibly resulting in segregation) and flocculation. The influence of the experimental conditions on the occurrence of these phenomena is also shown in Table 2.1.

In the zirconia-alumina suspensions sedimentation will occur during the consolidation step. In a sufficiently stable suspension this sedimentation will be very limited. In a non-stable suspension, sedimentation occurs more rapidly. This sedimentation may be either a collective movement of both types of particles (no segregation) or a separate movement of both phases (segregation). From the results it is found that if the alumina concentration is too low, the zirconia can easily move independently from the alumina particles and settle more rapidly. This means that sedimentation by gravitation takes place [26,27]. Concha and Almendra [28] describe sedimentation velocities of suspensions of spherical particles. They describe the sedimentation velocity of the particles according to Stokes' law, but the velocity is corrected for the influence of the solid concentration of the suspension. This correction is expressed as the hindrance factor, *h*. *h* is given by [29] for particle volume fractions, ϕ, up to 0.59 and a very low Reynolds number:

$$h(\phi) = \frac{(1-\phi)(1-1.45\phi)^{1.83}}{1-0.75\phi^{0.33}} \qquad (2.2)$$

If *h* is close to unity there is no hindrance (particles sediment according to Stokes' law) and if $h << 0.5$ there is a significant amount of mutual particle hindrance [29]. In Table 2.1, *h*-values are given, calculated with equation 2.2 and the assumption that both alumina and zirconia phases contribute to ϕ. In Table 2.1 an indication is given that the transition from individual particle movement to collective particle movement takes place at $\phi \approx 0.2$ and $h \approx 0.3$; these values are extrapolated from the values between 0.38 and 0.24 for the hindrance factor, *h*. This would correspond to an alumina solid loading of about 40 wt%. As a consequence, a minimum of 50 wt% alumina is used in the single phase suspension to minimise zirconia sedimentation after mixing, processing and sintering. Suspensions with larger concentrations of alumina (ZTA/5 and ZTA/6) do not have a visible segregation effect.

The large solid concentration does not only slow down the sedimentation of zirconia, but it also influences the amount of collisions between the particles in suspension. Because the number of collisions is higher, reversible flocculation of particles of both types will be more pronounced. This flocculation may prevent sedimentation from occurring [30,31]. Besides that, Williams *et al.* [31] state that when the particles in suspension are bi-disperse, this flocculating effect is enhanced. However, the use of solid concentrations of 75wt% in suspension ZTA/6, caused handling problems during consolidation because the viscosity of the suspension became too high.

The ϕ-value where transition from individual to collective particle behaviour is found is significantly lower than:

- The value of 0.4, reported by Locket *et al.* [32] for a bimodal particle system.

- The value of 0.5, reported by Velamakanni *et al.* [17] based on interparticle potential arguments.

The discrepancy is probably related to the fact that the systems investigated in [17,32] use powders that have a smaller BET surface area. Especially the zirconia powders used in this study have a very large surface area, meaning that particle interactions will be very strong. Thus, flocculation without segregation can take place at lower solid concentrations.

Separate flocculation of zirconia in the sintered ceramics is observed when too high nitric acid concentrations are used. This flocculation is caused by the classical "salt"-effect, explained by the DLVO-theory. This means that the stabilising effect of the acid is diminished by the increased concentration of counter-ions and the particles will flocculate and form clusters in the suspension structure. It is not known if these clusters are formed during removal of water from the binary suspension or that they are already formed in the single-phase suspension. The latter is more likely, because the very small zirconia particles show a natural tendency towards rapid agglomeration.

The optimisation of processing parameters for colloidal processing shows that suspensions should be stabilised using 0.05 M HNO_3 with a zirconia concentration of 33 wt% and an alumina concentration of 66 wt% in the single-phase starting suspensions (ZTA/5). ZTA/5 is chosen because the material already reaches near full density at 1400°C. The results show that by using the described consolidation technique (with the proper experimental parameters), a high green density of 66 vol% is obtained, resulting in dense sintered ceramics with a homogeneous phase distribution. In addition, the grain sizes for both phases in ZTA/5 are relatively small. Because both particle types tend to impede each other's grain growth process during sintering, it can be assumed that a limited grain growth of alumina in the colloidally processed compact is an indication for an initially homogeneous stacking of the alumina particles in the matrix. It is found that in the ZTA/5-based ceramics, alumina grains grew from 0.23 µm slightly agglomerated particles to 0.51 µm grains. In the same way zirconia grew from 10 nm highly agglomerated particles to 0.16 µm grains after sintering at 1400°C.

The mutual grain-growth impediment effect is clearly demonstrated if one looks at the final alumina grain size obtained with inhomogeneous green compacts. In ceramics made from the suspension with low solid loading and those made with a too high acid concentration, the alumina grain size is much larger: 1.6 and 1.1 µm, respectively.

2.5 Tribological properties

2.5.1 Results

Under relatively extreme conditions (initial mean contact pressure 1130 MPa, sliding speed 0.5 m/s), the wear of ZTA/5 remains in the mild regime until failure of the alumina test sphere. The specific wear rate, k_w, was $5 \cdot 10^{-8}$ mm^3/Nm, for the entire measurement (120 km sliding distance), while k_w for ZTACOM was as high as $2 \cdot 10^{-6}$ mm^3/Nm. In all cases the coefficient of friction was between 0.45 and 0.55. Microstructural observations were used to gain insight in the wear mechanisms. Figure 2.6 and Figure 2.7 show wear tracks for both materials. In Figure 2.6a the wear track of ZTACOM reveals a grooved pattern. Figure 2.6b shows a similar pattern for ZTA/5, but the distance between the grooves in the wear track of ZTACOM is smaller than that for ZTA/5.

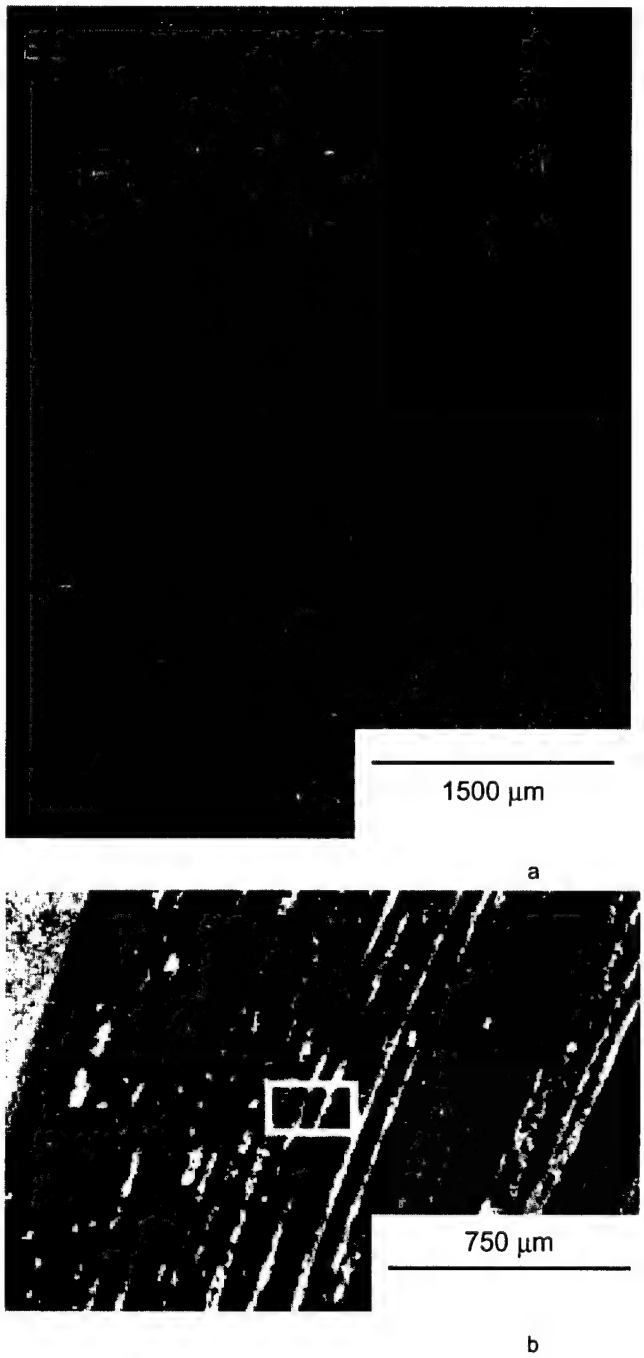

Figure 2.6: (a) Wear track (overview) of ZTACOM and (b) wear track (overview) of ZTA/5.

Figure 2.7a shows wear track details for ZTACOM. It is found that material in these grooves is fractured and smeared in the sliding direction. ZTA/5 (Figure 2.7b) shows the same features for wear inside the grooves as ZTACOM, but with a significantly smaller amount of grooves. The wear scar on the alumina pin is shown in Figure 2.8, revealing large "asperities" of about 10 µm. These "asperities" are likely to be caused by the microstructural inhomogeneities in the alumina ball.

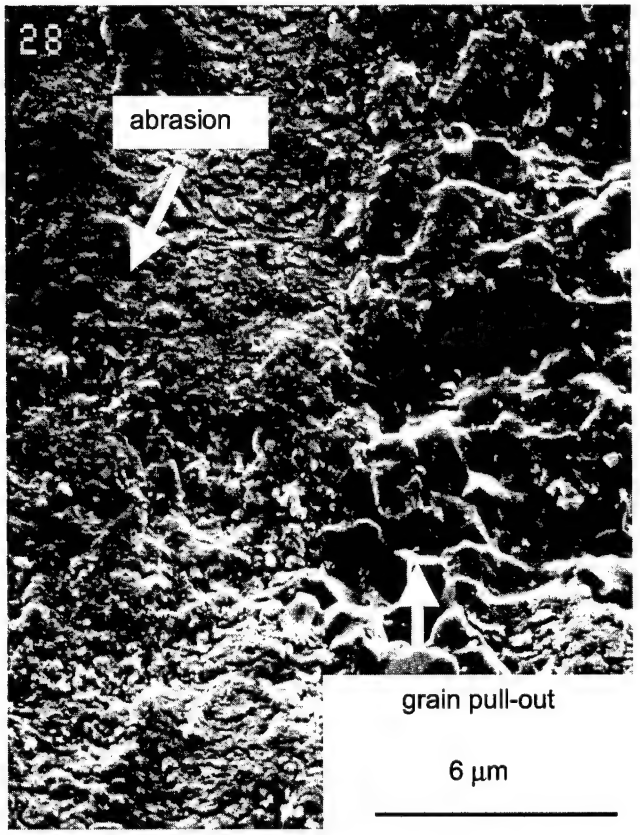

a

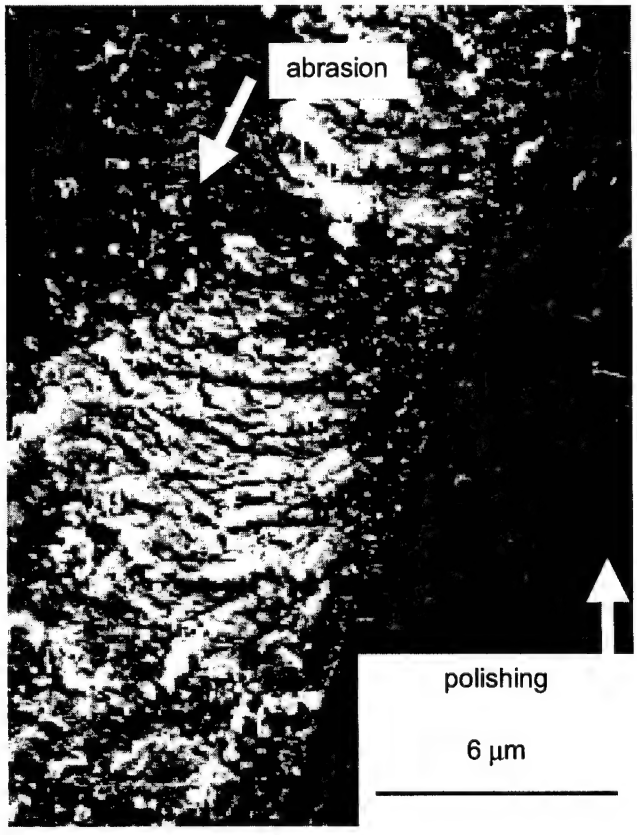

b

Figure 2.7: (a) Details of wear track of ZTACOM and (b) details of wear track of ZTA/5.

2.5.2 Discussion

The grooves in the wear tracks of the ceramic discs are caused by the asperities in the wear scars of the alumina pin because the size of the asperities are of the same size (app. 10 μm) as the groove widths. It is found that in the surface of the material next to the grooves, grain pull-out takes place for ZTACOM, whereas for ZTA/5 only a mild polishing/deformation effect takes place. This difference in wear mechanism is the main reason for the difference in the specific wear rate. The more homogeneous microstructure of the colloidal processed ZTA composite leads to a significant improvement in wear resistance compared to that of a commercially available, dry-pressed material.

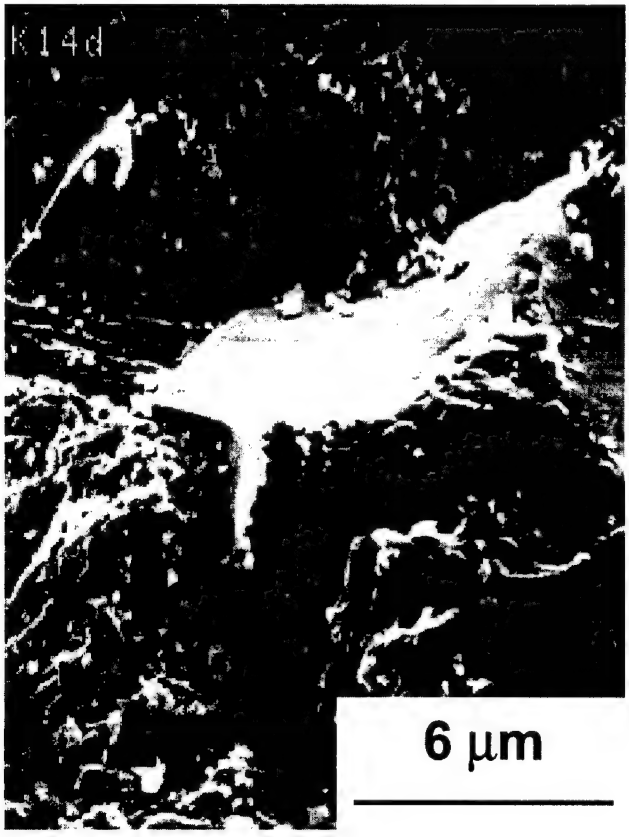

Figure 2.8: Wear scar of alumina pin.

2.6 Conclusion

Colloidal processing of zirconia-toughened alumina results in defect-poor, dense composites. A homogeneous composite ceramic could be obtained by colloidal filtration of an aqueous suspension stabilised using 0.05 M HNO_3. The suspension contained a mixture of fine-grained uniformly sized alumina (66 wt% solid in single-phase suspension) and zirconia (33 wt% solid in single-phase suspension). The ceramic, formed by colloidal processing and sintering, showed a more homogeneous phase distribution and also smaller average grain sizes than a ceramic processed and sintered from commercial material, used as comparison. The colloidal processed material sintered at 1400°C had grain sizes as small as 0.5 μm for

alumina and 0.2 μm for zirconia. During sintering, mutual grain-growth inhibition of alumina and zirconia grains in the colloidal processed ceramic is caused by a uniform distribution of the particles in the green compact.

The ZTA ceramics investigated, show mild wear under dry sliding testing conditions (initial contact pressure 1130 MPa, velocity 0.5 m/s). The specific wear rate is $5 \cdot 10^{-8}$ $mm^3/(Nm)$ for the colloidal processed material and $2 \cdot 10^{-6}$ mm^3/Nm for the reference materials made by dry pressing. The differences in wear rates are caused by grain pull-out in specific regions of the reference material, whereas the colloidal-processed material shows only polishing and deformation in these regions. These specific wear features are directly related to the microstructure of the material. It can therefore be concluded that the improved microstructure of the colloidal processed material leads to an improved wear resistance compared to the more coarse-structured and irregular reference material.

2.7 References

1. K. Adachi, K. Kato and N. Chen, *Wear*, 203-204 (1997) 291.
2. H. Czichos, D. Klaffke, E. Santner, M. Woydt, *Wear*, 190 (1995) 155.
3. C. He, Y.S. Wang, J.S. Wallace and S.M. Hsu, *Wear*, 162-164 (1993) 314
4. J.D. Sibold, in: Engineered Materials Handbook, Vol. 4. Ceramics and glasses, (1991) 973.
5. S. Sasaki, *Bull. Mech. Eng. Lab.* Japan, 58 (1992) 1.
6. Y.J. He, A.J.A. Winnubst, A.J. Burggraaf and H. Verweij, *J. Am. Ceram. Soc.*, 79 [**12**] (1996) 3090.
7. S.M. Hsu and M.C. Shen, *Wear*, 200 (1996) 154 .
8. Y.J. He, A.J.A. Winnubst, D.J. Schipper, P.M.V. Bakker, A.J. Burggraaf and H. Verweij, *Wear*, 184 (1995) 33.
9. K.J. Konsztowicz and R. Langlois, *J. Mater. Sci.*, 31 (1996) 1633.
10. R. Trabelsi, D. Treheux, G. Orange, G. Fantozzi, P. Homerin and F. Thevenot, *Trib. Trans.*, 32 [**1**] (1989) 77.
11. F.F. Lange and M.M. Hirlinger, *J. Am. Ceram. Soc.*, 67 [**3**] (1984) 164.
12. K. Cherif, B. Gueroult and M. Rigaud, *Wear*, 199 (1996) 113.
13. A. Ravikiran, G.R. Subbanna and B.N. Pramila Bai, *Wear*, 192 (1996) 56.
14. Y.J. He, A.J.A. Winnubst, D.J. Schipper, A.J. Burggraaf and H. Verweij, *Wear*, 210 (1997) 178.
15. H. Kamiya, M. Sakakibara, Y. Sakuri, G. Jimbo and S. Wada, *J. Am. Ceram. Soc.*, 77 [**3**] (1994) 666.
16. E.M. DeLiso, W.R. Cannon and A.S. Rao, *Advances in Ceramics, Vol. 24: Science and technology of zirconia III*, (1988) 335.
17. B.V. Velamakanni and F.F. Lange, *J. Am. Ceram. Soc.*, 74 [**1**] (1991) 166.
18. A. Bleier, P.F. Becher, K.B. Alexander and C.G. Westmoreland, *J. Am. Ceram. Soc.*, 75 [**10**] (1992) 2649.
19. J. Cesarano and I.A. Aksay, *J. Am. Ceram. Soc.*, 71 [**12**] (1988) 1062.
20. A. Roosen and H.K. Bowen, *J. Am. Ceram. Soc.*, 71 [**11**] (1988) 970.
21. F.F. Lange and K.T. Miller, *Am. Ceram. Soc. Bull.*, 66 [**10**] (1987) 1498.
22. A. Bleier and C.G. Westmoreland, *J. Am. Ceram. Soc.*, 74 [**12**] (1991) 3100.
23. T. Kimura, Y. Kaneko and T. Yamaguchi, *J. Am. Ceram. Soc.*, 74 [**3**] (1991) 625.
24. W.F.M. Groot Zevert, A.J.A. Winnubst, G.S.A.M. Theunissen and A.J. Burggraaf, *J. Mater. Sci.*, 25 (1990) 3449.
25. J.C. Wurst and J.A. Nelson, *J. Am. Ceram. Soc.-Disc. And Notes*, February (1972) 109.
26. A. P. Philipse, B. C. Bonekamp, and H. J. Veringa, *J. Am. Ceram. Soc.*, 73 [**9**] (1990) 2720.
27. F. M. Tiller, N.B. Hsyung, D.Z. Cong, *AIChE J.*, 41 [**5**] (1995) 1153.
28. F. Concha and E.R. Almendra, *Int. J. Mineral Proc.*, 6 (1979) 31.
29. P. M. Biesheuvel, A. Nijmeijer and H. Verweij, *AIChE J.*, 44 (1998) 1914.
30. J. F. Richardson and F. A. Shabi, *Trans. Instn Chem. Engrs.*, 38 (1960) 33.
31. R. A. Williams, W. B. K. Amarasinghe, S. J. R. Simons, and C. G. Xie, *Powder Techn.*, 65 (1991) 411.
32. M.J. Lockett and H.M. Al-Habbooby, *Trans. Inst. Chem. Eng.*, 51 (1973) 281.

3 Tribological properties of nanoscale alumina-zirconia composites*

Abstract

The tribological properties of zirconia (Y-TZP), alumina and their composites, alumina dispersed in zirconia (ADZ) and zirconia-toughened alumina (ZTA), were investigated. These ceramics are made by colloidal processing methods such that well-defined, homogeneous microstructures with sub-micron grains and few defects are obtained.
Dry sliding tests against alumina balls were performed on a pin-on-disc tribometer using varying test conditions. It was shown that, with initial Hertzian contact pressures up to 1 GPa and sliding velocities up to 0.5 m/s, the specific wear rate was the highest for Y-TZP, 10^{-6} $mm^3/(N \cdot m)$, and the lowest for ZTA, 10^{-9} $mm^3/(N \cdot m)$. For both single-phase zirconia and alumina ceramics it was found that addition of a harder (alumina) or a tougher (zirconia) phase, respectively, leads to an improved wear resistance. Depending on the test conditions the wear mechanisms are abrasion, delamination and polishing. The coefficients of friction were as high as 0.8 for Y-TZP and as low as 0.45 for ZTA.

The main conclusion of this work is that ZTA composites manufactured and tested in this study have a superior wear resistance and a relatively low coefficient of friction under dry sliding conditions.

3.1 Introduction

During the last ten years quite a number of papers on tribology of ceramics have been published. Industrial interest has risen as well, taking into account the broad array of ceramic products that is available for wear resistant applications - bearings of all types, cutting tools, thermal and erosion-resistant coatings. Especially for tribological applications, ceramics have a number of beneficial properties. In general, ceramics have high hardness and cannot easily be deformed. Besides this, ceramics are also known to maintain their mechanical properties at elevated temperatures better than metals.

Materials can also be characterised by some specific properties. Carbide- and nitride-based ceramics (e.g. SiC, Si_3N_4) have a very high hardness. This means that, for example, Si_3N_4 is a very suitable material for ball bearing applications. A problem with these materials is that they can undergo oxidation. Oxide ceramics like alumina and zirconia do not suffer from oxidation, but these ceramics have a lower hardness. The main advantage of the use of alumina in practice is the low cost compared to the other technical ceramics. Like the nitrides and carbides, alumina is a brittle material. This means that

---

* Taken from: B. Kerkwijk, A.J.A. Winnubst, H. Verweij, H.S.C. Metselaar, E.J. Mulder and D.J. Schipper, *Wear*, 225-229, (1999) 1293-1302.

alumina ceramics can have problems in structural applications where high strength and reliability are important. Here the enhanced toughness of stabilised zirconia is useful. By the addition of yttria, a meta-stable tetragonal phase (Y-TZP) is retained in zirconia after sintering, resulting in a ceramic, that has a high toughness connected with the presence of a stress-induced martensitic phase transition to the monoclinic phase.

However, zirconia has a disadvantage in its low thermal conductivity. In a tribological contact, frictional heating occurs, and this low thermal conductivity causes thermally induced crack formation, followed by severe wear processes. [1-6]. Alumina has a thermal conductivity that is at least 3 times higher than that of zirconia.

Given the properties of alumina and zirconia, it is interesting to combine the favourable properties of both ceramics (alumina and zirconia). This means that addition of a second phase of alumina to a zirconia matrix or vice versa may lead to ceramics with interesting properties. Addition of alumina to Y-TZP (alumina dispersed zirconia, ADZ) can improve the hardness of the ceramic and, if a percolative system can be made, the thermal conductivity. Addition of zirconia to alumina (zirconia-toughened alumina, ZTA) can improve the toughness of the matrix ceramic. If a homogeneous distribution of the zirconia phase is obtained, it must be possible to inhibit the grain growth of the alumina phase during sintering. Several investigations showed that a smaller grain size in alumina ceramics leads to improved wear-resistance and mechanical properties [7-9].

Previous investigations showed the importance and benefit of the use of alumina-zirconia composite systems for tribological purposes [10-15]. Especially for ZTA it is found that the transition from a mild wear process to a severe one can be shifted to more extreme operating conditions, for instance higher loads and higher velocities [10,11,13].

In the present investigation the results of pin-on-disc sliding wear measurements are shown for composites of alumina added to a Y-TZP matrix and undoped zirconia added to an alumina matrix. These materials were prepared to improve the tribological properties of both the single-phase ceramics. Tribological properties are measured using alumina pins at various high loads and velocities to find the limits of application of the ceramics mentioned. Wear was monitored on-line to gain insight in possible non-linear wear behaviour.

3.2 Experimental

Four types of ceramics, starting with various powders, were used for wear testing. Alumina ceramics were made from commercially available, high-purity α-alumina powder [AKP50, Sumitomo, Japan]. Yttria-stabilised tetragonal zirconia (Y-TZP) powder was prepared by a co-precipitation method of the metal-chlorides in an excess of ammonia. Alumina-dispersed zirconia (ADZ) composite powder was prepared by a modification of the previously mentioned precipitation method. In this case the precipitation of yttrium chloride and zirconium chloride (for ADZ) was performed in a suspension of AKP50-alumina powder in ammonia. All these powders were consolidated using dry pressing in a steel mould at 40 MPa, followed by isostatic pressing at 400 MPa. Zirconia-toughened alumina (ZTA) ceramics were made by colloidal filtration of the mixed suspension of AKP50-alumina and undoped precipitated ZrO_2 powder. The description of this process can be found else-

where [16]. The green bodies were sintered to relative densities of at least 95%. The properties of the sintered ceramics are given in Table 3.1.

Table 3.1: Properties of the ceramics used.

Material	Density [kg/m^3]	ν [–]	E [GPa]#	H_v [GPa]	Grain size ZrO_2 [µm]	Grain size Al_2O_3 [µm]
Y-TZP	5700	0.3	210	14	0.18	---
ADZ	5530	0.32	253	15	0.5	0.4
Alumina	3970	0.23	392	22	---	1.8#
ZTA	4210	0.23	370	20	0.2	0.5

Taken from [10]

3.2.1 Wear testing and characterisation

In traditional wear measurements the geometry of the specimen before and after testing is compared or the weight loss is measured. These measurements result in an average specific wear rate, k_w, using the following definition:

$$k_w = \frac{V_w}{F \cdot s}\left[\frac{\mathrm{mm}^3}{\mathrm{N \cdot m}}\right] \tag{3.1}$$

The wear volume, V_w, is often measured by means of surface height profiling. When dividing the wear volume by the applied force, F, and the sliding distance, s, the specific wear rate can be calculated. The value of k_w is set to a limit of 10^{-6} mm^3/(N·m) for unlubricated tribological applications, above which a material is no longer considered wear-resistant [17,18].

Several investigators [19-21] have used the method of on-line system wear measurement based on height displacement, in order to detect non-linear wear behaviour (as function of sliding distance). This method is applied here as well. A laser displacement sensor measures the vertical displacement of the load arm toward the rotating disc. In the case of equal specific wear rates for the ball and the disc, the height displacement can be mainly accounted for as ball wear (95%). This is due to the area effect, since assuming equal wear volume means that the height displacement of the worn ball must be higher than of the disc. For calculation of wear volumes, it is assumed that the wear scar of the ball is flat and circular*. The wear volume for the ball, $V_{w,ball}$, is then directly calculated from the height displacement:

$$V_{w,ball} = \frac{1}{3} \cdot \pi \cdot h^2 \cdot (3R - h) \tag{3.2}$$

* ASTM G99-90 standard test method for wear testing on a pin-on-disc apparatus

where R the ball radius and h the height of the worn ball segment. If h is measured on-line in time, the wear volume as a function of the sliding distance can be monitored as well. If the specific wear rate is constant, the resulting graph of $V_{w,ball}$ against the sliding distance should be a straight line. Deviations from the straight line are due to changes in specific wear rate.

Dry sliding wear tests are performed using a pin-on-disc tribometer [CSEM], placed in a climate chamber at 23°C and 40% relative humidity. As pin material, alumina balls of 6 or 10 mm diameter were used [grade 10, Gimex Technical Ceramics]. The investigated ceramics (alumina, Y-TZP, ADZ and ZTA) were cut to discs. The diameter of the discs was about 36.5 mm and the thickness varied between 2.5 and 4 mm. After cutting, the discs were polished to a final average roughness < 50 nm. A picture of the set-up is given in Figure 3.1.

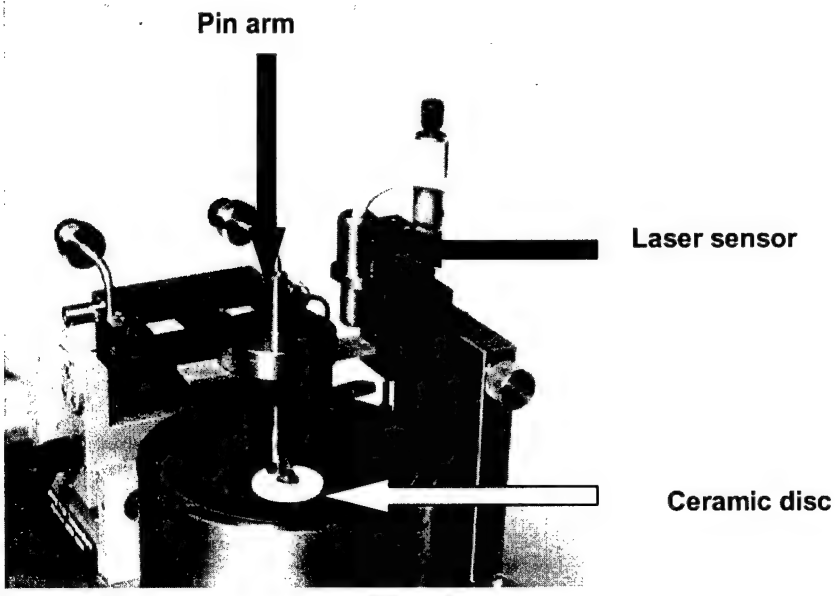

Figure 3.1: Pin-on-disc set-up with the on-line wear displacement laser sensor.

The two main test conditions, sliding velocity and applied load, were varied for each specific test between 0.1 and 0.5 m/s and 3 and 17.5 N, respectively. With the given geometry and properties of the materials used this leads to mean initial Hertzian contact pressures of 500 up to 1700 MPa. These values are calculated from the equations for the mean Hertzian contact pressure, P_{Hertz}:

$$P_{Hertz} = \frac{1}{3 \cdot \pi}\left(\frac{3 \cdot F \cdot E_r^2}{R_r^2}\right)^{\frac{1}{3}} \tag{3.3}$$

where F is the applied normal force, E_r is the reduced elastic modulus, R_r is the reduced radius. E_r and R_r are defined by:

$$E_r = \frac{2}{\left(\frac{1-\nu_1^2}{E_1} + \frac{1-\nu_2^2}{E_2}\right)} \tag{3.4}$$

where E_1 and E_2 the elastic moduli and ν_1 and ν_2 Poisson's ratios of pin and disc material, respectively.

$$R_r = \frac{R}{2} \tag{3.5}$$

where R the radius of curvature of the pin.

The sliding distance of the tests was varied for each specific measurement to obtain significant wear and to detect possible fatigue. The coefficient of friction was also measured on-line.

All wear tracks (disc) and wear scars (pin) were characterised by means of SEM. Cross-sectional characterisation of the tracks was performed as well. To determine phase distribution and the presence of impurities (or any strange phases) energy dispersive X-ray analysis (EDX) was used.

3.3 Results

3.3.1 Specific wear rates and coefficients of friction

Y-TZP and ADZ

Table 3.2 shows k and f for Y-TZP tested at sliding velocities between 0.1 and 0.5 m/s under initial contact pressure of 512 MPa (3 N). Because the thermal conductivity of zirconia ceramics is very low, tests were performed at various sliding velocities. In this way the thermal influence on the wear behaviour can be tested. The results show that up to a sliding velocity between 0.2 and 0.3 m/s, the specific wear rate is still below the limiting value of 10^{-6} mm^3/(N·m). Above this velocity wear becomes severe. The coefficient of friction has no apparent relation with the sliding velocity at moderate values. At higher sliding velocities (when wear is also high) the coefficient of friction is larger (0.8 instead of 0.6). Lee *et al.* [23] also reported transition behaviour of zirconia ceramics as function of velocity and load.

Table 3.2: Specific wear rate and coefficient of friction for Y-TZP disc at varying velocity and initial mean P_{Hertz} of 512 MPa (3N); k_w based upon wear track measurements.

Sliding velocity [m/s]	Specific wear rate, k_w [mm^3/N·m]	Coefficient of friction, f
0.1	$2.4 \cdot 10^{-7}$	0.6
0.15	$6.0 \cdot 10^{-7}$	0.6
0.2	$2.8 \cdot 10^{-7}$	0.6
0.3	$2.0 \cdot 10^{-6}$	0.6
0.4	$1.0 \cdot 10^{-4}$	0.8
0.5	$2.4 \cdot 10^{-4}$	0.8

An example of the development of the wear volume as a function of the sliding distance is given in Figure 3.2. It is clear that the wear volume increases linearly (except during a short initial period), meaning that the specific wear rate is constant during the test. For ADZ the same behaviour as for Y-TZP is found with respect to the development of the wear volume as a function of sliding distance.

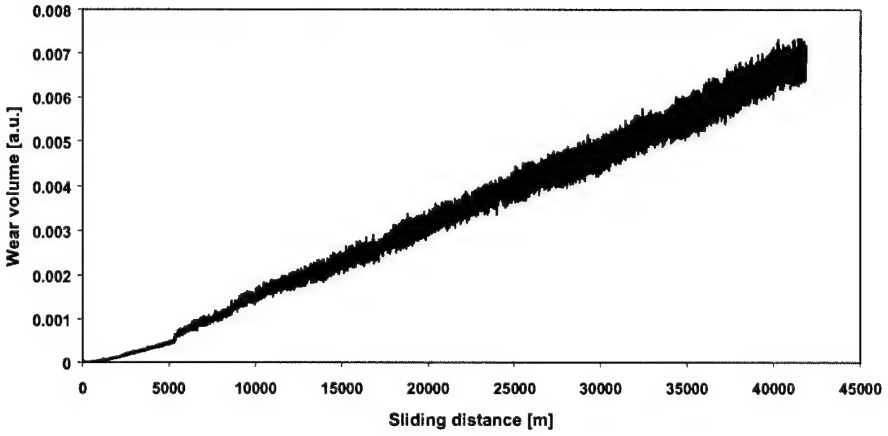

Figure 3.2: System wear measured for alumina ball against Y-TZP disc, wear volume was directly converted from height displacement; (F = 3 N, $P_{init,Hertz}$ = 512 MPa, v = 0.1 m/s, d_{Ball} = 10 mm).

At lower sliding velocities, the specific wear rates for ADZ are the same as for Y-TZP, but at higher velocities the specific wear rate is lower than for Y-TZP (Table 3.3). It can also be seen that for ADZ the coefficient of friction does not increase at higher sliding velocities.

Table 3.3: Specific wear rate and coefficient of friction for ADZ disc at with varying velocity and initial mean P_{Hertz} of 920 MPa (12N); k_w based upon wear track measurements.

Sliding velocity [m/s]	Specific wear rate, k_w [$mm^3/N{\cdot}m$]	Coefficient of friction, f
0.1	$3.8{\cdot}10^{-7}$	0.65
0.2	$1.6{\cdot}10^{-7}$	0.6
0.3	$3.1{\cdot}10^{-7}$	0.57
0.4	$4.8{\cdot}10^{-6}$	0.64
0.5	$2.6{\cdot}10^{-5}$	0.68

The positive influence of the alumina phase, besides the higher velocity before the limiting value of 10^{-6} $mm^3/(N{\cdot}m)$ is reached, can also be demonstrated when looking at tests per-

formed at a low sliding velocity (0.1 m/s) and increasing loads. At this velocity ADZ ceramics can be tested up to 1000 MPa (16 N) and show a specific wear rate of $1.3 \cdot 10^{-7}$ mm^3/(N·m). Y-TZP shows a specific wear rate that is already well above that value ($1.8 \cdot 10^{-6}$ mm^3/(N·m)) at even lower initial pressures of 800 MPa (12 N).

Alumina and ZTA

For alumina it is found (Table 3.4) that at 0.5 m/s the overall specific wear rate does not change significantly up to initial contact pressures of 1200 MPa (17.5 N). If tests are performed, however, at a given pressure and the velocity is varied, alumina shows, similar to Y-TZP and ADZ, a specific wear rate that increases with increasing velocity (Table 3.5). The coefficient of friction in all the experiments is about 0.5-0.6. No dependence on velocity and load was measured for *f*. Only at 17.5 N (0.5 m/s) and at 0.7 m/s (10N) *f* shows deviations.

Table 3.4: Specific wear rate and coefficient of friction for alumina disc at equal velocity of 0.5 m/s and varying loads (10 mm alumina balls); k_w based upon wear track measurements.

Mean contact pressure [MPa] (Load [N])	Specific wear rate, k_w [mm^3/N·m]	Coefficient of friction *f*
819 (5.5)	$2.5 \cdot 10^{-8}$	0.54
1000 (10)	$3.9 \cdot 10^{-8}$	0.55
1205 (17.5)	$3.9 \cdot 10^{-8}$	0.55-0.68

Table 3.5: Specific wear rate and coefficient of friction for alumina disc at equal load and varying velocity; k_w based upon wear track measurements.

Sliding velocity [m/s] $P_{Hertz,initial}$ 1000 MPa (10 N)	Specific wear rate, k_w [mm^3/N·m]	Coefficient of friction *f*
0.1	$<< 10^{-10}$	0.55
0.3	$1.9 \cdot 10^{-9}$	0.58
0.5	$3.9 \cdot 10^{-8}$	0.55
0.7	$6.5 \cdot 10^{-7}$	0.65

Figure 3.3, in which the on-line measurement of the wear volume at 1000 MPa (10 N) and 0.5 m/s is given, shows that after about 90 km of sliding distance a sudden increase of wear volume occurs. In the initial stage the wear volume increases very slowly, but after a certain sliding distance, suddenly a lot of wear takes place. After this short period of increased specific wear rate, it decreases again, probably due to the considerable decrease in average contact pressure. Previous investigations [24,25] also showed such a transition to severe wear, followed by a decrease in specific wear rate due to the decreased contact pressure. This type of measurements indicates the added value of on-line wear monitoring with respect to the measurement of the overall specific wear rate, k_w. Stopping this test

before 90 km would also mean that hardly any wear is measured, but in fact the system had not reached a steady state at that point.

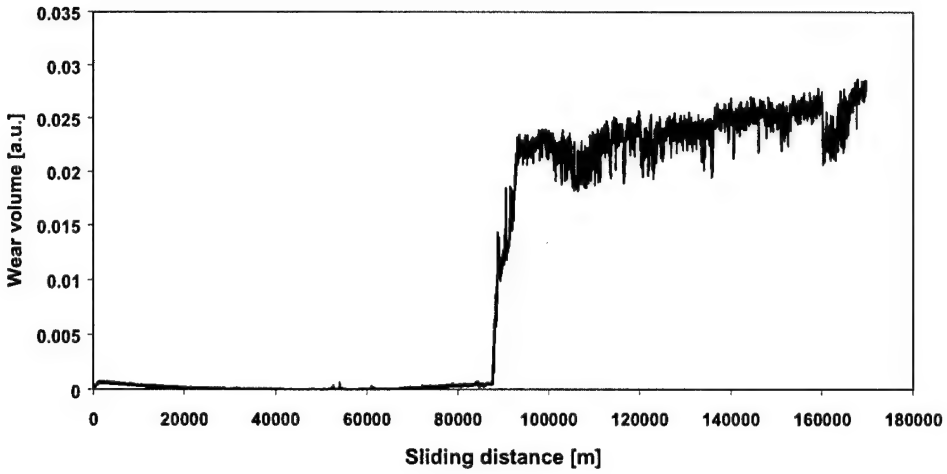

Figure 3.3: System wear measured for alumina ball against alumina disc, wear volume was directly converted from height displacement; (F = 10 N, $P_{init,Hertz}$ = 1000 MPa, v = 0.5 m/s, d_{Ball} = 10 mm).

Measurements on ZTA were performed to see the influence of the addition of zirconia to an alumina matrix. Previous work [10] showed that ZTA ceramics could withstand a high contact pressure and still have a good wear resistance. ZTA ceramics were all tested at 0.5 m/s and varying loads.

Table 3.6: Specific wear rate and coefficient of friction for ZTA disc at sliding velocity of 0.5 m/s and varying loads (6 mm alumina balls); k_w based upon wear track measurements.

Mean contact pressure [MPa] (Load [N])	Specific wear rate, k_w [$mm^3/N{\cdot}m$]	Coefficient of friction f
1175 (6)	$4.5{\cdot}10^{-8}$	0.46
1393 (10)	$1.7{\cdot}10^{-9}$	0.43
1480 (12)	$7.8{\cdot}10^{-8}$	0.45
1594 (15)	$2.3{\cdot}10^{-7}$	0.48

From Table 3.6 it can be seen that even at initial pressures up to 1600 MPa the specific wear rate is still below 10^{-6} $mm^3/(N{\cdot}m)$. The average coefficient of friction is 0.45 for all tests up to 15 N. For all dry sliding experiments, on the various ceramic materials against alumina as counter material, this is the lowest coefficient of friction that was measured. If the on-line wear measurements are examined (Figure 3.4), it is found that at an initial mean contact pressure of 920 MPa (8 N), the specific wear rate does not show any significant changes.

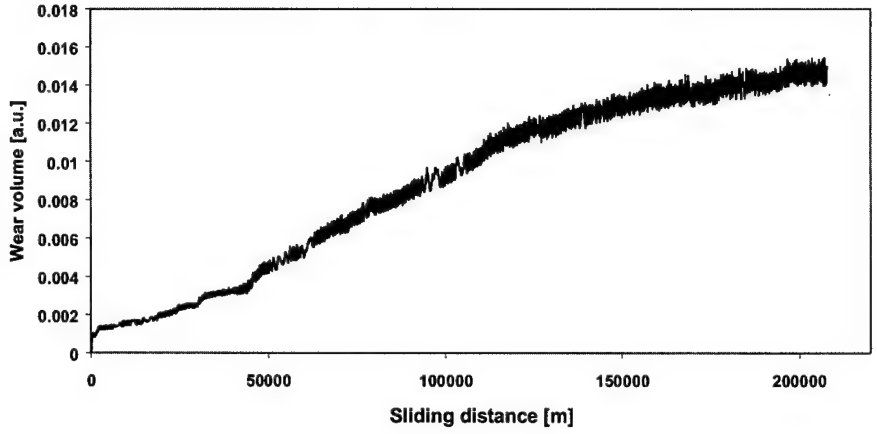

Figure 3.4: System wear measured for alumina ball against ZTA disc, wear volume was directly converted from height displacement; (F = 8 N, $P_{init,Hertz}$ = 920 MPa, v = 0.5 m/s, d_{Ball} = 10 mm).

The wear volume increases slowly, but not linearly. This indicates that the specific wear rate is not totally constant over the test period. Looking at a similar measurement at 1150 MPa (15.5 N), it is found that a sudden increase in wear takes place after about 15 km of sliding distance (Figure 3.5). Such a sudden failure was measured for alumina as well, where the increase occurred after 90 km. The sudden failure indicates that the failure of the alumina ball determines the behaviour of the tribological system. As for alumina, the specific wear rate for ZTA after the short failure period is small.

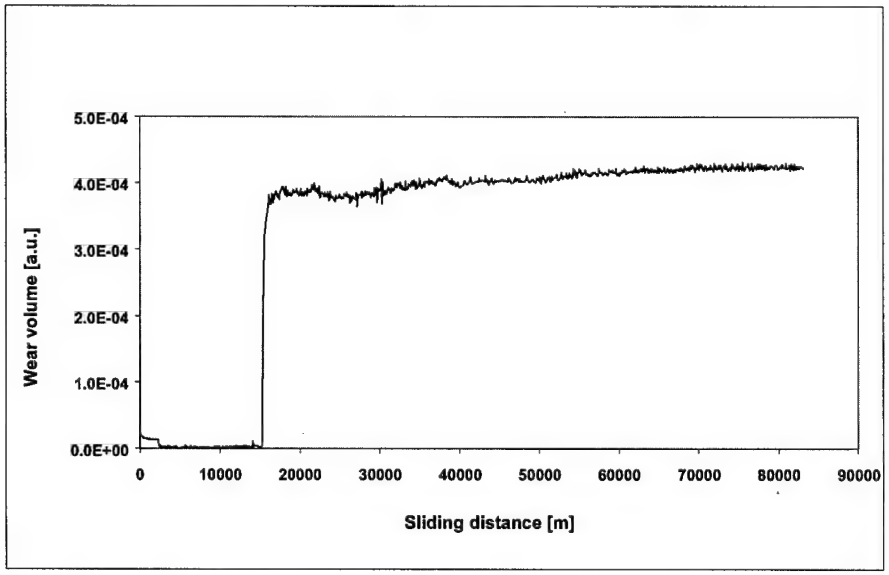

Figure 3.5: System wear measured for alumina ball against ZTA disc, wear volume was directly converted from height displacement; (F = 15.5 N, $P_{init,Hertz}$ = 1150 MPa, v = 0.5 m/s, d_{Ball} = 10 mm).

3.3.2 Wear mechanisms

SEM analysis of the wear tracks of Y-TZP shows that, when testing at 0.5 m/s and 512 MPa (3 N), wear takes place by abrasion, severe micro-fracture and grain pull-out (an extremely grooved wear track is found at low magnifications, not included). Figure 3.6a shows a detail of such a grooved part from the wear track where smeared-out wear debris is found as well. The amount of grooves caused by abrasion is decreasing at lower sliding velocities, resulting in a decreased specific wear rate. Wear most frequently takes place by fracture and grain pull-out. However, after testing at low sliding velocities it is found that a part of the wear track consists of grooves (formed by abrasion by the pin surface) and deposited wear debris at the edges of the track (Figure 3.6b).

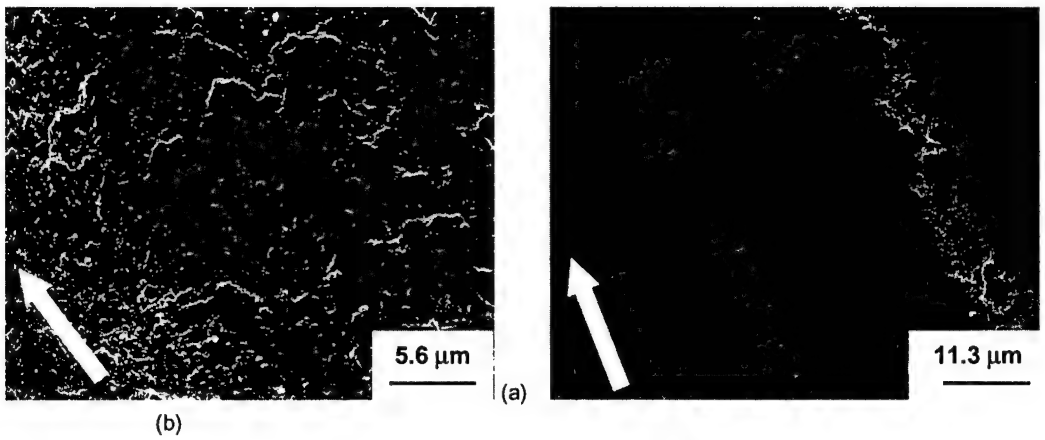

Figure 3.6: Wear track of Y-TZP after sliding against alumina at 512 MPa (3 N; 10 mm ball); (a) v = 0.5 m/s (b) v = 0.1 m/s (arrow indicates relative movement of ball over disc).

For ADZ materials, it is found that in principle the same wear mechanisms as for Y-TZP take place. Here too it is found that at low sliding velocities, part of the wear tracks consist of grooves (formed by abrasion by the pin surface) and polished parts (Figure 3.7).

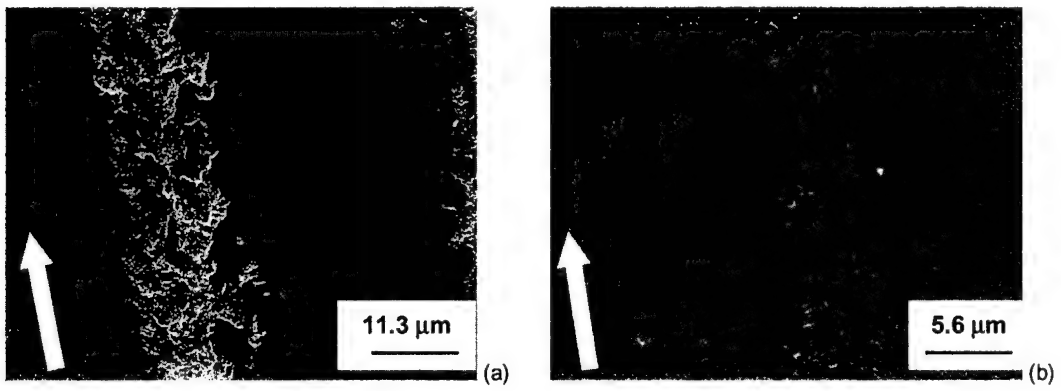

Figure 3.7: Wear track of ADZ after sliding against alumina at 900 MPa (12 N; 10 mm ball); (a) v = 0.5 m/s (b) v = 0.1 m/s (arrow indicates relative movement of ball over disc).

For alumina a grooved pattern is found as well. Analysis of the wear tracks with interference microscopy shows that the grooves in the track are less deep than in ADZ. Analysis of the grooves reveals that wear takes place mainly by grain pull-out (Figure 3.8a) and abrasion (Figure 3.8b).

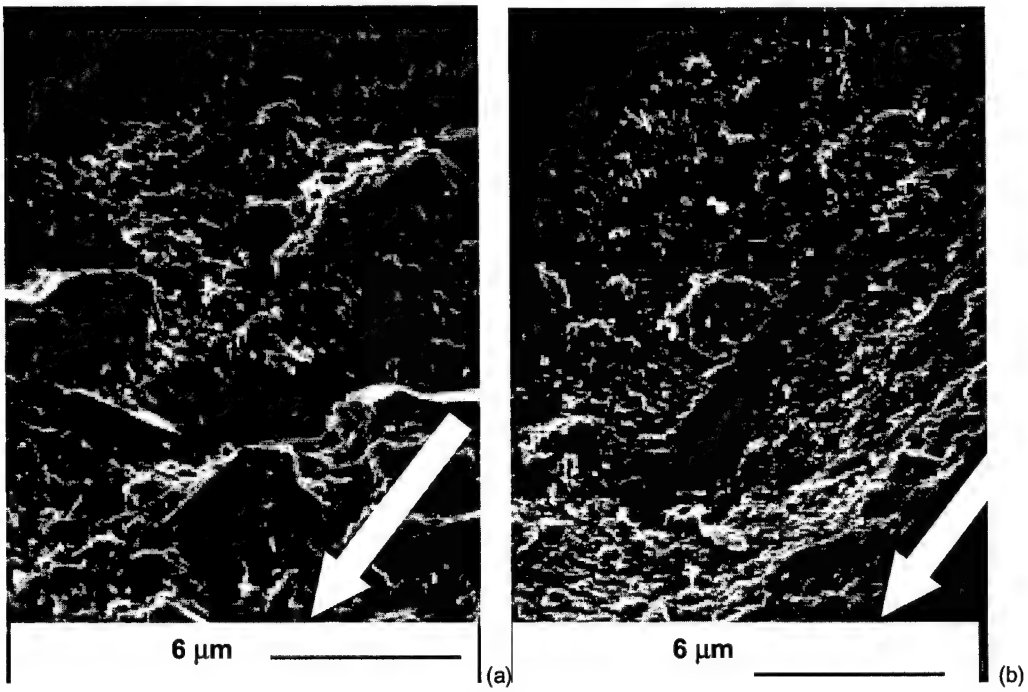

Figure 3.8: Wear track of AKP50-alumina after sliding against alumina at 1000 MPa (10N, 10 mm ball); (a) detail next to groove (b) detail inside groove (arrow indicates relative movement of ball over disc).

SEM pictures of wear tracks of ZTA, from tests performed at 0.5 m/s, show the same grooved patterns, caused by abrasion of the asperities on the ball wear scar (Figure 3.9a). A detail of such a groove, where smeared-out wear debris can be found inside these grooves is given in Figure 3.9b. In more detail, polished parts were found next to these grooves in Figure 3.9c.

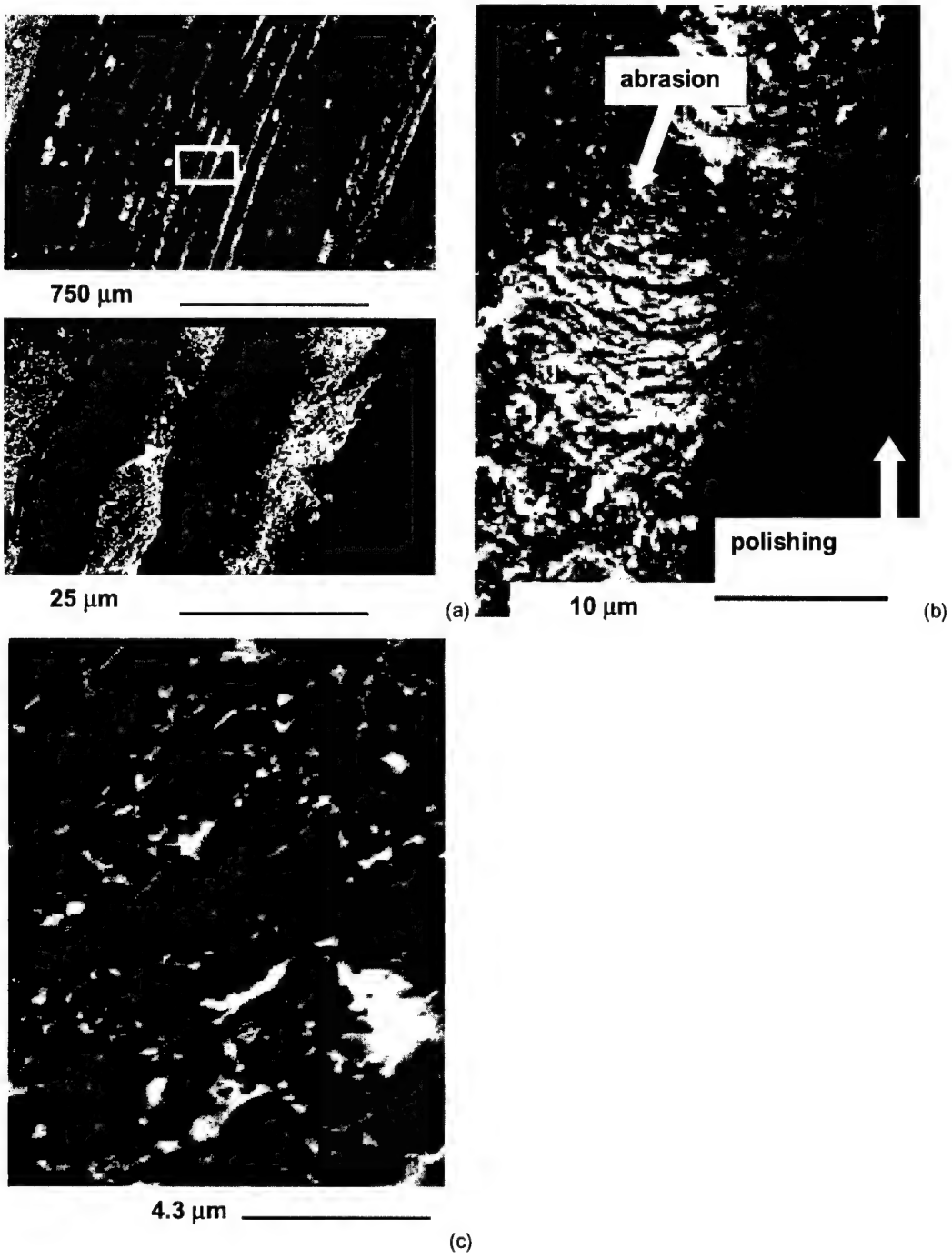

Figure 3.9: Wear track of ZTA after sliding against alumina at 1150 MPa (15.5 N, 10 mm ball); (a) double overview of wear track, showing the grooved pattern formed by abrasion by the ball (b) detail of grooved pattern from abrasion, showing smeared out debris in the groove (arrow indicating abrasion shows relative movement of ball over disc indicates sliding direction) (c) detail of polished surface next to groove.

3.4 Discussion

3.4.1 Y-TZP

The sliding velocity is a very critical parameter for the wear behaviour of Y-TZP. Above sliding velocities of 0.2 m/s wear becomes severe. As suggested before, this is related to the low thermal conductivity of Y-TZP ceramics and wear is dominated by thermally induced micro-cracking. Metselaar *et al.* [22] use a model in which these well-known thermally induced fracture processes by means of mechanical and thermal severity of the contact are described. They use this thermal severity to predict in what regime (velocity, load) wear will become severe. The sliding velocity in combination with the thermal conductivity mainly influences this thermal severity.

At low sliding velocities the load can be increased, but it also has a limit (contact pressures up to 700 MPa), which is related to micro-cracking due to mechanical stresses [18]. The final density (94%) of the material is not the most important limiting property, because tests on commercially available, 100% dense, Y-TZP ceramics (not included in this chapter) show the same limitations.

3.4.2 ADZ

Compared to Y-TZP, ADZ has a specific wear rate that is approximately a factor 10 lower. However, at high velocities both ceramics suffer from thermally induced micro-cracking, because of their relatively bad thermal properties (ADZ has zirconia as main phase). The real difference is found at lower velocities and increased load. ADZ can take higher loads, showing that the thermally induced processes are less dominant at lower velocities. Above a certain velocity, these thermally induced processes dominate the mechanical ones.

For ADZ the transition from mild to severe wear occurs at a higher sliding velocity (between 0.3 and 0.4 m/s). This transition also takes place at even higher contact pressures (920 MPa instead of 512 MPa for Y-TZP). Both the increased density (> 98% instead of 94%) and the presence of 20 wt% harder alumina play a role in this improved wear resistance. This influence is also described by He *et al.* [10]. It is unlikely that the presence of 20 wt% alumina in ADZ results in an improved thermal conductivity. The amount of alumina (app. 27 vol%) is not likely to result in a percolative system, when the second phase is homogeneously distributed. It is possible, however, that the alumina phase has some influence on the thermal properties of the surface, but this is very difficult to determine. Hence, the main effect of the improved hardness by the presence of the alumina must account for the improved tribological properties. This is also deduced from the occurring wear mechanisms. At 0.5 m/s, microstructural observations show no differences in wear mechanism between Y-TZP and ADZ. Wear takes place by severe abrasion and wear debris is smeared out in the contact. At lower velocities wear takes place by the same mechanisms but to a smaller extent. For ADZ the amount of abrasion is smaller than for Y-TZP. This means that the sliding velocity and the contact pressure do not influence the type of wear that takes place.

3.4.3 Alumina

For alumina a dependence on the sliding velocity is found as well, but wear remains in the mild regime at velocities up to 0.3-0.4 m/s. The main critical wear parameter is the load that can be used for the alumina pins. Table 3.4 shows that no apparent changes in specific wear rate are found with increasing load. From on-line measurements it is found that in the initial stage of the wear test very little wear is found and most of the wear takes place in a very short period of sliding (Figure 3.3). This may be explained by failure of the alumina balls that are used, since ball wear determines 95% of the height displacement that is measured. The phenomena found for alumina are not new [24,25], but they are necessary to show in relation with the results found for the composite (ZTA).

3.4.4 ZTA

The same failure effect for the alumina ball, which was also found in tests against alumina, is found for testing alumina against a ZTA disc. ZTA has a lower specific wear rate than alumina, even at higher initial mean contact pressures. Looking at wear mechanisms it is found that the grooved pattern is also found for alumina and ZTA and again, depending on the load, the morphology of the surface of the pin is the main cause for the abrasion that is found in the wear tracks. The main difference between alumina and ZTA is that the parts of the surface besides the grooves suffer less from wear for ZTA (polishing) than for alumina (fracture).

Wear for the alumina-alumina couple is very low, but failure of the pins and non-linear wear behaviour are found at more severe test conditions. The ZTA ceramics show extremely low specific wear rate, because the disc material has a very fine, homogeneous microstructure due to the colloidal filtration process used. It is reported by Kerkwijk *et al.* [16] that the improved microstructure of such a composite ceramic (compared to a commercially available composite) improves the wear resistance by two orders of magnitude. Besides this, the toughening character of the zirconia phase contributes to the occurrence of polishing rather than fracture for ZTA [10].

3.5 Conclusions

The addition of a second phase to either a zirconia or an alumina matrix improves the tribological properties. For Y-TZP ceramics, the addition of 20 wt% (app. 27 vol%) alumina results in the possibility of applying the ADZ-ceramic can be applied at higher velocities and contact pressures. Thermally induced fracture processes are not prevented by the presence of alumina, since the second phase does not create a percolative system.

Alumina shows low specific wear rates at all test conditions. However, the specific wear rate does increase significantly with increasing sliding velocity. The load dependence (i.e., the sudden change in wear rate for a short period of time) is not necessarily accounted for in the overall specific wear rate (average value for entire test length). On-line wear measurements show that after a short period of severe failure of the ball, the low specific wear rate is achieved again.

The addition of alumina as second phase decreases the load dependence of Y-TZP. The material can be tested at higher contact pressures and also higher velocities before transition to severe wear takes place. The addition of zirconia as second phase improves the wear resistance in all cases. Moreover, the materials can still be tested up to initial contact pressures of 1600 MPa, without showing significant wear. In this case, the overall specific wear rate of the ZTA discs is still below the limiting value of 10^{-6} $mm^3/(N \cdot m)$.

3.6 References

1. N.B. Thomsen, B.L. Karihaloo, *J. Am. Ceram. Soc.*, 78 (1995) 3.
2. Y.M. Chen, B. Rigaut, F. Armanet, *J. Eur. Ceram. Soc.*, 6 (1990) 383.
3. G.W. Stachowiak, G.B. Stachowiak, *Wear*, 143 (1991) 277.
4. M. Woydt, J. Kadoori, K.-H. Habig, H. Hausner, *J. Eur. Ceram. Soc.*, 7 (1991) 135.
5. R.W. Davidge, F.L. Riley, *Wear*, 186-187 (1995) 45.
6. H. Liu, Q. Xue, *Trib. Trans.*, 40 (1997) 627.
7. A. Krell, *Mater. Sci. Eng.*, A209 (1996) 156.
8. K.-H. Zum Gahr, W. Bundschuh, B. Zimmerlin, *Wear*, 162-164 (1993) 269.
9. T. Senda, J. Drennan, R. McPherson, *J. Am. Ceram. Soc.*, 78 (1995) 3018.
10. Y.J. He, A.J.A. Winnubst, D.J. Schipper, A.J. Burggraaf, H. Verweij, *Wear*, 210 (1997) 178.
11. Y.S. Wang, C. He, B.J. Hockey, P.I. Lacey, S.M. Hsu, *Wear*, 181-183 (1995) 156.
12. T.A. Libsch, P.C. Becker, S.K. Rhee, *Wear*, 110 (1986) 263.
13. A. Ravikiran, G.R. Subbanna, B.N. Pramila Bai, *Wear*, 192 (1996) 56.
14. L. Esposito, R. Moreno, A.J. Sanchez Herencia, A. Tucci, *J. Eur. Ceram. Soc.*, 18 (1998) 15.
15. V. Sergo, V. Lughi, G. Pezzotti, E. Lucchini, S. Meriani, M. Muraki, G. Katagiri, S. Lo Casto, T. Nishida, *Wear*, 214 (1998) 264.
16. B. Kerkwijk, A.J.A. Winnubst, E.J. Mulder, H. Verweij, *J. Am. Ceram. Soc.*, accepted for publication, (1999).
17. H. Czichos, D. Klaffke, E. Santner, M. Woydt, *Wear*, 190 (1995) 155.
18. K.Adachi, K.Kato, N.Chen, *Wear* 203-204 (1997) 291.
19. M.G. Gee., C.S. Matharu, *Int. J. High. Tech. Cer.*, 4 (1988) 319.
20. M. Woydt, K-H. Habig, *Trib. Int.*, 22 (1989) 75.
21. H.E. Sliney, C. Dellacorte, *Lubr. Eng.*, 47 (1991) 314.
22. H.S.C. Metselaar, A.J.A. Winnubst, D.J. Schipper, Proceedings of AUSTRIB 98, Brisbane, Australia, (1998) 185.
23. S.W. Lee, S.M. Hsu, M.C. Shen, *J. Am. Ceram. Soc.*, 76 (1993) 1937.
24. Y.S. Wang, S.M. Hsu, R.G. Munro, *Lubr. Eng.*, 47 (1991) 63.
25. X. Dong, S. Jahanmir, S.M. Hsu, *J. Am. Ceram. Soc.*, 74 (1991) 1036.

4 Dry sliding wear of self-mated couples of zirconia, alumina and zirconia-alumina composites*

Abstract

Homogeneously structured, dense and fine-grained ceramic composites consisting of 11 vol% ZrO_2 and 89 vol% α-alumina were prepared by controlled packing of colloidal particles followed by sintering. These zirconia-toughened alumina (ZTA) ceramics show an improvement in wear resistance of >3 orders of magnitude under the most severe testing conditions compared to less homogeneous ZTA (prepared by conventional processing of commercial powders). Dry sliding wear tests with self-mating couples at contact pressures up to 1.7 GPa revealed low coefficients of friction (0.43), while wear only occurred by polishing. The composite ceramics also show superior tribological behaviour compared to α-alumina and yttria-stabilised zirconia.

4.1 Introduction

Wear and friction at sliding contacts in moving parts are often minimised by the use of lubricants. The use of these lubricants is undesirable for environmental and maintenance reasons. This causes an increased interest in the development of materials with stable sliding contacts under unlubricated conditions. Hence, the development of engineering ceramics has received a lot of attention in research over the last 20 years. In most of this work, a specific test set-up (with typical conditions) or a specific material combination is chosen to characterise the tribological conditions of the developed materials. This usually results in a judgement on the tribological behaviour over a limited range of parameters. If many studies like these are combined, one can usually find some kind of application limit as function of system properties like load and sliding velocity or properties of the materials used, like hardness, strength or corrosion resistance. These limitations are usually characterised by a transition from mild to severe wear in the investigated ceramics, i.e. the onset of this transition imposes the practical limit for use of the material.

Normally, severe wear is caused by local contact-surface roughening from the break-out of pieces of material and is affected by:

- Microstructural inhomogeneities,
- The presence of a high surface roughness,
- The presence of third body particles,
- A low intrinsic material toughness,
- The occurrence of local "flash heating" at microscopic contact points [1], and

* Taken from: B. Kerkwijk, E.J. Mulder, H. Verweij, accepted for publication, *Adv. Eng. Mater.*, 1999.

- Transfer of material from one surface to the other if the materials show some (chemical or physical) affinity with each other.

If the contacting materials of wear-resistant dry sliding couples only polish each other, this may result in low specific wear rates (mild wear) and possibly low coefficients of friction. Most probably, the use of inert [2], hard and preferably tough [3] ceramic materials with a high thermal conductivity [4] is the only option for unlubricated sliding contacts, especially when load and sliding speed are high.

The choice for suitable and cheap single-phase materials becomes limited to dense α-Al_2O_3 ceramics. Alumina is relatively inert in normal atmospheres, non-toxic, hard, cheap to produce and it has a high thermal conductivity. However, most state-of-the-art alumina ceramics have a poor homogeneity with respect to grain size and a low toughness.

The poor homogeneity of most state-of-the-art alumina materials is connected with the high temperatures needed for sintering of particle compacts. This results in growth of alumina grains to a size much larger than 1 µm [5] during sintering together with the occurrence of anomalous grain growth. The physical properties of the hexagonal α-Al_2O_3 grains are anisotropic, meaning that hardness and stress across the ceramic microstructure vary from grain to grain.

Hence, a promising strategy for developing highly wear-resistant materials is to obtain a fine-grained, homogeneous α-Al_2O_3 matrix phase with a tough zirconia (ZrO_2) second phase, so called "zirconia-toughened alumina" (ZTA) [3,6-8]. The role of the insoluble ZrO_2 is to increase toughness [6-8] and to avoid the development of a coarse and, hence, inhomogeneous microstructure of the alumina phase [9] during sintering. On the other hand, the presence of the connected α-Al_2O_3 phase in ZTA makes certain that the favourable hardness and thermal conductivity of pure α-Al_2O_3 are maintained. The ZrO_2 phase itself is known as a tough engineering ceramic in its tetragonal stabilised phase.

At present, few ZTA composites are commercially available. These composites are usually processed by conventional methods, such as dry pressing. They show a poor microstructural homogeneity, particularly with respect to grain size and the dispersion of the second phase (ZrO_2). In order to obtain the finest grain size in combination with a microstructure that is as homogeneous as possible, a ceramic processing route must be selected that starts with a colloidal suspension and consolidation process. In the colloidal consolidation process, nanoscale particles with an isometric shape and a relatively narrow particle size distribution are random-close-packed to compacts. This process is then followed by sintering at high temperatures to a dense microstructure [10].

Since engineering ceramics are to be applied in a wide variety of operating conditions, it is necessary to test these materials under extreme tribological conditions. This means that tests have to be performed not only under unlubricated conditions with a high velocity and load. The materials combination in a system influences the severity of the tribological conditions as well. In a so-called "self-mated" test, only one specific material is tested. Generally dry sliding contacts of identical materials lead to high specific wear rates and coefficients of friction [11-18]. This is ascribed to the occurrence of naturally strong cohesion forces between similar materials. This chapter describes the unlubricated self-mated

wear behaviour of ZTA composite ceramics under high loads and at high sliding velocities. Their behaviour is compared to that of the singe-phase engineering ceramics Y-TZP and α-alumina that are the basic constituents of the composite ceramic. Furthermore, commercially available ZTA ceramics are used as well.

4.2 Experimental

Al_2O_3 ceramics were made by dry pressing and sintering of a commercially available α-Al_2O_3 powder (AKP-50, Sumitomo Chemical Co. Ltd, Osaka, Japan) with a BET-surface area of 11 m^2/g. These ceramics were sintered at 1500°C for 2 hours.

Y-TZP powder was made by co-precipitation of YCl_3 and $ZrCl_4$ in ammonia. The resulting powder was washed with water and ethanol and subsequently calcined at 500°C. The crystalline phase is tetragonal and the BET-surface area is 100 m^2/g. Details of this process can be found elsewhere [19]. After dry isostatic pressing, the material was sintered at 1150°C for 10 hours to obtain a dense material with the smallest possible grain size.

ZTA-CF was made by colloidal filtration from a mixed suspension in 0.05 M HNO_3 of AKP-50 (85 wt% of total solid phase) and undoped ZrO_2 (15 wt% of total solid phase). The ZrO_2 particles were made by the same precipitation process as used for Y-TZP. After consolidation, the green bodies were sintered to relative densities of >98% at 1400°C for 2 hours. This process is described in detail in another study [22]. Wear tests on similar ZTA composites prepared by conventional ceramic processing were performed, to study the influence of microstructural parameters such as homogeneity and grain size. Therefore, commercially available spray-dried ZTA-SD powder (Daichii, Zirconia Sales, Surrey, Great Britain) was used to prepare compacts by dry isostatic pressing. The compacts were sintered at 1575°C for 2 hours.

All sintered ceramics were cut into discs or machined to rounded pins. The diameter of the discs was about 36.5 mm and their thickness up to 4 mm. The pins were made at a length up to 10 mm with a one-end radius of curvature of 5.2 mm. The samples were polished to a final average surface roughness, R_a, of < 0.1 μm.

Wear and friction of the self-mating sliding couples were tested under extreme tribological conditions. This means high loads and high velocities were used and both contacts were made of the same material. Dry sliding wear tests were performed using a pin-on-disc tribometer [CSEM, Neuchatel, Switzerland] placed in a climate chamber at 23°C and 40% relative humidity. The sliding velocity was 0.1 m/s for Y-TZP and 0.5 m/s for the other two ceramics. These conditions were chosen such that a meaningful comparison between the various ceramics was possible, since using 0.5 m/s for Y-TZP would cause extremely severe wear processes solely by thermally induced fracture [20]. The applied load was varied up to 15 N for each specific test. This was done to find the limitation in practical use and to explore the wear transition load of the various ceramics. The given geometry and properties of the materials used allowed initial Hertzian contact pressures, $P_{Hertz,i}$, up to 1.7 GPa. In the wear tests the average specific wear rate, k_w, was determined by:

$$k_w = \frac{V_w}{F \cdot s}\left[\frac{\mathrm{mm}^3}{\mathrm{N \cdot m}}\right] \tag{4.1}$$

in which V_w is the measured wear volume, F the applied normal force and s the sliding distance. The wear volume was determined from either weight loss measurements or by means of surface height profiling of the wear track. Furthermore, overall wear was also monitored on-line by means of a nano-displacement sensor that was mounted at the back of the pin arm. The measured height difference from the laser is converted into a wear volume. The coefficient of friction, f, i.e. the ratio between the measured friction force and the applied normal force, and the wear volume were monitored on-line during the entire test.

4.3 Material properties

The properties of the tested materials are listed in Table 4.1. The grain size of both alumina and zirconia in the ZTA-CF ceramic are small (0.5 and 0.2 μm, respectively). The grain size of zirconia is similar to the grain size of normal Y-TZP ceramics, although the ZTA-CF is sintered at a higher temperature (1400°C compared to 1150°C for Y-TZP). The commercial ZTA ceramic has the largest grain size due to the high sintering temperature necessary to obtain full density. The most important mechanical properties are also listed in Table 4.1. Alumina and ZTA have a Vickers hardness that is significantly higher than that of Y-TZP. This difference should be reflected in the results from the self-mating wear tests.

Table 4.1: Properties of the four ceramics used in this study.

Material	Density [kg/m^3]	Grain size [μm]	Hardness [GPa]	E-modulus [GPa]	Strength[4] [MPa]	Fracture toughness[5] [MPa·√m]
Y-TZP	5700	0.18	13[1]	210[3]	570	8
Al_2O_3	3900	1.5	20[1]	400[3]	350	4.5
ZTA-CF	4200	A: 0.5; Z: 0.2	18[1]	380[3]	420	5.2
ZTA-SD	4200	A: 3.1; Z: 1.0	18[2]	380[2]	420	5.2

[1] Vickers hardness; [2] values from supplier; [3] [23]; [4] 4-point bending tests; [5] SENB-method.

4.4 Tribological characterisation

4.4.1 Specific wear rates

Table 4.2 shows the results for Y-TZP. The material always shows high wear in a self-mating set-up, even when the velocity is lowered to 0.1 m/s at moderate contact loads/pressures. We find that Y-TZP cannot be tested at velocities of 0.5 m/s and pressures more than 700 MPa, where wear is always severe due to thermally induced fracture processes [20,21]. At 0.1 m/s, the wear volume of Y-TZP appears to increase linearly with time, from which it may be concluded that no changes in wear mechanism can be found during the entire length of the test.

Table 4.2: Wear and friction of Y-TZP from self-mating tests under varying conditions.

	0.7 GPa; 0.5 m/s	0.8 GPa; 0.1 m/s
Wear rate disc, k_w [$mm^3/(N \cdot m)$]	Failure	$2.9 \cdot 10^{-5}$
Wear rate pin, k_w [$mm^3/(N \cdot m)$]	Failure	$3.1 \cdot 10^{-4}$
Coefficient of friction, f	0.8	0.8

Alumina has a low specific wear rate, even at high contact pressures (Table 4.3). The main disadvantage in the use of alumina is that the measurements with loads of 10 N (1 GPa) and higher show failure with increasing sliding distance. Even though the overall specific wear rates are still at an acceptable level, wear does not increase linearly in time. In principal this means that transition from mild to severe wear occurs repeatedly. For alumina, a constant increase of the wear volume was only found when the applied load was 10 N maximum. The average specific wear rate in this case was 10^{-9} $mm^3/(N \cdot m)$. Similar behaviour was found in a previous study where commercially availale alumina balls were used [21].

Table 4.3: Wear and friction of alumina from self-mating tests at 0.5 m/s at different initial Hertzian contact pressures.

	1.0 GPa	1.2 GPa
Wear rate disc, k_w [$mm^3/(N \cdot m)$]	$4.7 \cdot 10^{-8}$	$2.3 \cdot 10^{-8}$
Wear rate pin, k_w [$mm^3/(N \cdot m)$]	$1.6 \cdot 10^{-8}$	$3.0 \cdot 10^{-8}$
Coefficient of friction, f	0.55	0.55

Some results on self-mating ZTA couples are given in Table 4.4. Tests with commercial ZTA-SD gave irreproducible results, similar to those found for alumina. Wear remained mild in some tests at 1.3 GPa (app. 10^{-9} $mm^3/(N \cdot m)$, while during others severe wear ($>10^{-4}$ $mm^3/(N \cdot m)$) and catastrophic failure occurred. Tests performed at higher pressures (1.6 GPa) always revealed severe wear. Therefore, the material cannot be regarded as reliable under these tribological conditions.

Table 4.4: Wear and friction of ZTA ceramics from self-mating tests at 0.5 m/s.

	ZTA-CF (1.6 GPa)	ZTA-SD (1.3 GPa)	ZTA-SD (1.6 GPa)
Wear rate disc, k_w [$mm^3/(N \cdot m)$]	$2.0 \cdot 10^{-10}$	$\approx 10^{-9}$ if no failure	$>>10^{-4}$
Wear rate pin, k_w [$mm^3/(N \cdot m)$]	$2.0 \cdot 10^{-10}$	$\approx 10^{-9}$ if no failure	$>>10^{-4}$
Coefficient of friction, f	0.43	0.45 if no failure	---

Self-mated tests under the most extreme testing conditions for ZTA-CF made by colloidal filtration show the best wear resistance of all tested materials (Table 4.4). Even at an extremely high initial contact pressure of 1.6 GPa (12 N), ZTA-CF showed that wear is dominated by polishing. The coefficient of friction, f, is low (0.43), while the specific wear rate, k_w, of $2.0*10^{-10}$ $mm^3/(N \cdot m)$ is at least 3 orders of magnitude lower than previously reported literature values [11-17]. Even at 1.7 GPa (14 N) the material still has a specific wear rate as low as $6.3*10^{-10}$ $mm^3/(N \cdot m)$, while this contact pressure immediately resulted in severe wear for the other ceramic materials. Figure 4.1 shows a typical on-line measurement of the wear volume of ZTA-CF (at 1.3 GPa) using the nano-displacement sensor. The figure reveals a linear increase of the measured wear volume with distance and this indicates a constant specific wear rate. This also implies that there are no significant changes in the dominant wear mechanism. Particularly noteworthy is a sliding distance of 160 km (about 140 hours of testing), which is significantly higher than typically reported values of up to 40 km [11-17]. In fact, these large test lengths were needed to be able to detect any significant wear at all.

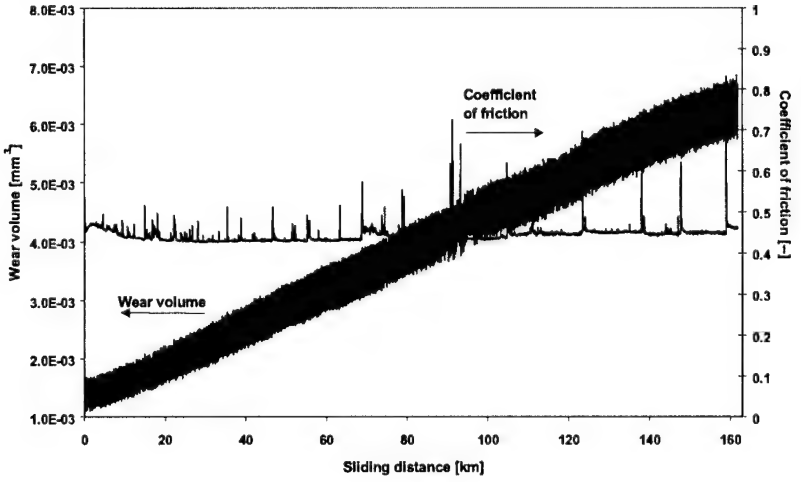

Figure 4.1: On-line analysis of the wear volume and coefficient of friction of the tribo-system measured for ZTA pin against ZTA disc made by colloidal filtration (Test conditions: F = 6 N, $P_{Hertz,i}$= 1.3 GPa, v = 0.5 m/s, $r_{curv.}$ = 5.2 mm, total sliding distance = 162 km).

4.4.2 Wear behaviour

Comparing the self-mating wear behaviour of the investigated ceramics, it is clear that ZTA-CF made by colloidal filtration is the material with superior tribological behaviour (both low specific wear rate and coefficient of friction). The ZTA-SD made from commercially available powder shows similar wear behaviour, but the application is limited to a maximum load that is lower than can be applied for ZTA-CF. Alumina also shows good wear behaviour, but here too, the load where transition from mild to severe wear occurs, is low. Compared to alumina and ZTA, Y-TZP has very poor wear behaviour. This is mainly related to both the relatively low hardness and low thermal conductivity. Even at low load and velocity, the material shows severe type wear processes, even though the specific wear rate is in the order of 10^{-7} $mm^3/(N \cdot m)$. The fact that a very bad wear behaviour is measured, stresses the importance of self-mating tests, since a previous study [21] on these Y-TZP ceramics against alumina balls showed that at low velocities and moderate pressures the material has an acceptable wear rate of app. 10^{-7} $mm^3/(N \cdot m)$. The differences in wear behaviour can be characterised by looking at the microstructural characterisation of the wear tracks.

Characterisation of the wear tracks for Y-TZP by means of SEM shows that severe fracture and smeared out wear debris are always found (Figure 4.2). The overview shows that after testing at 0.5 m/s, the edges of the track are really clear, since the surface inside the track is very rough compared to the polished surface. The pins are ploughing in the disc surface causing a lot of deformation, delamination and material removal besides creating a rough surface with a lot of smeared-out debris deposited inside the track.

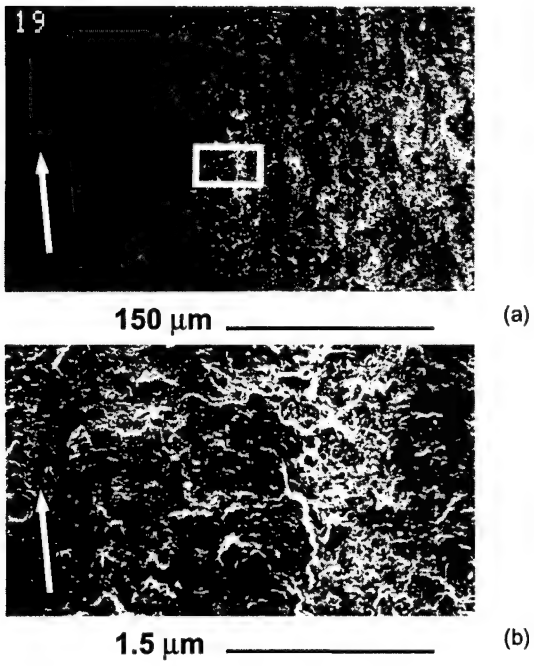

Figure 4.2: SEM micrographs of the wear track of Y-TZP disc after sliding at 0.5 m/s and 0.7 GPa (6 N) for 30 km; (a) overview of the edge of the wear track showing the differences between the polished and the worn surface, and (b) detail of the worn surface, where extreme smear-out of wear debris is found (arrow indicates sliding direction).

For alumina, typical wear tracks are found, showing wear by microfracture along grain boundaries of alumina. This is an indication of weak grain boundaries in the material. Characteristic features of failure behaviour are shown in Figure 4.3. In Figure 4.3a an overview is shown of the entire track just before failure. Part of the wear track shows a relatively smooth morphology, whereas in some parts grain pull-out (by micro-fracture) is visible. The edges of the wear track are not very clear. The picture was made after 78 km of sliding. A picture of the wear track after failure is shown Figure 4.3b, where the edges of the track are clearly visible. Here the wear track shows fracture (resulting in grooving) over the entire surface after 180 km of sliding. This grooving is caused by partial failure of both disc and pin. Here, no more roughening takes place, but direct material removal occurs by the rubbing of two rough surfaces. This also results in a much wider wear track (app. 850 μm instead of 200 μm).

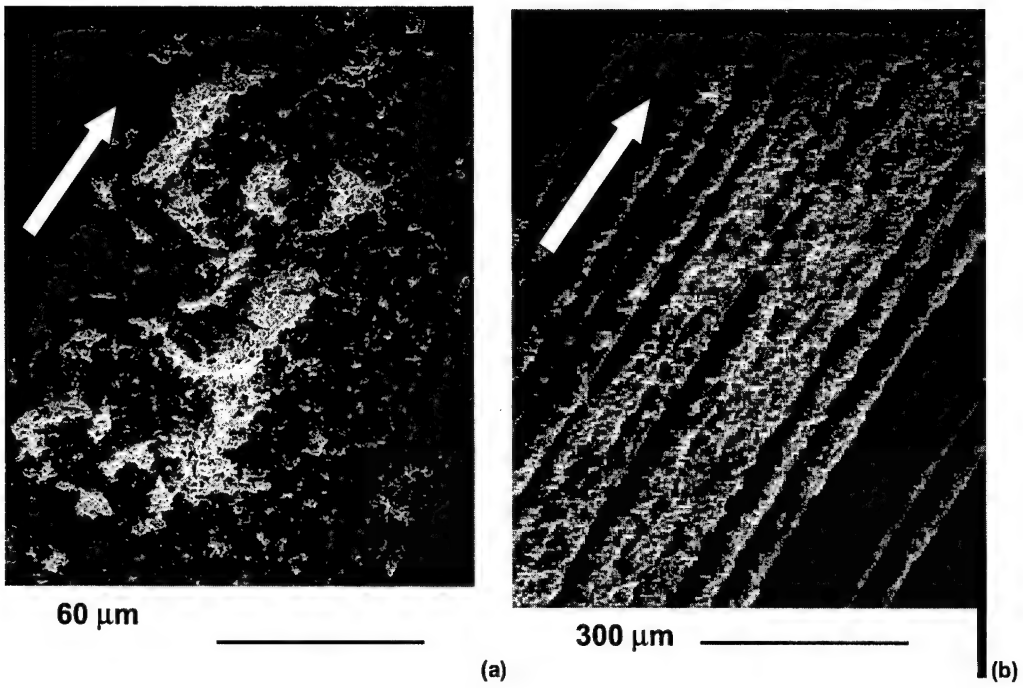

Figure 4.3: SEM micrographs of overviews of the wear tracks of alumina discs after sliding at 0.5 m/s and 1.0 GPa (10 N): (a) after 78 km of sliding just before failure, showing some material removal, and (b) after 180 km of sliding after failure, showing groove formation by partial failure of both ball and disc (arrow indicates sliding direction).

Microstructural investigations of the wear track of ZTA-CF (Figure 4.4) showed that wear solely occurs by polishing for all pressures. The wear track shows no features of ceramic wear, such as abrasion, grain pull-out or fracture. The mild wear track has a very smooth morphology; it even has a lower surface roughness than before testing. The detailed picture also shows the homogeneous phase dispersion of zirconia (white phase) in alumina (dark phase). Analysis by surface profiling also indicates a low surface roughness (Figure 4.5). The polishing scars in the wear track are partly removed after 160 km of sliding. A very shallow and smooth wear track of 80 nm depth is found with an average surface roughness, R_a, in the wear track of < 2 nm, in the sliding direction. This is very low, compared to the average surface roughness of the polished material (app. 10 nm). If the morphology of these tracks is compared to those for ZTA-SD, no real differences are found when wear is mild (polishing).

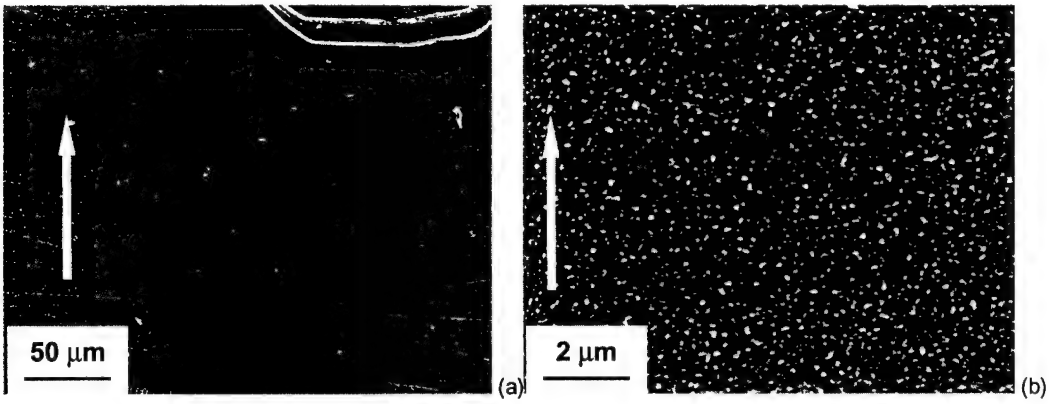

Figure 4.4: SEM micrographs of wear tracks of disc of ZTA-CF after sliding at 0.5 m/s and 1.3 GPa (6 N) for 162 km: (a) wear track overview, and (b) detail of the wear track, showing no features of typical ceramic wear processes (arrow indicates sliding direction). The detailed picture also gives an indication of the very homogeneous distribution of the zirconia (white) in the alumina (dark) created by colloidal filtration consolidation followed by sintering.

The main reason for the better wear resistance of the ZTA-CF composite compared to the commercially available ZTA-SD is found in the improved microstructural homogeneity for ZTA-CF (both the smaller grain size and the better dispersion of the second phase). This influence of homogeneity was also found for tests against alumina [22]. Both the smaller grain size and the more homogeneous dispersion of the second phase zirconia in the matrix phase alumina contribute to the improved wear behaviour. Compared to alumina, an improvement in wear resistance is found together with a lower coefficient of friction. Here too, the zirconia phase in ZTA acts a stabiliser of the microstructure of the alumina phase, since grain growth was inhibited. The presence of the second phase diminishes the amount of material removed by microfracture, as is typical for alumina. The coefficients of friction are the lowest for the ZTA ceramics. In this case, it must be directly related to the low wear, since no evidence is found that surface roughening takes place.

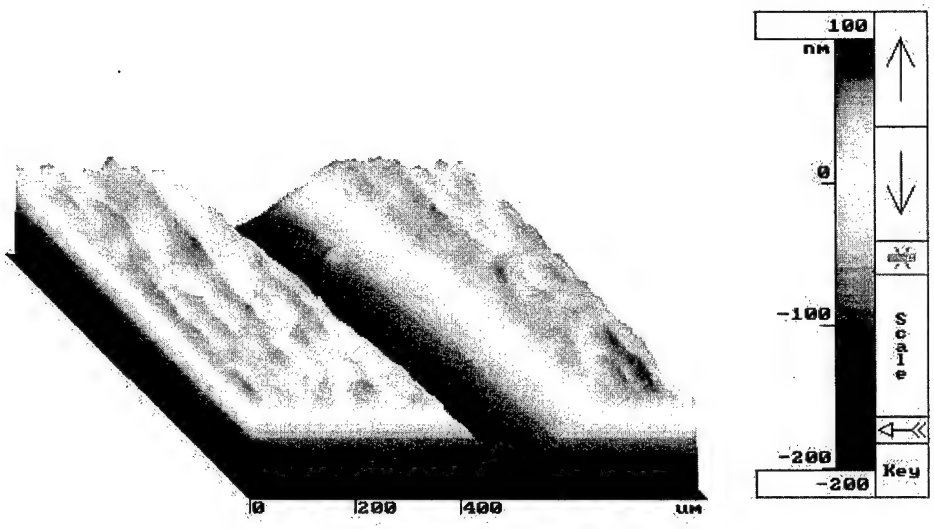

Figure 4.5: Wear track roughness mapping of ZTA by colloidal filtration; the track depth is only about 80 nm (note that the height axis is extremely enlarged!!!). (Test conditions: $F = 6$ N, $P_{Hertz,i} = 1.3$ GPa, $v = 0.5$ m/s, $r_{curv.} = 5.2$ mm, total sliding distance = 162 km). The pictures were made using interferometric surface height profiling (ATOS micromap, Pfungstadt, Germany).

4.5 Conclusions

The results from this study show that ZTA ceramics have a self-mating, dry sliding specific wear rate of $6.3 \cdot 10^{-10}$ mm^3/(N·m) under extreme pressures (1.7 GPa, 14 N). This is significantly lower than values reported so far in literature [11-18]. Self-mating tests with Y-TZP and Al_2O_3 show that Y-TZP has an extremely high wear rate and Al_2O_3 has similar wear behaviour as found for ZTA. However, alumina has more limitations in practical use, since the maximum applicable load before a wear transition occurs is lower than for ZTA composite ceramics. From these results it is found that ZTA is extremely wear-resistant, keeping in mind the generally noted upper limit of acceptable wear-rates: $k_w = 10^{-6}$ mm^3/(N·m) [15,18]. Wear occurs mainly by polishing, giving a strong indication that cohesion does not play an important role for the ZTA materials. This finding further supports the use of homogeneous and fine-grained ceramic materials to extend the lifetime of dry-sliding contacts in moving equipment parts.

4.6 References

1. R. Holm, *J. Appl. Phys.*, 19 (1948) 361.

2. S. Lawson, *J. Eur. Ceram. Soc.*, 15 (1995) 485.
3. C. He, Y.S. Wang, J.S. Wallace, S.M. Hsu, *Wear*, 162-164 (1993) 314.
4. J.D. Sibold, Engineered Materials Handbook, Vol. 4. Ceramics and glasses, (1991), 973.
5. S.J. Bennison and M.P. Harmer, *Ceram. Powders*, (1983), 929.
6. Y.J. He, A.J.A. Winnubst, D.J. Schipper, P.M.V. Bakker, A.J. Burggraaf, H. Verweij, *Wear*, 184 (1995) 33.
7. K.J. Konsztowicz and R. Langlois, *J. Mater. Sci.*, 31 (1996) 1633.
8. R. Trabelsi, D. Treheux, G. Orange, G. Fantozzi, P. Homerin, F. Thevenot, *Trib. Trans.*, 32 (1989) 77.
9. F.F. Lange and M.M. Hirlinger, *J. Am. Ceram. Soc.*, 67 (1984) 164.
10. F.F. Lange and K.T. Miller, *Am. Ceram. Soc. Bull.*, 66 (1987) 1498.
11. A. Krell, *Mater. Sci. Eng. A*, A209 (1996) 156.
12. K.-H. Zum Gahr, W. Bundschuh, B. Zimmerlin, *Wear*, 162-164 (1993) 269.
13. M. Woydt, J. Kadoori, K.-H. Habig, H. Hausner, *J. Eur. Ceram. Soc.*, 7 (1991) 135.
14. L. Esposito, R. Moreno, A.J. Sanchez Herencia, A. Tucci, *J. Eur. Ceram. Soc.*, 18 (1998) 15.
15. H. Czichos, D. Klaffke, E. Santner, M. Woydt, *Wear*, 190 (1995) 155.
16. S.B. Krefetz and T.E. Fischer, *Wear*, 211 (1997) 141.
17. M. Terheci, *Wear*, 211 (1997) 289.
18. K.Adachi, K.Kato, N.Chen, *Wear*, 203-204 (1997) 291.
19. W.F.M. Groot Zevert, A.J.A. Winnubst, G.S.A.M. Theunissen and A.J. Burggraaf, *J. Mater. Sci.*, 25 (1990) 3449.
20. H.S.C. Metselaar, A.J.A. Winnubst, D.J. Schipper, *Wear*, 225-229 (1999) 857.
21. B. Kerkwijk, A.J.A. Winnubst, H. Verweij, H.S.C. Metselaar, E.J. Mulder and D.J. Schipper, *Wear*, 225-229 (1999) 1293.
22. B. Kerkwijk, A.J.A. Winnubst, E.J. Mulder and H. Verweij, *J. Am. Ceram. Soc.*, accepted for publication, (1999).
23. Y.J. He, "Tribological and mechanical properties of fine-grained zirconia and zirconia-alumina ceramics", Ph. D. thesis, University of Twente (1995), ISBN 90-9008624-2.

5 Wear of ceramics due to thermal stresses: a new thermal severity parameter*

Abstract

The objective of this study is to introduce a wear map of ceramics which shows the different regimes of dominant wear modes observed for a wide range of material properties and operational conditions. Furthermore, from the wear map, common demanding conditions for the application of various ceramics as wear-resistant materials in a wide range of operational conditions are discussed. For this purpose, friction and wear tests are carried out using two types of tetragonal zirconia discs sliding against various pin materials under various contact pressures and sliding velocities. Sliding wear phenomena of ceramics observed in all tests can be classified into two types: "mild wear" and "severe wear". If the specific wear rate exceeds the value of $3 \cdot 10^{-6}$ $mm^3/(N \cdot m)$, wear is indicated as "severe". This criterion is closely related to the criterion based on the ratio of process surface roughness over mean grain size as described by Adachi *et al.* [1]. The mild wear region is supposed to be necessary for the application of ceramics as wear-resistant materials. The critical condition for transition from mild to severe wear is analysed with an intergranular fracture model from the view points of both mechanical and thermal aspects. A wear map of ceramics, in which the regimes of mild and severe wear can be distinguished, is introduced using two dimensionless parameters, namely an existing mechanical severity of contact (*MS*) and a newly developed thermal severity of contact (*TS*). The availability of the wear map constructed by this method is proven by the experimental results observed for a wide range of test material properties and operational conditions.

5.1 Introduction

Advanced ceramics are promising wear-resistant engineering materials because of their high hardness and chemical inertness as compared to the widely used engineering materials such as metals and polymers. In fact, their superior wear resistance over metals in the mild wear regime has been proven in many applications [2,3]. However, transitions to the unfavourable severe wear regime are frequently reported to be dependent on operational conditions and test-material characteristics such as, for example, normal load [4], sliding velocity [5], temperature [6], sliding distance [7], porosity and grain size [8] and microstructural homogeneity [9].

In order to apply advanced ceramics as wear-resistant engineering materials, it is essential to be able to predict the transition from mild to severe wear. The tribological reliability of ceramics will be determined by this necessary condition.

---

* H.S.C. Metselaar, B. Kerkwijk, E.J. Mulder, H. Verweij, D.J. Schipper, submitted for publication, 1999.

On the other hand, the concept of wear mapping has been popular in tribology, see e.g. [10]. A wear map can be considered as one of the better methods to c larify comprehensively the common demanding conditions for tribological use of various materials under the wide range of operational conditions. Wear maps can be classified into two types, based on the dimensions of parameters used along the axes.

The first type is a wear map using experimental parameters along the axes, such as no rmal load, sliding velocity, temperature, sliding distance, etc. The "wear map" [11], the "tribomapping" technique [12], the "wear transition diagram" [13,14] and the "wear mode diagram" [15] belong to this first type of wear map. These wear maps are uses systematic methods for understanding the height of wear rate and the effects of operational conditions on tribological performance of a given material. However, because of the different mechanical and thermal properties of different materials, these wear maps are only valid for a specific materials combination, necessitating a wear map for each material combination of interest.

In contrast, a second type of wear map uses dimensionless parameters along the axes. The "wear-mechanism map" [10], "flow regime map" [16], "deformation map" [17] and "abrasive wear mode diagram" [18] have been proposed for widely used materials such as metals and polymers. These maps using dimensionless parameters are useful for a unified understanding of wear phenomena obtained under a wide range of operational conditions. In particular, in the case of a wear map [1] using dimensionless parameters which dominate wear modes, it is possible to give the unified critical condition(s) for each wear mode caused by individual factors such as material properties and operational conditions. Furthermore, these kinds of wear maps can provide guides for improving wear resistance, because the generation of each wear mode can be correlated with dimensionless parameters which include material properties and operating parameters.

In the case of ceramics, four kinds of wear maps have been proposed using dimensionless parameters. The "wear-mechanism map" proposed by Kong and Ashby [19] showed characteristic wear transition boundaries of seven kinds of wear modes of alumina using normalised pressure and normalised velocity as proposed by Lim and Ashby [10]. Although this type of wear map is useful for unified understanding of wear phenomena of each material obtained over a wide range of operational conditions, it cannot be synthetically used to evaluate the critical conditions of each wear mode obtained in various materials.

Ting and Winer [20] constructed a "thermomechanical wear map" from theoretical considerations which showed a region for thermomechanical wear of PSZ using dimensionless parameters which included the effect of frictional heating based on a yielding criterion. This map can give unified understanding of thermomechanical wear obtained under a wide range of operational conditions and various materials.

On the other hand, Hokkirigawa [21] proposed a "wear mode map" of ceramics using dimensionless parameters of severity of contact $S_{c,m}$, $S_{c,t}$ and the coefficient of friction f based on fracture mechanics. In these analyses, it had been considered that wear of ceramics was caused by crack propagation due to its brittleness [22]. Therefore, a critical condition of each wear mode had been discussed from the viewpoint of fracture mechanics, whose suitability had been proven in some earlier works, [e.g 19].

These maps could predict three wear modes of ceramics, such as flake-formation mode, powder-formation mode and ploughing mode. Furthermore, their suitability had been proven by experimental results from tests with various ceramic materials. However, they are useful only when experimental results are obtained under certain conditions in which effects of sliding velocity or atmospheric temperature on stress distribution, and changes of material properties or chemical reactions are negligible.

Acknowledging the influence of sliding velocity [23] and temperature [e.g. 13] on wear transitions, it is clear that it is essential to construct a wear map which comprehensively evaluates wear behaviour obtained under widely varied operational conditions, including high sliding velocity and temperature.

Therefore, the purpose of this paper is to introduce a wear map of ceramics by using dimensionless parameters, which shows the regions of dominant wear modes observed in a wide range of material properties and operational conditions.

5.2 Transition from mild to severe wear

5.2.1 Critical condition for severe wear

In this paper the critical condition is analysed from the viewpoint of inter-granular fracture, which will cause removal of grains.

Here, we assumed the following two points for this analysis:

- Micro-cracks are present at the grain boundaries. Their length is directly proportional to the grain size [24], and is smaller than the length of the contact area.
- Fracture is caused by the propagation of these microcracks, which may be enhanced by the tensile stress induced by friction.

These assumptions and wear models have been employed by many researchers [21] in order to explain the transition mechanism in the mechanical wear of ceramics. Based on linear elastic fracture mechanics, the critical condition for crack growth can be expressed by the following equation:

$$\beta\sigma_{max}\sqrt{\pi d} \geq K_{Ic} \tag{5.1}$$

where σ_{max} is the maximum tensile stress at the tip of the crack, d the pre-existing crack length, K_{Ic} the fracture toughness of the material, and β a constant, taken here as 1.12 [25].

Normally, two kinds of tensile stresses are introduced in σ_{max} in equation 5.1. They are based on mechanical and thermal aspects of the system.

5.2.2 Tensile stress induced by mechanical contact

In a sliding contact a friction force is generated as a result of normal and shear stresses in the contact. The maximum tensile stress σ_{max} induced by these stresses is expressed in the following equation [26] in the case of a contact between a sphere and a flat surface:

$$\sigma_{max} = P_{max}\left(\frac{1-2\nu}{3} + \frac{4+\nu}{8}\pi f\right) \tag{5.2}$$

where P_{max} is the maximum Hertzian contact pressure, ν the Poisson ratio and f the coefficient of friction. Noting that the exact value of ν does not significantly influence σ_{max}, this can be simplified by taking ν as 0.25:

$$\sigma_{max} = \frac{P_{max}(1+10f)}{6} \tag{5.3}$$

Substituting equation 5.3 into equation 5.1, the critical condition for the onset of severe wear can be expressed as:

$$\frac{(1+10f)P_{max}\sqrt{d}}{K_{Ic}} \leq \frac{6}{\beta\sqrt{\pi}} \tag{5.4}$$

If we define the left hand side of equation 5.4 as the mechanical severity of contact, *MS* (equation 5.5), and noting that the right hand side should ideally be a constant, then mild wear will occur as long as *MS* is smaller than a critical value and severe wear will occur when *MS* is larger than that value.

$$MS = \frac{(1+10f)P_{max}\sqrt{d}}{K_{Ic}} \tag{5.5}$$

5.2.3 Tensile stress induced by thermal strain

A sliding contact generates heat pulses by frictional heating, which in turn causes thermal strain at the contact surface. The thermal stress, which is introduced by the thermal strain, applied to the crack tip as a tensile stress σ_{max}, is defined by the following equation:

$$\sigma_{max} = \frac{E\alpha}{1-\nu}\Delta T \tag{5.6}$$

where E is the Young's modulus, α the coefficient of thermal expansion and ΔT the temperature rise relative to the bulk temperature.

Bos [27] derived an equation for the temperature rise in an elliptic contact with an elliptic heat source, taking into account the partition of the heat across the bodies due to different thermal properties and different Péclet numbers:

$$\Delta T = \frac{fWV}{\sqrt{ab}} \frac{1}{\frac{K_1}{\theta_1} + \frac{K_2}{\theta_2}} \tag{5.7}$$

in which f is the coefficient of friction, W the contact load, V the velocity, a and b are the half widths of the elliptic contact in the direction of sliding and perpendicular to this direction, respectively, K is the thermal conductivity and θ is a dimensionless contact number, where indices 1 and 2 denote the bodies in contact.

For a configuration with a moving (*mov*) and a stationary(*stat)* body, θ_{mov} is given by:

$$\theta_{mov} = \left((\theta_l)^2 + \left(\frac{\theta_r}{\sqrt{\frac{aV}{\kappa_{mov}}}} \right)^{-2} \right)^{-\frac{1}{2}} \tag{5.8}$$

where κ is defined by $K/(\rho \cdot c)$ (ρ is the density and c is the specific heat of a material).

θ_{stat} is given by:

$$\theta_{stat} = \theta_l \tag{5.9}$$

θ_l and θ_r are numerically derived constants for the case of a semi-elliptical heat source distribution. They have values of 0.375 and 0.589, respectively [27] and combined with equations 5.8 and 5.9 this gives:

$$\theta_{mov} = \frac{1}{\sqrt{7.111 + \frac{aV}{\kappa_{mov}} 2.878}} \quad and \quad \theta_{stat} = 0.375 \tag{5.10}$$

A circular contact will be considered. This means $b=a$ and $\sqrt{ab}$ in equation 5.7 can be replaced by a. Combining equations 5.10 and 5.7 yields the following:

$$\Delta T = \frac{fWV}{aK_{eff}} \tag{5.11}$$

In which $K_{eff} = 2.667 \cdot (K_{stat} + \sqrt{\{K_{mov}^2 + 0.4 Va\rho_{mov} c_{mov} K_{mov}\}})$.

Note that while K_{eff} has the dimension of thermal conductivity, it is dependent on the contact conditions.

Combining equations 5.11 and 5.6 gives the maximum stress:

$$\sigma_{max} = \frac{E\alpha}{1-\nu} \frac{fWV}{aK_{eff}} \tag{5.12}$$

Finally this equation, combined with equation 5.1 means that crack growth will be possible when:

$$\beta\sqrt{\pi d} \frac{E\alpha}{1-\nu} \frac{fWV}{aK_{eff}} \geq K_{Ic} \tag{5.13}$$

or:

$$\frac{fWV}{aK_{eff}} \frac{E\alpha\sqrt{\pi d}}{(1-\nu)K_{Ic}} \geq \frac{1}{\beta} \tag{5.14}$$

It has been argued that the material properties in equation 5.14 can be related to the thermal shock resistance of the material, with the following linear relation [1]:

$$\Delta T_s = \Delta T_{s0} + c\frac{(1-\nu)K_{Ic}}{E\alpha\sqrt{\pi d}} \tag{5.15}$$

In which c is a proportionality constant and ΔT_{s0} is an offset value.

When equations 5.14 and 5.15 are combined, the thermal severity of contact (TS) is now defined as:

$$TS = \frac{fWV}{\Delta T_s aK_{eff}} \tag{5.16}$$

5.3 Experimental procedure

For the evaluation of the thermal severity number (*TS*), pin-on-disc experiments were performed using a pin-on-disc tribometer shown in Figure 5.1. In order to obtain constant test conditions the tribometer was placed in a climate chamber with the temperature set at 23°C and the relative humidity at 40%.

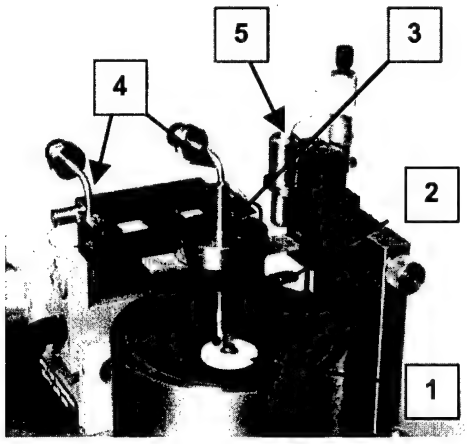

Figure 5.1: Picture of the pin-on-disc tribometer used; (1) rotating sample, (2) stationary sample, (3) dead weight providing the contact load, (4) two transducers measuring the friction force from the deflection of the arm, and (5) a laser for performing on-line wear measurements.

To obtain wear data for different *TS* values, experiments were performed at different loads and velocities. The ranges of velocity and load are shown in Table 5.1.These were chosen in such a way that *TS* was close to the expected transition, depending on the material properties of the various pin materials, Table 5.2.

Table 5.1: Velocities and loads used in the experiments.

Pin materials	Velocity [m/s]	Load [N]
Al_2O_3	0.1-0.5	3-12
SiC	0.1-0.6	5-15
Si_3N_4	0.05-0.4	5-15
Y-TZP	0.02-0.08	5-10
ZY5	0.02-0.07	5

The discs had a diameter of 36 mm and a thickness of 4 mm. The discs were polished to an RMS roughness of ≤ 0.1 µm. The commercial pins were balls with a radius of 5 mm and were mirror polished, whereas the ZY5 pins were cylinders with a spherical cap with a radius of 2.6 mm. Both discs and pins were ultrasonically cleaned in water and ethanol for 30 minutes,

then dried at 120°C prior to use. To clarify the general validity of the model, various pin materials were used, namely alumina, silicon carbide, silicon nitride, and two types of zirconia. All pins, except the home made zirconia pins, were commercially available. The home-made zirconia pins were processed to give a material with submicron grains.

Table 5.2: Properties of materials used.

Property			Z3500[d]	ZY5[d,p]	Al2O3[p]	SiC[p]	Si_3N_4[p]	Y-TZP[p]
Grain size	d	[µm]	0.6	0.18	6	n.a.	n.a.	4
Strength	σ	[MPa]	1400	454	214	400	650	1000
Fracture toughness	K_{IC}	[MPa√m]	10	7	3.5	4	8	10
Young's Modulus	E	[GPa]	205	210	390	430	320	210
Poisson's ratio	ν	[-]	0.3	0.3	0.23	0.17	0.24	0.31
Density	ρ	[10^3 kg/m^3]	6.05	5.7	3.9	3.2	3.1	6.05
Thermal expansion coefficient	α	[10^{-6} K^{-1}]	10	9	8	n.a.	3	9.8
Thermal conductivity	K	[W/(m·K)]	2	2.5	29	110	35	3
Specific heat	c	[J/(kg·K)]	400	400	600	1000	800	400
Thermal shock resistance	ΔT_s	[K]	250	280	200	380	600	250

[d] disc materials; [p] pin materials; n.a. not available.

5.3.1 Microstructures of ZY5 and Z3500

As disc material a tetragonal zirconia was chosen, because of the low thermal conductivity, which allows high thermal stresses at low loads. Two types of zirconia were used: a commercial material, Z3500, and a home-made material with controlled, submicron grains, ZY5. Z3500 discs were sawn from a bar whereas ZY5 was pressed and sintered in disc shape. It is thought that the difference in microstructure between these materials significantly influences the wear behaviour.

Both materials are yttria-stabilised zirconia ceramics. They are made from powders containing Y_2O_3 as stabilising agent. Major differences between the materials can be found in initial powder properties, chosen processing route and sintering temperature.

ZY5 ceramics are made from co-precipitated zirconia-yttria salts that were dry pressed in disc shapes to a "green" density of 40%. These discs were then sintered at 1150°C for 10 hours to a relative density of 94%. Z3500 ceramics are made by dry-pressing powder into large cylinders that are given a heat treatment under isostatic gas pressure (so-called HIP treatment). This HIP-process is conducted at 1420°C for 2 hours under 40 MPa nitrogen gas pressure leading to full theoretical density. The HIP treatment improves the mechanical properties compared to the ZY5 ceramic as can be seen in Table 5.2.

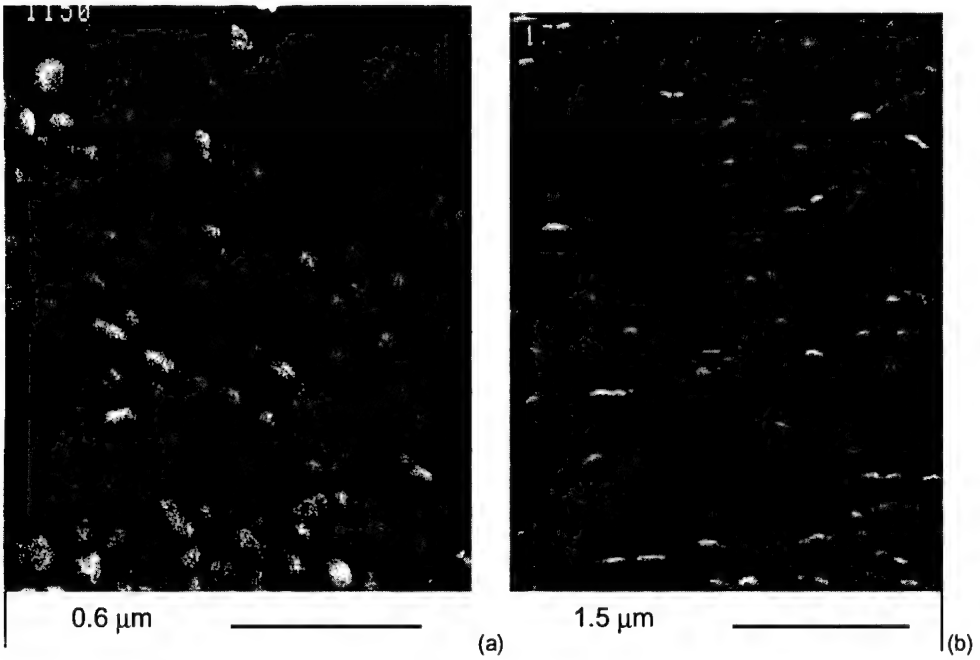

Figure 5.2: Microstructures of the two Y-TZP materials; (a) ZY5 and (b) Z3500.

Figure 5.2 shows the microstructure of the materials. The average grain size of the ZY5 ceramics is 0.18 µm and for Z3500 ceramics a grain size of 0.6 µm is measured using the linear intercept method [28]. It is also found that not only the grain size of ZY5 is smaller, but the grain size distribution (visual inspection) as well.

5.4 Results

5.4.1 Specific wear rates

In order to make the distinction between mild and severe wear, several criteria can be used. In this work, "severe" wear is characterised by the specific wear rate exceeding $3 \cdot 10^{-6}$ mm^3/(N·m). Adachi *et al.* [1] based the difference between mild and severe wear on the ratio of worn surface roughness R_y to the mean grain size D_g. For the present work and the results presented by Adachi *et al.* [1], it is found that the specific wear rate is generally less than $3 \cdot 10^{-6}$ mm^3/(N·m) when the worn surface roughness is lower than half the grain size. On the other hand, a worn surface roughness larger than half the grain size indicates severe

wear and generally gives a wear rate higher than $3 \cdot 10^{-6}$ mm^3/(N·m). The criteria as described by Adachi *et al.* [1] were compared to the values for the specific wear rate by a visual inspection of the wear tracks, indicating whether a "polishing" (mild type) or severe-type wear mechanism occurred.

The experiments using Al_2O_3 pins have been described before by Metselaar *et al.* [29]. In Figure 5.3 the results from that work are summarised.

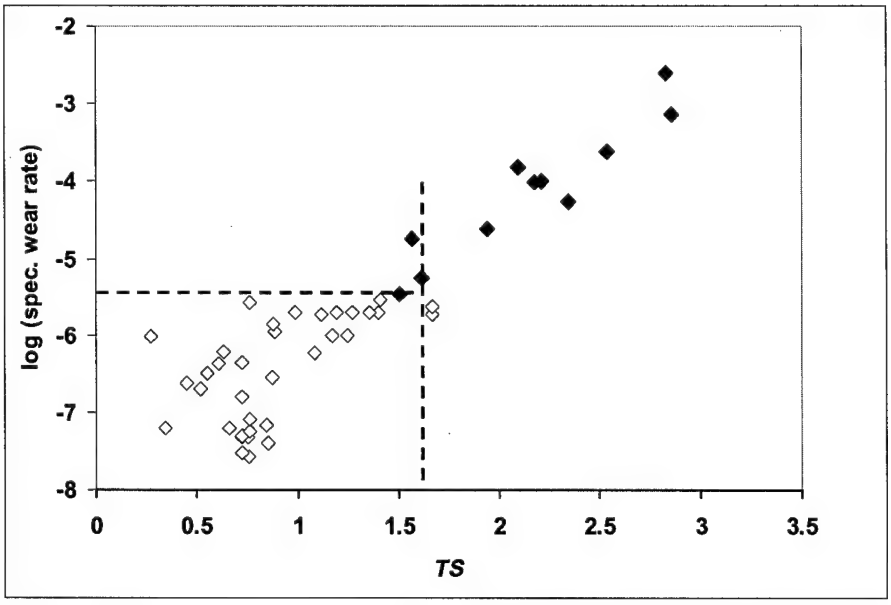

Figure 5.3: Specific wear rates of Z3500 and ZY5 discs sliding against an alumina pin at different *TS*-values [adapted from 29], open markers: mild wear and solid markers: severe wear.

Results from the present experiments are represented in Figure 5.4 to Figure 5.7. In these figures the specific wear rate is plotted against the *TS*-value of each experiment.

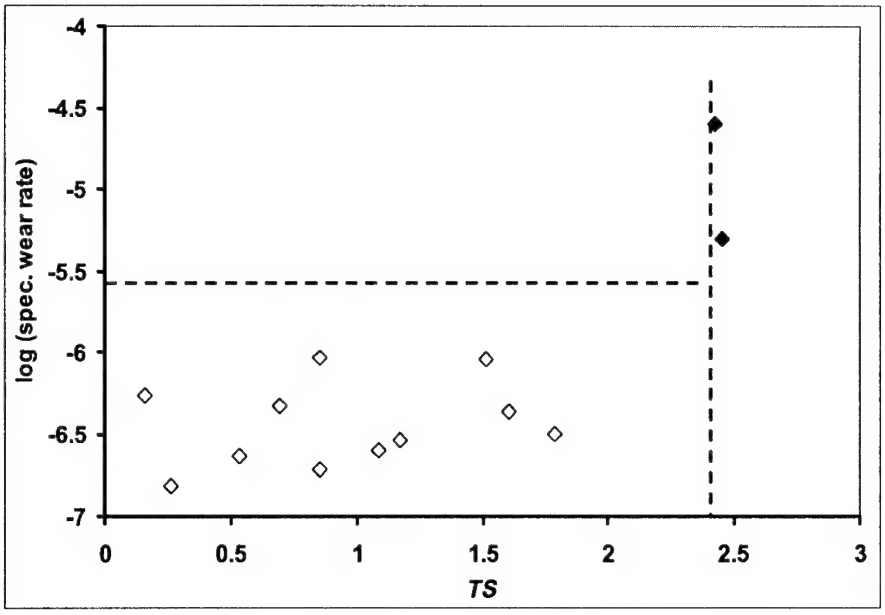

Figure 5.4: Specific wear rates of a Z3500 disc sliding against SiC pins at different *TS*-values; open markers: mild wear and solid markers: severe wear.

As can be seen from these figures, for all material combinations that have been tested, there is a transition at a specific *TS*-value. This transition occurs at $TS \approx 2.5$ ($\pm$ 0.3) for SiC, Si_3N_4, Y-TZP and ZY5 pins. From Metselaar *et al.* [29] it is found that the transition, using Al_2O_3, pins occurred at $TS \approx 1.5$, see Figure 5.3.

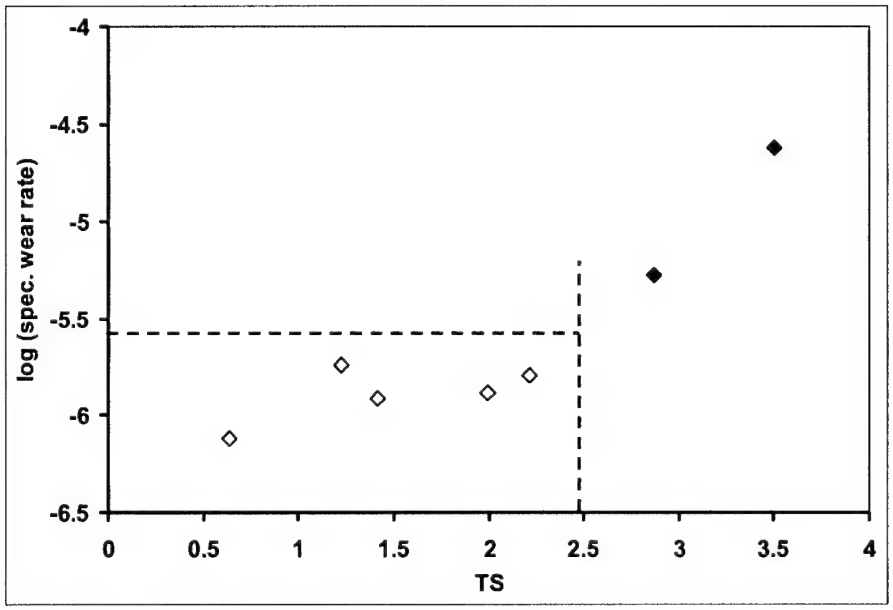

Figure 5.5: Specific wear rates of a Z3500 disc sliding against Si_3N_4 pins at different *TS*-values: open markers: mild wear and solid markers: severe wear.

When comparing the results obtained with Z3500 discs and ZY5 discs in Figure 5.6, it can be seen that these materials behave very similarly, even though their mechanical properties are different. This is because of the smaller grain sizes and narrower grain size distribution in ZY5, which both contribute to the similar wear behaviour of ZY5 compared to Z3500 in spite of the lower density and the worse mechanical properties of the first material. This is explained by He *et al.* [8], who reported that such a small grain size has a positive influence on the wear resistance. The resulting grain pull-out has a less detrimental influence, but also the amount of transformation from tetragonal to monoclinic phase is less. This transformation is not beneficial for the wear behaviour of the monolithic Y-TZP ceramics. It creates a lot of stress in the surface, resulting in easier delamination type wear processes under these circumstances.

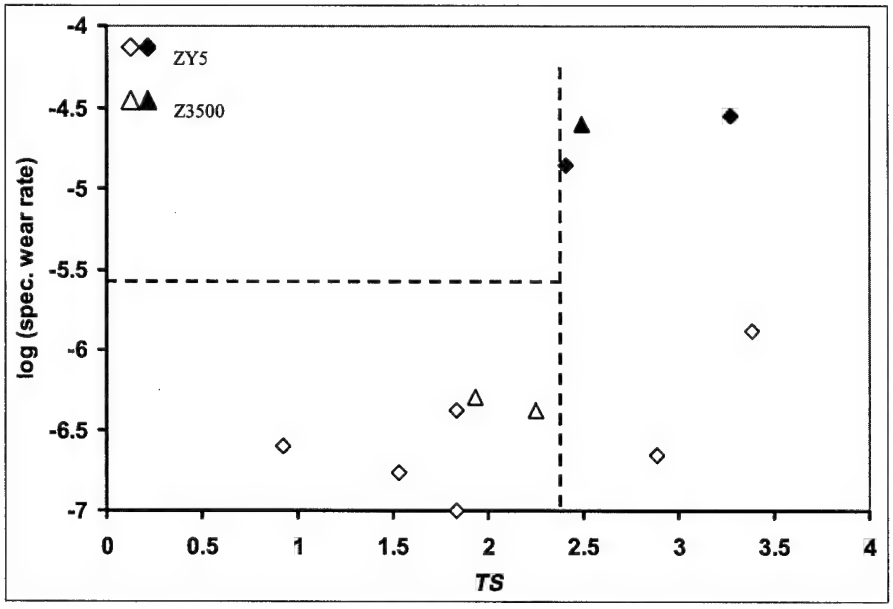

Figure 5.6: Specific wear rates of Z3500 and ZY5 discs sliding against Y-TZP pins at different *TS*-values; open markers: mild wear and solid markers: severe wear.

Thus, while the transition for each material combination is clear from these results, the transition occurs at slightly different values of *TS* for different material combinations.

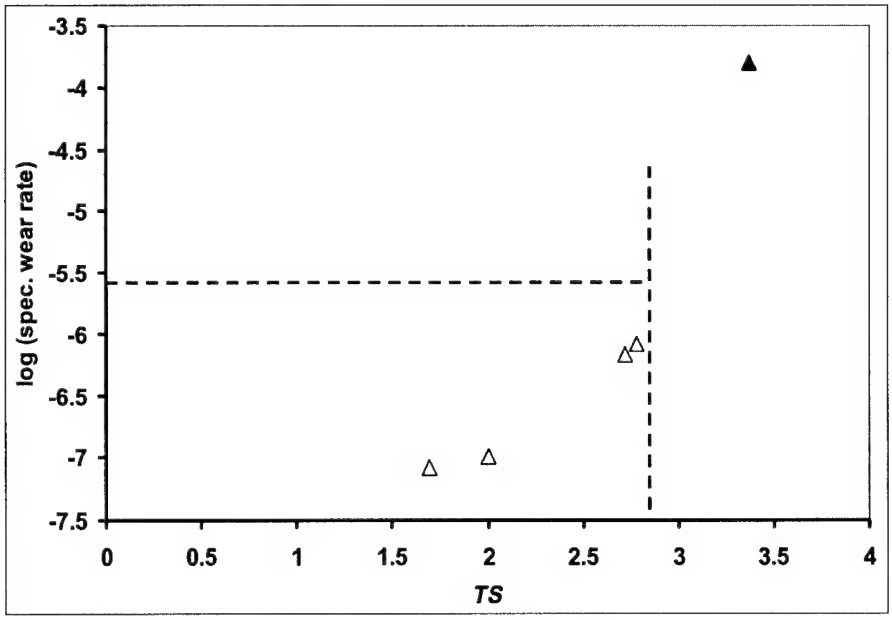

Figure 5.7: Specific wear rates of ZY5 discs against ZY5 pins at different *TS*-values; open markers: mild wear and solid markers: severe wear.

In Figure 5.8 all present results for the specific wear rate as function of the *TS*-parameter are represented. This figure indicates the transition value of app. 2.5 is valid for all material combinations presented.

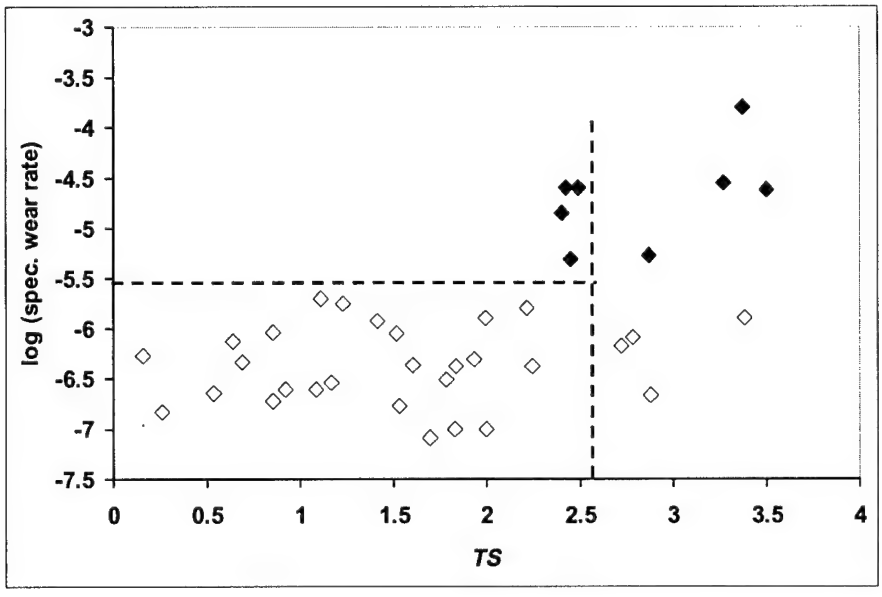

Figure 5.8: Overview of results of all present experiments; open markers: mild wear and solid markers: severe wear.

5.4.2 Wear tracks

Depending on the test conditions and material used for the counterface for ZY5, mild or severe wear was found. Wear track investigations clearly showed the presence of very small grains in the wear track of ZY5 after sliding against Y-TZP pins at 0.07 m/s and 5 N (Figure 5.9a), which is an indication of wear taking place by grain pull-out, followed by deformation and smear-out of the worn material. The cases of mild wear were characterised by some grain pull-out in the track accompanied by mild plastic deformation of the surface. Only very little grooving was found after sliding against ZY5 pins at 0.04 m/s and 5 N (Figure 5.9b). This also indicates that the properties (grain size, homogeneity) of the counterface are important. ZY5 pins have a very small grain size compared to the commercial Y-TZP pins that are used. So, in spite of a very small difference in the low sliding velocity, we find an extremely great difference in wear behaviour that is related to the microstructural properties of the zirconia counterface material that is used. Previously reported measurements on these materials [29] showed that after sliding against Al_2O_3 usually severe wear was found, caused by micro-fracture.

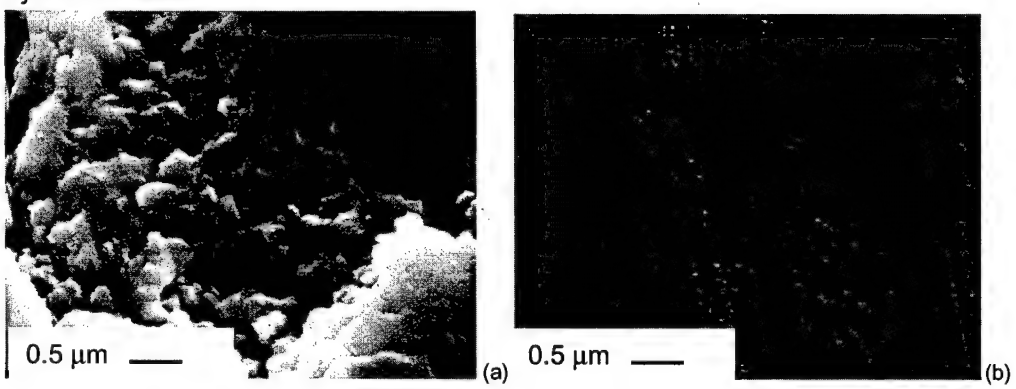

Figure 5.9: Wear tracks on ZY5 discs after sliding against two zirconia pins. Both tests were performed at 5 N. (a) Y-TZP pin at 0.07 m/s, showing severe wear, (b) ZY5 pin at 0.04 m/s, showing mild polishing.

As can be seen in Figure 5.10a for Z3500, we find clear evidence of severe wear after sliding against a Y-TZP pin, similar to what was found for ZY5 (5 N, 0.08 m/s). After sliding against both non-oxide ceramics, grooved wear patterns are found, caused by the hard asperities on the ceramic pins. The wear track of Z3500 after sliding against SiC is shown in Figure 5.10b. Here we find clear evidence of extreme grain pull-out, corresponding to the reported grain size. Figure 5.10c shows the wear track of Z3500 after sliding against Si_3N_4. Tests against SiC could be performed at much higher sliding velocities and loads without showing catastrophic wear (example after sliding at 15 N and 0.5 m/s). Z3500 ceramics show severe wear behaviour typical for Y-TZP materials at the given conditions.

No real differences in wear behaviour are found between ZY5 and Z3500, in spite of the differences in density (in favour of Z3500) and grain size (in favour of ZY5). The better microstructural properties of ZY5 apparently compensate for the worse mechanical properties compared to Z3500 commercial material.

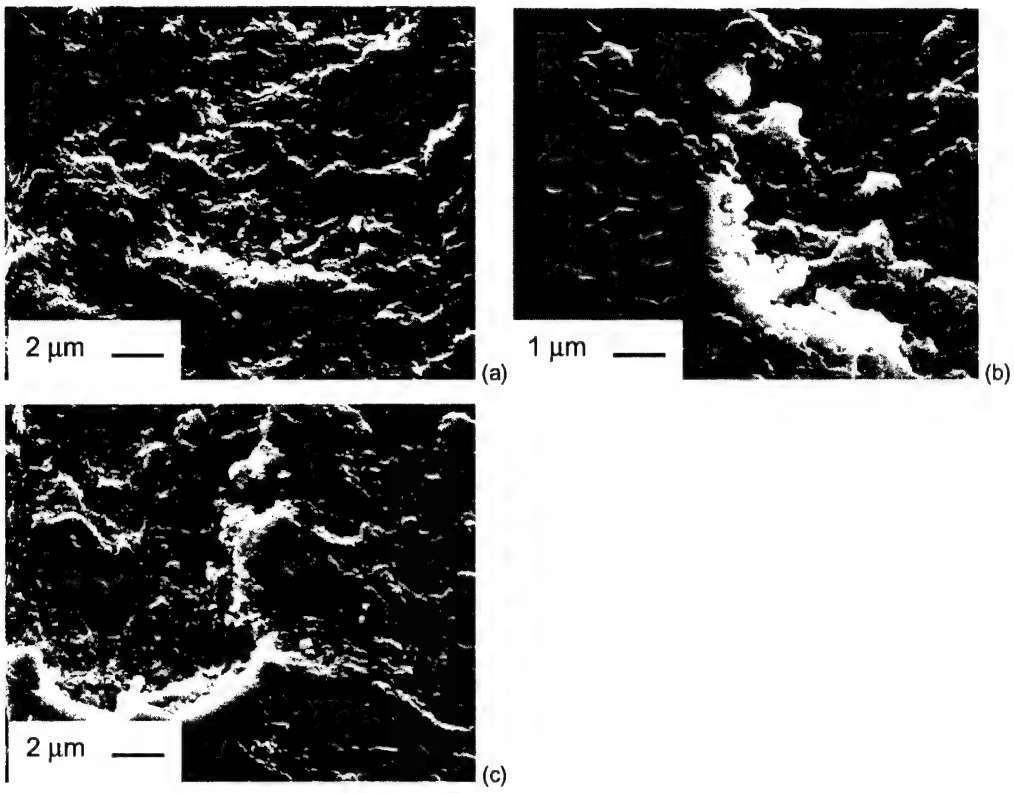

Figure 5.10: Wear tracks of Z3500 all showing severe wear after sliding against various pins; (a) Y-TZP, (b) SiC and (c) Si_3N_4.

Examples of mild wear processes are found after sliding Z3500 against SiC. In Figure 5.11a, an example of the wear track shows that polishing occurs with some grain pull-out after sliding at 0.4 m/s and 5 N. Larger holes are also found when grain pull-out has occurred, again indicating the influence of the grain size on the wear behaviour. At even milder conditions (0.1 m/s), the investigation shows that the surface is hardly worn. Only some minor polishing is found [Figure 5.11b]. Closer investigations show, however, that there is evidence of the onset of severe wear. Figure 5.11c shows that there is evidence of delamination wear in the track. Although this is a severe-type wear process, which was found locally, the overall wear process is still mild.

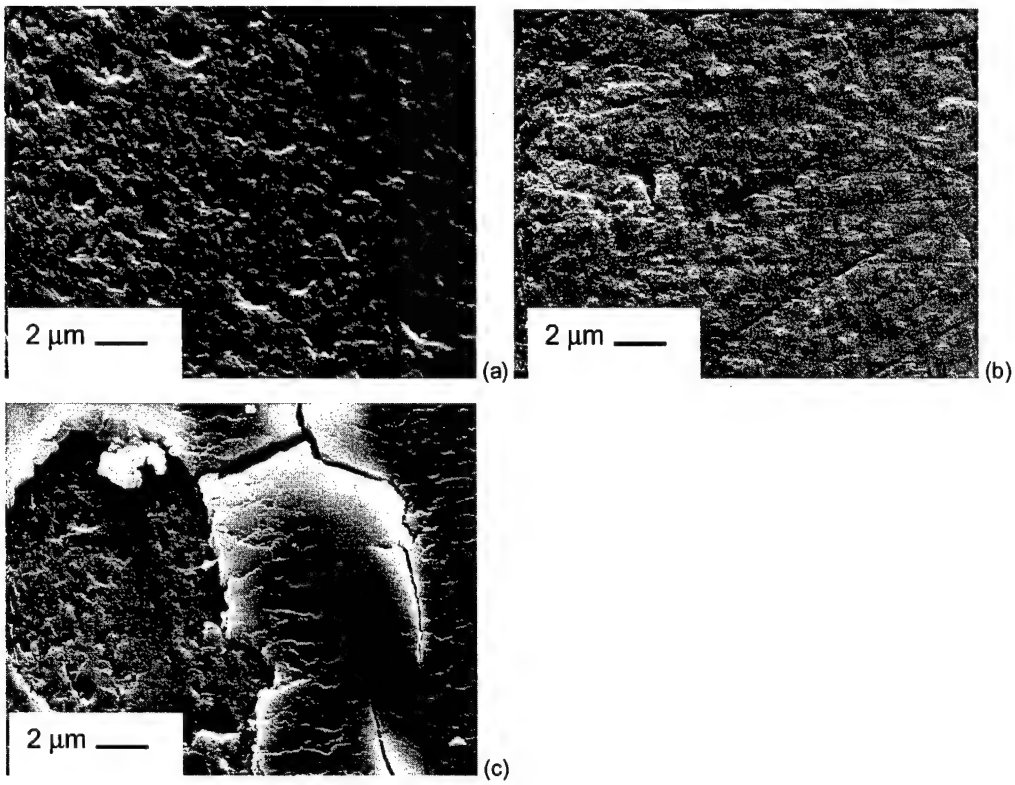

Figure 5.11: Wear tracks of Z3500 showing mild wear after sliding against SiC at milder testing conditions than given in Figure 5.10; (a) 0.4 m/s, 5N, (b) general view (0.1 m/s, 5N and (c) typical example of start of severe wear inside a wear track from the mild region.

5.5 Discussion

A new thermal severity parameter was introduced in this work. This parameter is developed on the basis of crack growth induced by thermal stress. In literature some numbers are given, as summarised in paragraph 5.1. A promising parameter was introduced by Adachi *et al.* [1]. Besides the fact that this parameter is not dimensionless, the major drawback of this parameter is found in the use of an estimated parameter that accounts for the partition of heat in the contact. They assumed in most of their work that the heat flows equally to both materials in contact. In fact, this may be doubted, since frequently material combinations are used with different thermal properties and types of motion (operational conditions). Therefore, Adachi *et al.* [1] conducted only self-mating tests to verify their model. This partition problem is solved by using the model developed by Blok *et al.* [27], describing the heat partition ratio that accounts for the varying thermal properties of material combinations and operational conditions. Using this heat partitioning, it is possible to develop a thermal severity parameter that should be valid for all materials.

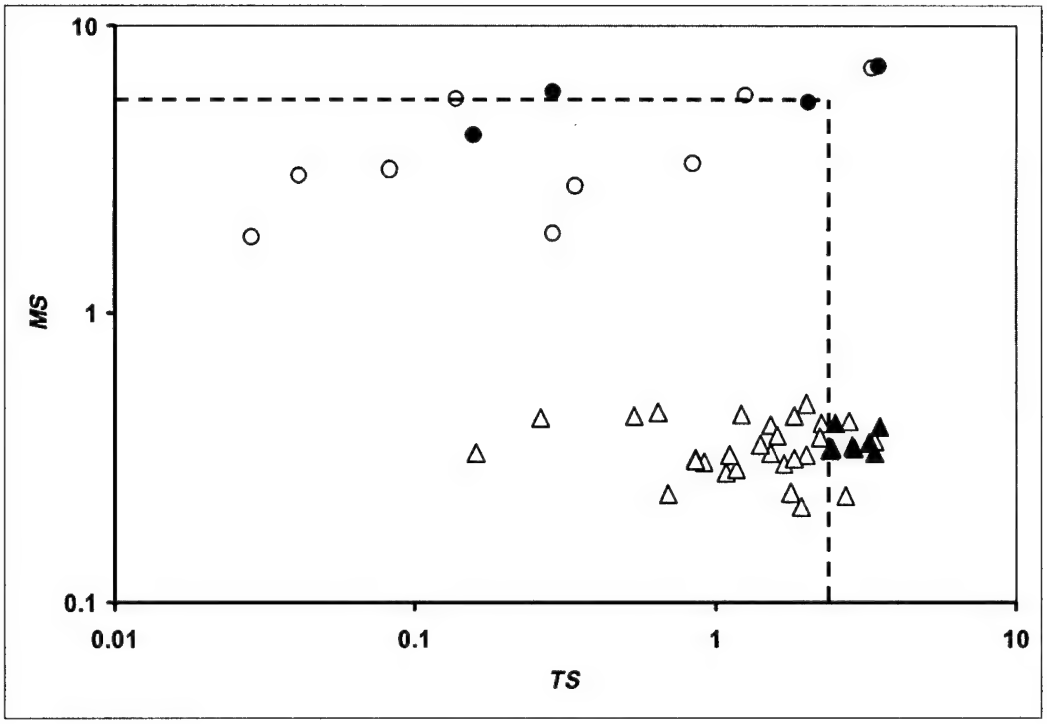

Figure 5.12: Overall picture of the wear measurements on both ZY5 and Z3500; open markers: mild wear and solid markers: severe wear.

In this work we initially performed experiments to verify the validity of the newly introduced thermal severity parameter. Adachi *et al.* [1] introduced the wear map including the mechanical severity as given in paragraph 5.2.2. With the results from the experiments presented in this paper, a similar wear map is created, making use of the existing *MS* and the new *TS*. In Figure 5.12 results of present experiments and results adapted from Adachi *et al.* [1] are given to show the validity of the thermal severity parameter in an overall valid wear map. The transition line from mild to severe wear on the thermal side is clearly defined. The validity of the *MS* transition value at low *TS* values is under investigation.

In general the modelling seems to be improved by introducing a thermal severity parameter, accounting for varying thermal properties of the materials in contact.

5.6 References

1. K. Adachi, K. Kato and N. Chen, *Wear*, 203-204 (1997) 291.
2. R. Stevens, "An introduction to zirconia", Magnesium Elektron Ltd., Litho 2000, Twickenham UK, (1986).
3. G. Willmann, *Bioceramics: proceedings of the 10th international symposium on ceramics in medicine*, (1997) 123.
4. S.M. Hsu and M. Shen, *Wear*, 200 (1996) 154.
5. M. Woydt and K.H. Habig, *Trib. Int.*, 22 (1989) 75.
6. M.G. Gee, Y.S. Wang and R.G. Munro, *Wear*, 138 (1990) 169.
7. H. Kim, D. Shim and T.E. Fischer, *Proceedings international tribology conference JAST*, (1990) 1437.
8. Y.J. He, *PhD thesis*, University of Twente, The Netherlands (1995).
9. B. Kerkwijk, A.J.A. Winnubst, H. Verweij, E.J. Mulder, H.S.C. Metselaar and D.J. Schipper, *Wear*, 225-229 (1999) 1293.
10. S.C. Lim and M.F. Ashby, *Acta Metall.*, 35 [1] (1987) 1.

11. S. Lee, S.M. Hsu and M.C. Shen, *J. Am. Ceram. Soc.*, 76 (1993) 1937.
12. A. Blomberg, M. Olsson and S. Hogmark, *Wear*, 171 (1994) 77.
13. X. Dong, S. Jahanmir and S.M. Hsu, *J. Am. Ceram. Soc.*, 74 (1991) 1036.
14. X. Dong and S. Jahanmir, *Wear*, 165 (1993) 169.
15. M. Akawaza, *Proceedings international tribology conference - Eurotrib'89*, (1989) 126.
16. T.H. Childs, *Proceedings institution mechanical engineers*, 202 (1988) 379.
17. B.J. Briscoe and P.D. Evans, *Proceedings Wear of Materials*, (1989) 449.
18. K. Kato and K. Hokkirigawa, *Proceedings international tribology conference - Eurotrib'85*, (1985) 1.
19. H. Kong and M.F. Ashby, *Acta Metall.*, 40 [11] (1992) 2907.
20. B.Y. Ting and W.O. Winer, *J. Trib.*, 111 (1989) 315.
21. K. Hokkirigawa, *Wear*, 151 (1991) 219.
22. K. Kato, *Wear*, 136 (1990) 117.
23. M.G. Gee and D. Butterfield, *Wear*, 162-164 (1993) 234.
24. H. P. Kirchner and R. M. Gruver, *J. Am. Ceram. Soc.*, 53 (1970) 232.
25. W.T.Koiter, *J. Appl. Mech.*, 32 (1965) 237.
26. G.M.Hamilton, *Proc. Inst. Mech. Eng.* 197C (1983) 53.
27. J. Bos and H. Moes, *J. Trib.*, 117 [1] (1995) 171.
28. J.C. Wurst and J.A. Nelson, *J. Am. Ceram. Soc.*, 55 (1972) 109.
29. H.S.C. Metselaar, A.J.A. Winnubst and D.J. Schipper, *Wear*, 225-229 (1999) 857.

6 Self-lubrication of alumina and zirconia ceramics by use of soft oxide additives*

Abstract

This chapter describes the preparation and frictional properties of alumina and yttria-stabilised tetragonal zirconia (Y-TZP) ceramic composites with small amounts of soft oxide additives. The concentration of additive was kept low to preserve the mechanical properties of the matrix ceramics. Powder mixing was performed by wet milling in ethanol. In most cases, composite ceramics with a relative density > 92% were easily produced. Various single oxide additives (ZnO, MgO, CuO, B_2O_3 and MnO_2) were used to establish which oxides could result in a significant friction reduction in dry sliding pin-on-disc experiments against alumina or Y-TZP balls. All additives resulted in medium friction (app. 0.5) for dry sliding of ceramics with alumina and high friction (> 0.65) for ceramics with Y-TZP. The addition of CuO in alumina or Y-TZP reduced the coefficient of friction from 0.65 to 0.45.

6.1 Introduction

Dry sliding wear of ceramics has been extensively studied over the last 15 years. Most studies focused on the development of wear-resistant materials and with little attention for coefficients of friction. The development of wear-resistant ceramics has been quite successful lately, leading to materials with an extended lifetime in practical applications. Materials like alumina, Y-TZP, ZTA, SiC and Si_3N_4 have been extensively studied. These materials all have their specific advantages and disadvantages under dry sliding conditions. Y-TZP is not recommended for situations with high sliding velocities. Alumina always shows transition behaviour from mild to severe wear at increasing contact load. SiC and Si_3N_4 are known to suffer from excessive wear due to oxidation.

In dry sliding wear, the minimum coefficient of friction obtained in ceramic couples is 0.4, when at least one sliding partner with a high thermal conductivity (e.g. SiC) is present [1,2]. To avoid large energy losses, the coefficient of friction value should be < 0.2 for practical situations [3]. This low friction is necessary to minimise heating that leads to temperature gradients in the contacting materials, which in turn result in wear created by fatigue processes. A high coefficient of friction can be related to a high surface roughness. This results in an increased intensity of the contacting asperities, creating large stresses in the contacting surfaces.

---

* Taken from: B. Kerkwijk, H.S.C. Metselaar, M.M.L. Garcia-Curiel, E.J. Mulder and H. Verweij, to be submitted for publication, 1999.

In practice, the use of a wide variety of lubricants is suitable for friction reduction [1-3]. There are, however, several reasons why their use should be avoided:

- detrimental influence on the environment,
- contamination of products in production equipment,
- finite lifetime causing increased equipment maintenance to ensure continuous operation.

In addition, when ceramics are applied at high temperatures or under vacuum, these lubricants, mainly based on organic materials, will not function properly anymore. This calls for the need of lubrication by means of solid state lubricants or low friction surfaces that can be used under extreme loads and velocities, at high temperatures or under vacuum.

Several authors have described the use of solid state lubricants, mainly based on materials like graphite, MoS_2 and CF_x. Nice examples can be found in the work of Baumann *et al.* [1] and Woydt *et al.* [2], who described the use of materials-based concepts for ceramic lubrication, since the development of new wear-resistant materials leads to new demands on lubrication techniques. In the work of Peterson *et al.* [4,5] similar solid state lubricants were described for use at high temperatures. Bridgeman [6] and Hensley [7] as well, used a variety of oxide materials as solid state lubricants, either in powder form or as a coating/film. Others described the use of TiB_2 and Ti_3N_4 as hard coatings [8], or low friction surfaces [9] but these are mainly intended to protect materials from wear or corrosion and not specifically for friction reduction.

To overcome the problems described above, it may be interesting to create a self-lubricating system. In this route a specific solid state lubricant is incorporated in a ceramic matrix. Slight wear of such a material results in the presence of a soft phase at the surface and, consequently, in the contact between the opposing surfaces. This soft phase overcomes the difference in sliding velocity between the surfaces and shear takes place in this layer resulting in a low coefficient of friction.

Self-lubricating composites are known in literature for metals [10], but are not often described for ceramics. Ideas proposed for ceramics are described by Gangophadyan *et al.* [11]. An example is given in the work of Wang *et al.* [12], in which the preparation of Y-TZP ceramics with a wide variety of volume fractions of graphite is described. The addition of large volume fractions (up to 30 vol%) of graphite lowered friction of Y-TZP, but significantly increased wear.

Many investigators [13-17] describe the preparation of alumina and Y-TZP ceramics with various types of oxide added in small amounts. Incorporation of these oxides, however, was not intended for friction reduction. These materials were used to study their influence on a variety of properties (e.g. strength, chemical stability) of the matrix ceramic phase. Addition of CuO to Y-TZP for superplastic deformation is a well-known example [13,14]. The same goes for the addition of MgO to alumina and Y-TZP for improvement of the homogeneity. In alumina, MgO acts as a grain growth inhibitor [15] and in Y-TZP it acts as a stabiliser of the tetragonal phase.

In previous work, the preparation of ceramic composites with an extremely high dry-sliding wear-resistance (obtained by controlling the microstructural homogeneity of

these materials), was described [18]. The resulting low wear rates were accompanied by a relatively low coefficient of friction of 0.43. Here, no attention was paid to friction reduction. In this chapter, a description is given of the preparation and tribological properties of alumina and Y-TZP ceramics with solid lubricating soft oxides as additives to provide the materials with a self-lubricating mechanism. Small amounts are used to preserve the mechanical properties of the matrix phase so that the specific wear rate is not increased. In this stage of the investigation, limited attention was paid to control the dispersion homogeneity of the additive, which may significantly influence the final properties. The frictional properties are monitored on-line and microstructural investigations show the influence of the additives on the wear tracks of the single-phase materials and their tribological properties.

6.2 Experimental

6.2.1 Materials

Commercially available powders were used to prepare the matrix materials:

- α-alumina (AKP50, Sumitomo, Japan) with a crystallite size of 0.23 μm,
- zirconia powder (TZ3Y, Tosoh, Japan), stabilised in the tetragonal phase by the addition of 3 mol% Y_2O_3, with a crystallite size of 40 nm (Y-TZP).

Their respective BET-surface areas are 10 and 16 m^2/g. Up to 5 wt% of other commercially available oxide powders, CuO, ZnO, TiO_2, MnO_2 or B_2O_3 (Alfa Chemicals, Germany) were added to the matrix powders. All these oxides have a lower hardness and melting point than alumina and Y-TZP. Properties of the additive materials are given in Table 6.1.

Table 6.1: Properties of various additives (applied as solid state lubricant) used in the preparation of the composites; hardness (Moh) values for alumina and Y-TZP are 9 and 8, respectively.

Additive	Density [kg/m^3]	Hardness (Moh)	T_{melt} [°C]	Crystal structure	Lowest friction value reported
CuO	6400	4	1326	Monoclinic	0.14 [4,5,7,12]
MgO	3580	6-7	2852	Cubic	0.14 [6]
MnO_2	5026	*	reduction, 535	Rhombohedral	*
ZnO	5606	4-5	1975	Hexagonal	0.22 [6,7]
B_2O_3	2460	4	1860	Rhombohedral	0.25-0.3 [17]

* not known.

The composite powders are made by wet-milling and mixing in ethanol for 24 hours using 2 mm Y-TZP milling balls. The mixtures are dried in air at 80 to 120°C for 16 hours to remove the ethanol. The powders are dry-milled and subsequently sieved through a 180 μm sieve. Consolidation is performed by dry pressing uniaxially at 30 MPa, followed by isostatic pressing at 400 MPa. All ceramics were sintered to relative densities larger than 92% at temperatures and dwell times normally used for Y-TZP and alumina without additives (1400°C for 4 hours and 1500°C for 2 hours, respectively).

6.2.2 Testing procedure and tribological characterisation

The investigated ceramics were cut into discs. The diameter of the discs was about 36.5 mm and their thickness varied between 2.5 and 4 mm. Finally, the discs were polished to an average surface roughness of 0.1 μm. Dry sliding wear tests were performed using a pin-on-disc tribometer [CSEM], placed in a climate chamber at 23°C and 40% relative humidity. As pin material, polished alumina or Y-TZP balls of 6 or 10 mm diameter [Gimex Technical Ceramics, Geldermalsen, The Netherlands] were used. A picture of the set-up is given in Figure 6.1.

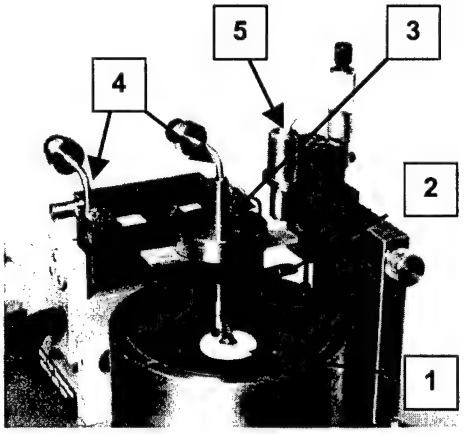

Figure 6.1: Pin-on-disc set-up. (1) Rotating ceramic sample, (2) stationary ceramic ball, (3) dead weight providing contact load, (4) two inductors measuring friction force from the deflection of the arm, (5) laser sensor for on-line wear measurement.

The sliding velocity for the Y-TZP ceramics was set at 0.1 m/s to avoid the occurrence of any severe thermally induced fracture processes [19]. The load was varied between 3 and 10 N. In this way, a meaningful comparison between all investigated ceramics could be made. With the given geometry and materials properties the loads mentioned lead to mean initial Hertzian contact pressures between 300 and 1000 MPa. For alumina ceramics, a sliding velocity of 0.5 m/s was used. The applied load was 10 N, resulting in an initial contact pressure, for alumina without additive, of 1000 MPa.

All testing conditions were chosen in such a way that the results from the measurements could be compared to similar ones performed for ceramics without friction-reducing additives. The sliding distance of the tests was adapted for each specific measurement to obtain significant wear and to detect possible fatigue. Typically, a measurement for alumina composites took 32 km of sliding distance and for Y-TZP 16 km. Longer sliding distances were used in tests for identification of possible fatigue processes. The coefficient of friction was measured on-line. This was done by monitoring the ratio between the measured shear force and the applied normal force by measuring the deflection of the pin-arm with two inductors.

Analysis of the crystal structure was performed by XRD (Philips PW3710). Furthermore, microstructures and wear tracks were characterised by means of SEM (Hitachi S800). To determine phase distribution and the presence of impurities energy-dispersive X-ray analysis (EDX, Kevex) was used together with SEM.

6.3 Materials characterisation

Properties of the composites with Y-TZP and alumina are presented in Table 6.2. Some of the materials could not be mirror-polished, in spite of sufficient density. On the other hand, an average surface roughness after polishing of < 0.1 µm was obtained for these samples which is similar to roughness values obtained for dense materials. Hence, the poor polishing appearance of these samples could be explained by the fact that the polished surfaces were not dense. This is also demonstrated by SEM micrographs of the microstructures which will be discussed later.

Table 6.2: Physical properties of composites of Y-TZP and alumina with various additives sintered at 1400°C for 4 hours and 1500°C for 2 hours, respectively.

Matrix	Additive	Maximum density [kg/m^3]	Crystal structure*	Grain size [µm]
Y-TZP	none	6050	Tetragonal	0.4
	CuO	5551	Tetragonal	2.6
	MnO_2	5856	Tetragonal, Monoclinic, cubic	^
	MgO	5917	Cubic, tetragonal	8.2
	B_2O_3	5445	Cubic, tetragonal	^
Al_2O_3	none	3970	Hexagonal	2
	CuO	3732	Hexagonal	^
	MnO_2	3930	Hexagonal	4.8
	MgO	3930	Hexagonal	2.3
	ZnO	397	Hexagonal	3.7
	B_2O_3	3891	Hexagonal	4.3

* Qualitative analysis, major phase detected is mentioned first.

^ Not measured.

Generally, the preparation of the composites with Y-TZP was more problematic than with alumina, since more difficulties were met to obtain dense materials. This is probably due to phase transitions of Y-TZP during sintering. The chosen preparation route with MgO as an additive did not result in a homogeneous distribution of two phases. For Y-TZP, MgO is a known stabilising agent dissolved in the matrix phase. All Y-TZP ceramics with additives reached relative densities of 92-94% based on the theoretical density for single-phase Y-TZP*. All additives resulted in Y-TZP ceramics with larger grains than in the pure Y-TZP material. The addition of ZnO resulted in serious crack formation and no suitable disc material could be made for wear testing. Some examples of microstructures of Y-TZP material with additives before wear testing are shown in Figure 6.2.

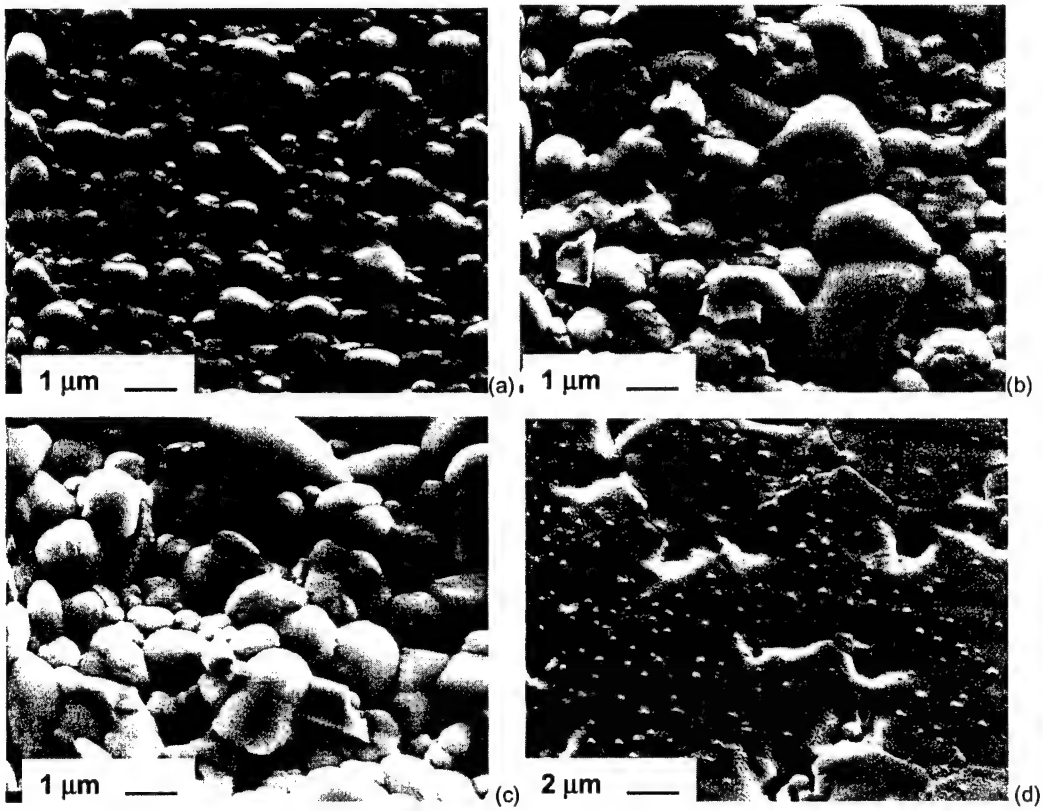

Figure 6.2: Microstructures of Y-TZP with addition of (a) MnO_2, (b) B_2O_3, (c) CuO and (d) MgO.

The addition of MnO_2 (Figure 6.2a) resulted in dense ceramics with a grain size between 0.4 and 1 µm and the microstructure clearly shows two phases with different grain sizes. This is probably related to the presence of both monoclinic and tetragonal zirconia, as was indicated by XRD-analysis. For B_2O_3 additions (Figure 6.2b) clear evidence of liquid phase sintering was found which caused enhanced grain growth, resulting in grain

* This density value was used, since it was not sure what the effect of the various additives is on the theoretical density. In this way, the same theoretical density was obtained for all materials.

sizes > 1 µm. Addition of CuO resulted in problems to obtain a fully dense material, but by increasing the sintering temperature (to 1600°C) satisfactory densities were reached. Also for the material with CuO (Figure 6.2c) a larger grain size compared to Y-TZP without the addition of CuO (typically 0.4 µm) was found. The SEM micrographs of the microstructure show clear boundaries of Y-TZP grains. XRD measurements revealed that the tetragonal zirconia phase is always present in combination with traces of cubic and monoclinic phase. In the case of MgO addition (Figure 6.2d) a strong presence of the cubic phase is revealed. Here, grain growth was considerable due to the fact that this cubic phase was formed because the addition of 5 wt% MgO resulted in extra stabilisation.

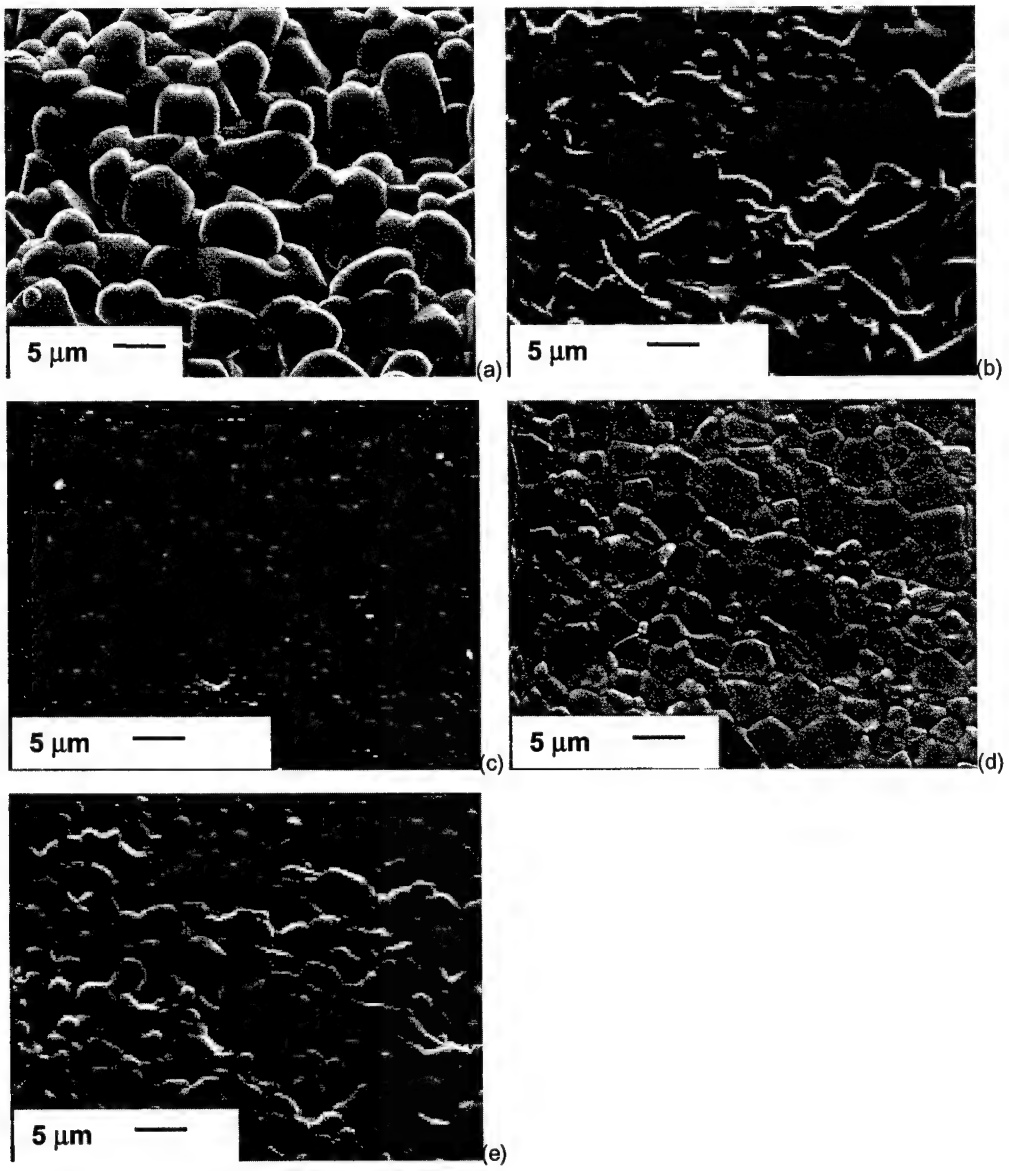

Figure 6.3: Microstructures of Al_2O_3 with addition of (a) CuO, (b) MnO_2, (c) MgO, (d) ZnO and (e) B_2O_3.

All alumina composite discs could be made with densities > 94%. Again, the addition of CuO did not result in a fully dense system (94%, based on the theoretical density of α-alumina). For all other additives near full densities were reached by sintering at 1500°C for 2 hours, which are normal conditions to obtain dense alumina without additives. The presence of additives in the matrix resulted in significant colour changes in the material. The MnO_2-containing alumina sample had a red/magenta colour after sintering. This colour indicates that Mn^{4+} from the initial MnO_2 had been reduced to Mn^{2+}. Most probably a spinel-type structure like $MnAl_2O_4$ is formed, since this material is known to have a red/magenta colour. Another possibility is the reduction to Mn^{3+}, since this oxidation state is also known to result in red-coloured materials. From EDX measurements it is found that a phase is present containing indeed aluminium and manganese. Figure 6.3 shows the microstructure of some of the alumina materials. The grain size of alumina ceramics with MgO (Figure 6.3c) and ZnO (Figure 6.3d) is comparable to the values measured for alumina without additives. Normally the alumina used in this study shows a grain size of 2-3 μm, whereas the materials with the other additives have grain sizes up to almost 5 μm. The fact that MgO inhibits grain growth for alumina is well known in literature [15].

6.4 Tribological characterisation

6.4.1 Coefficients of friction

Tribological measurements were performed to determine the steady-state coefficient of friction for the various composites against either alumina or Y-TZP pins. An overview of all measured coefficients of friction is given in Table 6.3.

Table 6.3: Tribological properties of all investigated materials, after sliding against 10 mm ceramic balls (Al_2O_3 or Y-TZP).

		Al_2O_3 ball		Y-TZP ball	
Disc	Additive	f[–]	k_w [mm^3/(N·m)]	f[–]	k_w [mm^3/(N·m)]
Y-TZP	none	0.7	> 10^{-6}	0.9	failure
	CuO	0.43	≈ 10^{-7}	0.8	failure
	MnO_2	0.77	≈ 10^{-7}	*	*
	MgO	0.85	≈ 10^{-7}	*	*
	B_2O_3	0.75	≈ 10^{-7}	*	*
Al_2O_3	none	0.55	10^{-8}	0.7	failure
	CuO	0.65	≈ 10^{-8}	0.43	10^{-7}
	MnO_2	0.47	≈ 10^{-9}	*	*
	MgO	0.48	≈ 10^{-9}	*	*
	ZnO	0.49	≈ 10^{-9}	0.9	*
	B_2O_3	0.48	≈ 10^{-9}	*	*

* not measured

Generally, addition of soft metal oxides did not result in a significant friction reduction for most Y-TZP materials except for the one with CuO. Figure 6.4 shows a typical plot of the coefficient of friction versus sliding distance measured for Y-TZP with 5 wt% CuO sliding against alumina. The same is shown for Y-TZP without additive. The coefficient of friction reduces from about 0.62 down to 0.47. The steady-state value is reached after a short running-in period starting at an initial value of about 0.2. The values reported in Table 6.3 are the extreme values found in all tests.

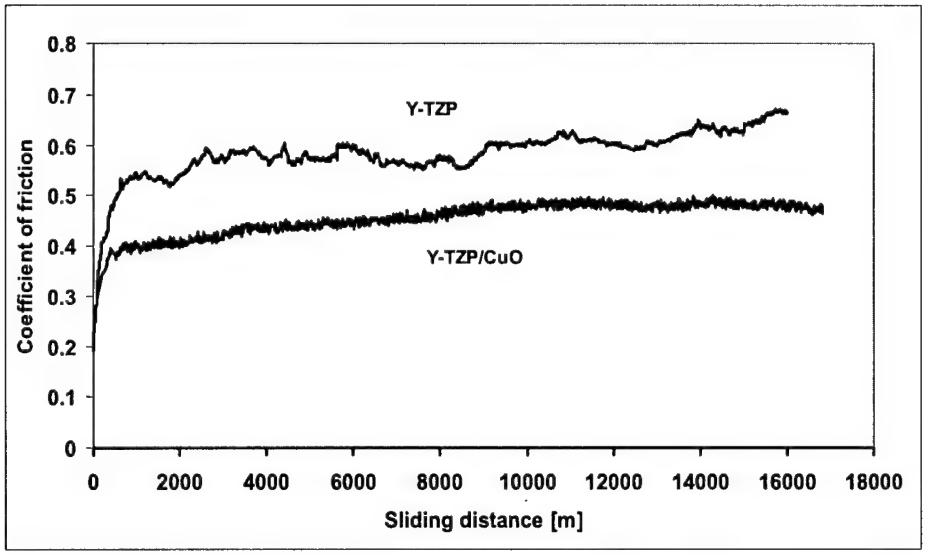

Figure 6.4: Plot of coefficient of friction versus sliding distance measured for Y-TZP with and without CuO sliding against alumina.

Several conclusions can be drawn:

- The effect of the addition of CuO is dependent on the combination of materials in the friction couple.
- Wear is similar to what is found for the combination without additive and is very low. Compared to results found in literature it is especially striking that this result is found after such a long sliding test. Typically, measurements reported up to now have been performed for a couple of hundreds of meters [12], so that it is not always sure if the steady-state was already reached or that a material can have the same performance for a longer period of time.
- The friction decrease together with a low wear rate indicates that the CuO additive behaves as a "lubricating phase". The exact mechanism behind this friction reduction is not yet clear.
- The development of friction with distance showed that friction gradually increased from a low initial value. If second phase release would be the reason for friction reduction to occur, the coefficient of friction would have been higher in the initial stage than in the steady-state.
- For Y-TZP with CuO sliding against Y-TZP balls, no friction reduction is found.

For alumina with MnO_2 sliding against alumina the coefficient of friction is plotted in Figure 6.5, where is given. Here, a friction reduction from 0.55 to 0.47 is found, which is similar to the results found for most of the other additives. When alumina containing CuO is tested against an alumina ball, however, no friction reduction is found, but friction increases from 0.55 to 0.65. Tests with alumina containing CuO against Y-TZP balls revealed that the coefficient of friction is again reduced from about 0.7 to 0.43. For

CuO-containing ceramics, it seems that only Y-TZP/alumina couples show a friction reduction regardless of the material used for disc and pin and vice versa. If similar tests with, for instance, ZnO in alumina and Y-TZP balls are performed, the coefficient of friction is increased to app. 0.9.

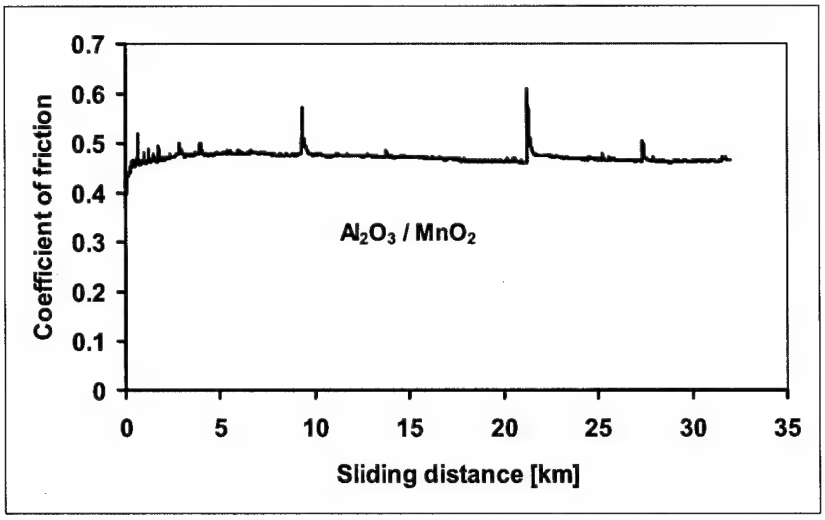

Figure 6.5: Plot of coefficient of friction versus sliding distance measured for alumina containing MnO_2, sliding against alumina.

Besides CuO, the use of all other additives to alumina when sliding against alumina balls, results in low coefficients of friction, mostly in the order of 0.5. Besides lower friction values, the ceramics also show low specific wear rates (app. 10^{-9} $mm^3/(N \cdot m)$). Normally values in the order of 10^{-9} to 10^{-8} $mm^3/(N \cdot m)$ are measured. This indicates that only very little material is worn off and is actually present in the contact. This again raises the question what the reason is for the low friction that is measured. It is not likely that an actual second phase is present in the matrix, given the small amounts of additive. It is, however possible that some kind of lubricating solid film is created. If this would be the case friction would be high at the start of the experiment and this was not measured so far.

6.4.2 Wear mechanisms

The wear track of Y-TZP with MnO_2 shows the presence of a manganese- and alumina-containing compound after sliding against alumina. Wear debris of the alumina testing balls reacts with the Mn-containing phases present in the matrix, as indicated by EDX-measurements of the darker phase in the wear track (Figure 6.6).

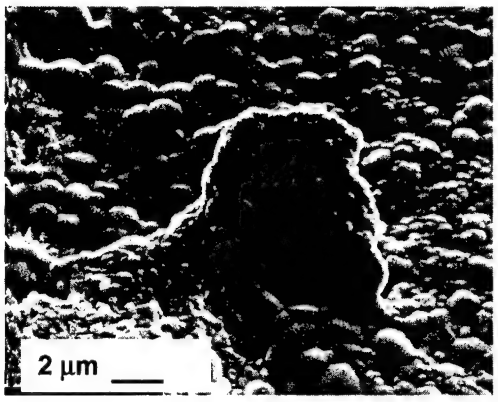

(a)

Figure 6.6: Special cases found in wear tracks of (a) Y-TZP with MnO_2, black phase consists of an oxide phase containing Mn and Al.

Inspection of all wear tracks of the Y-TZP ceramics showed that deformation of grains has occurred (Figure 6.7). Especially along the edges clear evidence for deformation is present whereas the middle of the track shows extreme material pull-out. This severe wear is one of the reasons for the high coefficient of friction that is found. Hence, even though no significant friction reduction was found, the preparation of these materials resulted in ceramics with structural changes that cannot be accounted for, so far. For the addition of MgO to Y-TZP, these changes can be explained by the stabilising effect of MgO on the cubic or tetragonal structure. MnO_2 shows the presence of a distinct second phase. This may be explained in terms of the presence of zirconia with a different structure (the monoclinic phase was found together with the tetragonal phase from XRD analysis), since no significant amounts of Mn-containing compounds were found.

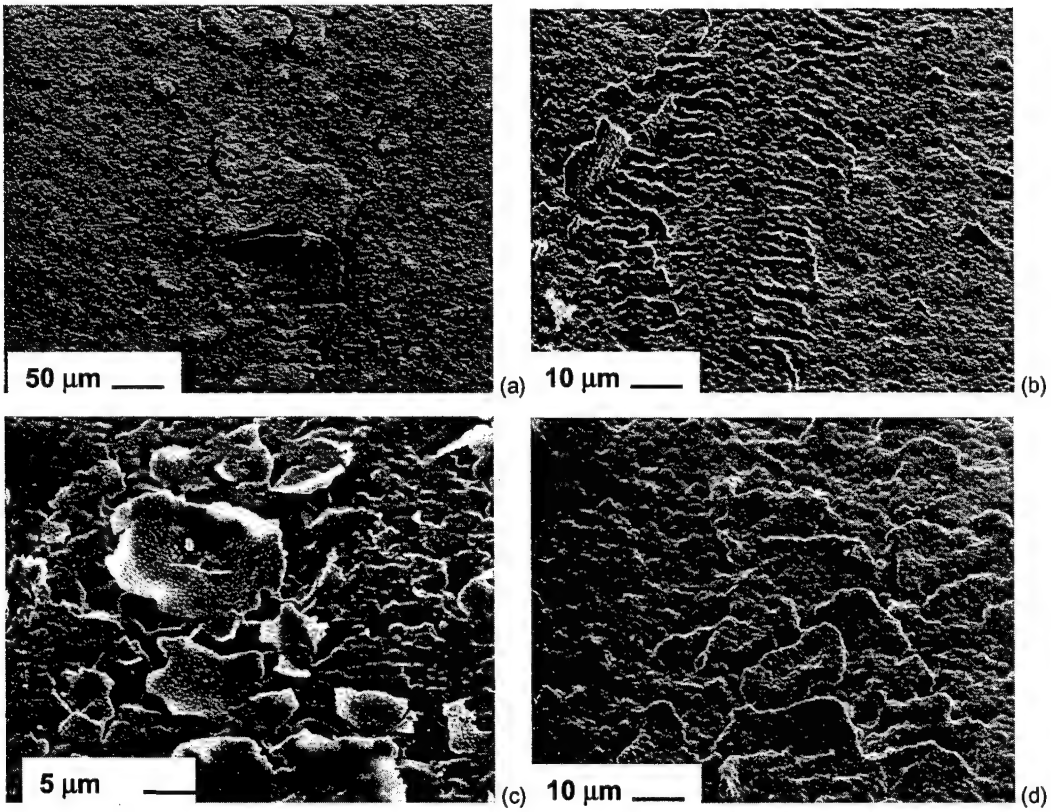

Figure 6.7: Wear tracks of Y-TZP with the addition of (a) CuO, (b) MnO_2, (c) MgO and (d) B_2O_3, after sliding against alumina balls.

Contrary to what was the case for Y-TZP, alumina was present in its most stable α-phase. For alumina it is well-known that MgO acts as a grain growth inhibitor. In addition, MgO may have lubricating properties when applied as a solid state lubricant [1]. In our alumina ceramics, however, MgO does not seem to act as a lubricant, but it plays a significant role in the microstructural improvement and this, in turn, causes a reduction in both friction and wear. For the alumina ceramics, a friction reduction for all materials is measured, except for the CuO additive. After sintering the material with MnO_2, the colour of the discs had changed from black to red. This can be explained by a reduction from Mn^{4+} to Mn^{3+} or Mn^{2+}, as was found for Y-TZP. This reduction is probably caused by the formation of a $MnAl_2O_4$-phase. This phase could not be detected in the wear track with XRD, since only small amounts of additives are used. It is obvious that friction reduction occurs but the exact mechanisms could not be revealed. Unlike what is found for the Y-TZP materials, no evidence is obtained for any film formation due to the presence of a softer phase (Figure 6.8).

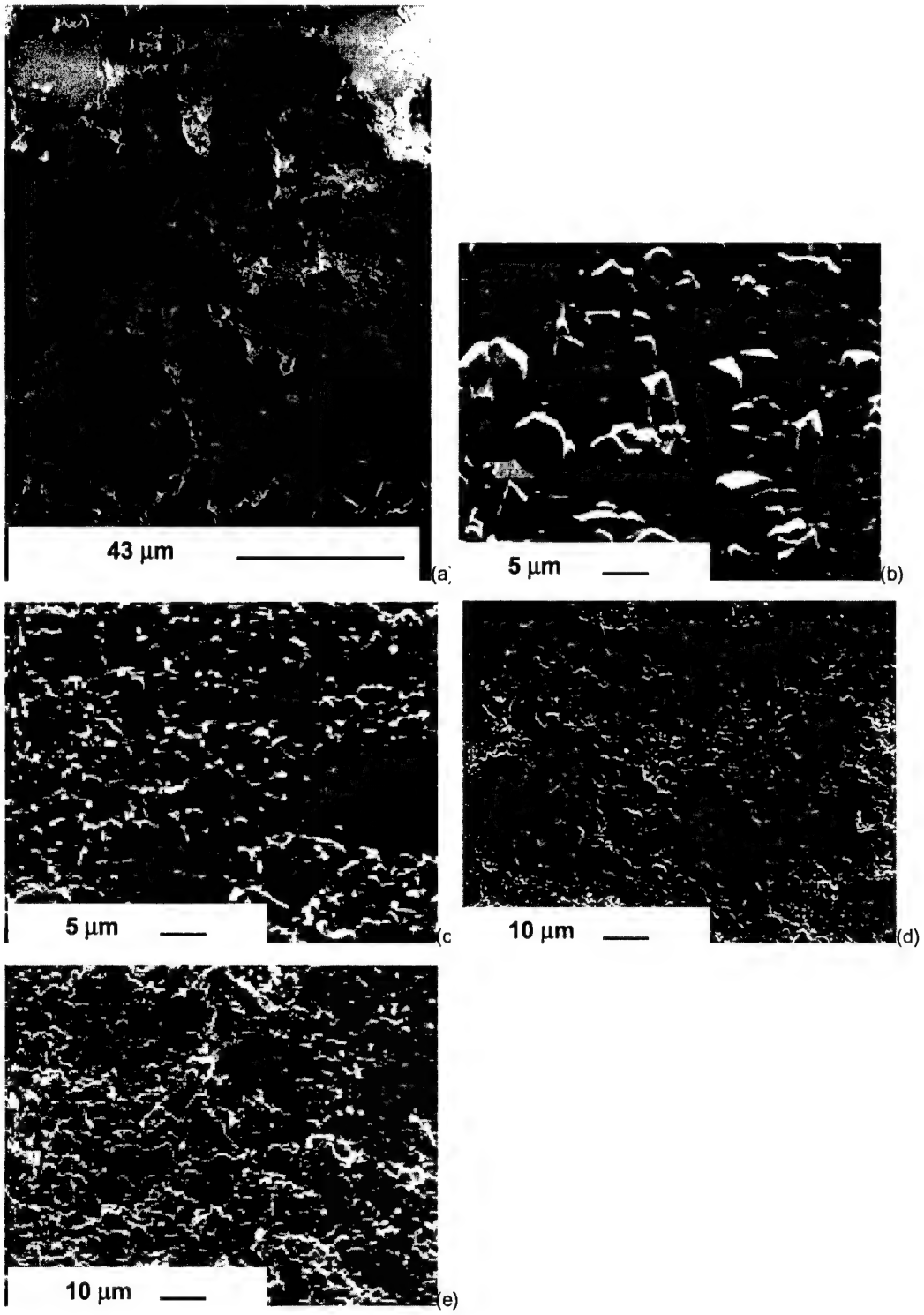

Figure 6.8: Wear tracks of Al_2O_3 with the addition of (a) CuO, (b) MnO_2, (c) MgO, (d) ZnO and (e) B_2O_3, after sliding against alumina balls.

The other additives probably have a positive influence on the improvement of the alumina microstructures. This is supported by the fact that the accompanying specific wear rates are in the order of 10^{-9} $mm^3/(N \cdot m)$, which is lower than the values found for alumina sliding against pure alumina without any additive. Obviously, this low wear is indirectly related to the lower friction. On the other hand, for the case of Y-TZP with CuO sliding against alumina, a coefficient of friction of 0.43 is measured, with a specific wear rate in the order of 10^{-7} $mm^3/(N \cdot m)$, indicating that wear and friction do not automatically go hand in hand. Here, a high wear rate (compared to the value of 10^{-9} $mm^3/(N \cdot m)$ for the undoped compound) was found in combination with a low coefficient of friction.

CuO-containing alumina material showed a significantly lower friction compared to undoped material when sliding against a Y-TZP ball: 0.43 instead of 0.7. This is similar to what was found for a CuO-containing Y-TZP disc sliding against an alumina ball. So, CuO lowers friction in heterogeneous wear couples with both alumina and Y-TZP. The explanation may be the fact that alumina always reacts with CuO to form $CuAlO_2$, which is a softer compound with possibly good friction-reducing properties in the specific combination. Such a $CuAlO_2$-compound was detected in XRD measurements of materials containing larger fractions of CuO [21]. Another possibility may be that, due to the presence of both Y-TZP and CuO, the superplastic deformation behaviour of Y-TZP is improved [13,14] which, in turn, may be the reason for an important friction reduction. This difference in deformation behaviour may ease shear in the contact to a considerable extent and thus decrease friction. The deformation behaviour may also explain the fact that in most of the cases, during sliding less grain pull-out occurs which usually is the on-set of severe wear of alumina ceramics.

6.5 Conclusion

This study shows the possibility of preparation and use of alumina and Y-TZP ceramics with soft metal oxide additives (as second phase) intended to lower friction in dry-sliding couples. All oxide additives had a relatively low melting point and hardness. The contents of additives were low (1 to 5 wt%) to preserve the mechanical properties of the single-phase ceramics. All materials could be made with sufficient densities, but some materials that showed liquid-phase sintering were more difficult to densify. The frictional properties of the materials are diverse.

For most of the Y-TZP ceramics no significant friction reduction is found. The CuO containing materials, however, showed a friction reduction of almost 40% (0.7 to 0.43), when sliding against alumina balls. For alumina, it is found that the use of additives resulted for most of the materials in a friction reduction from 0.55 to about 0.47. The addition of CuO results in the same friction reduction as described before, but only in wear couples in which the alumina disc is tested against Y-TZP balls. The grain size of the alumina is similar to that of materials without additive. This makes sure that it does not contribute to differences in the specific wear rates.

From the preparation point of view, it is interesting to use more advanced processing methods like colloidal filtration. Previous studies with colloidal-processed composite materials revealed improved tribological behaviour (low wear and friction), because of the

enhanced microstructural homogeneity [18]. Colloidal filtration may yield a better homogeneity of the ceramic microstructure when compared to dry-pressing, e.g. a better dispersion of the additive through the ceramic matrix. With a better dispersion of the lubricating phase it may also be possible to introduce larger or smaller amounts of additives while still retaining the favourable mechanical properties of the matrix. The preparation of more complicated systems (non-oxides, graphite) may be considered as well, but their processing may be more difficult.

Acknowledgement

Special thanks are due to Dik Schipper, Manon Timmerman and Louis Winnubst for their useful comments to the manuscript.

6.6 References

1. M. Baumann and K.H. Zum Gahr, (in German), *Trib. und Schmier. Techn.*, 43 **[1]** (1996) 23.
2. M. Woydt, (in German), *Trib. und Schmier. Techn.*, 44 **[1]** (1997) 14.
3. H. Czichos, D. Klaffke, E. Santner and M. Woydt, *Wear*, 190 (1995) 155.
4. M.B. Peterson, S.F. Murray and J.J. Florek, *ASLE Trans.*, 2 **[2]** (1960) 225.
5. M.B. Peterson, S.J. Calabrese, S.Z. Li and X.X. Jiang, Proceedings Leeds-Lyon symposium, edited by D. Dowson, Trib. Series, 16 (1990) 15.
6. P.W. Bridgeman, *Proc. Am. Acad. Arts Sci.*, 71 (1936) 387.
7. C.F. Hensley, A.T. Male and C.W. Rowe, *Wear*, 11 **[3]** (1968) 233.
8. B. Longson, *Trib. Int.*, 16 **[4]** (1983) 221.
9. K.J. Wahl, L.E. Seitman, R.N. Bolster, I.L. Singer and M.B. Peterson, *Surface and Coatings Technology*, 89 (1997) 245.
10. N. Alexeyev and S. Jahanmir, *Wear*, 166 (1993) 41.
11. A. Gagyopadhyan, S. Jahanmir and M.B. Peterson, in "Friction and wear of ceramics" edited by S. Jahanmir, (Marcel Dekker, New York, 1994) 163.
12. Y. Wang, F.J. Worzala and A.R. Lefkow, *Wear*, 167 (1993) 23.
13. J.R. Seidensticker and M.J. Mayo, *Scr. Metall. Mater.*, 31 **[12]** (1994) 1749.
14. C-M.J. Hwang and I-W. Chen, *J. Am. Ceram. Soc.*, 73 **[6]** (1990) 1626.
15. Bateman, Bennison, *J. Am. Ceram. Soc.*, 72 **[7]** (1989) 1241.
16. H. Erkalfa, Z. Misirli and T. Baykara, *Ceram. Int.*, 24 **[2]** (1998) 81.
17. N. Wang, B. Gallois and T.E. Fischer, *J. Soc. Trib. Lub. Eng.*, 49 **[10]** (1992) 763.
18. B. Kerkwijk, E.J. Mulder and H. Verweij, *Adv. Eng. Mater.*, accepted for publication (1999).
19. H.S.C. Metselaar, A.J.A. Winnubst and D.J. Schipper, *Wear*, 225-229 (1999) 857.
20. B. Kerkwijk, A.J.A. Winnubst, H. Verweij, H.S.C. Metselaar, E.J. Mulder and D.J. Schipper, *Wear*, 225-229 (1999) 1293.
21. B. Kerkwijk, M.M. Garcia-Curiel and H. Verweij, unpublished work, (1998).

7 Wear resistant ceramics: two practical cases verified by tribological tests*

7.1 Introduction

Development and properties of wear-resistant ceramics have received increasing interest in recent years. Particular attention is paid to wear-resistance and friction of dry sliding contacts under harsh conditions such as high temperatures, contact pressures and sliding velocities and chemically aggressive environments. Tribological laboratory studies of ceramic materials at such conditions revealed wear rate values ranging from nearly undetectable up to unacceptably high.

Hard and dense ceramics with a homogeneous microstructure can be good candidate materials for stable dry sliding contacts. Additional requirements are: sufficient chemical inertness with respect to the opposite material and the operating environment and a thermal conductivity that is high enough to avoid local thermal flash phenomena [1]. Thermal conductivity becomes less important if wear-resistant ceramic materials can be applied as a thin coating on other, thermally conductive materials. Dry sliding friction values can be improved further by making use of solid lubricants present in the material matrix that are supplied to the contact surface during operation [2]. The requirements mentioned make that ceramics of mainly alumina, zirconia and mixtures of these come readily into scope. The optimum ceramic material depends largely on the actual application. If chemical inertness is more important than thermal conductivity, fine-grained zirconia may be the material of choice. At very high sliding speeds and contact pressures zirconia-toughened alumina might be the best material [3]. If requirements are less severe, cheaper but more coarse-grained alumina ceramics can be the best solution.

Development of ceramics can be done in a synthesis/properties program with a focus on microstructure control in which feed-back is provided by tribological tests performed at standardised conditions in the laboratory. In that case one may encounter the problem, that in such tests the practical circumstances can never be simulated. If, on the other hand, promising materials are directly tested in practice, it is usually difficult to define (or retrieve afterwards) exactly the actual tribological conditions that the materials have been subjected to. This makes that systematic studies based on feed-back from practical tests are nearly impossible. Hence one needs a significant number of practice tests to be sure that the materials choice made sense at all while systematic development of promising materials should be done in a parallel program with lab tests using fully defined tribological tests that approach the practical situation as closely as possible.

---

* Taken from: B. Kerkwijk, J.J.C. Buizert, E.J. Mulder and H. Verweij, submitted for publication, 1999.

The rather formal statements of the above paragraph can be made more explicit with recently obtained tests of the application of wear-resistant ceramics in axial bearings (in pumps) and in high-definition cutting blades. For both applications particularly promising results were obtained with fine-grained zirconia-toughened alumina (ZTA) composite material and yttria-stabilised tetragonal zirconia (Y-TZP), respectively. The objective of this chapter is to present these results and to compare them critically with the most relevant tribological tests performed under standardised laboratory conditions.

7.2 Materials

Fine grained zirconia powder was prepared by co-precipitation of YCl_3 and $ZrCl_4$ in concentrated ammonia. After washing and drying, the powder was calcined at 500°C and the resulting Y-TZP (5 at% Y) powder had a crystallite size of 8 nm as obtained from X-ray line broadening and BET measurements (surface area of 100 m^2/g). To obtain a ZTA powder with 85 wt% α-Al_2O_3, $ZrCl_4$ was precipitated in a suspension of α-Al_2O_3 powder (AKP50, Sumitomo Chemical Ltd., Tokyo, Japan) in ammonia. After washing and drying, the powder was calcined at 550°C. Both Y-TZP and ZTA powders were consolidated by dry pressing the powders into disc shapes. After consolidation, the Y-TZP and ZTA ceramics were sintered to 94% and 99% of their theoretical density at 1150°C for 10 hrs and 1450°C for 2 hrs, respectively.

To establish the ultimate limits in wear-resistance, ZTA ceramics were also made with an extremely fine-grained and homogeneous microstructure via a (more elaborate and expensive) colloidal filtration route. For this process undoped zirconia powder was used, made by the Y-TZP route and AKP50 alumina powder again. These powders were first ball-milled separately in a 0.05 M HNO_3 aqueous solution. Consolidation was performed by colloidal filtration of the thoroughly mixed suspensions under vacuum. The resulting green body was dried in air and sintered to full density at 1400°C for 2 hrs. All preparation procedures were described more extensively in a previous study [4].

The following commercially available materials (provided by Dynamic Ceramic, England and Gimex Technical Ceramics, The Netherlands) were tested as well:

- ZY-C, hot isostatic pressed high-strength Y-TZP, Technox Z3500,
- A100, alumina, Dynalox,
- ZTA-C, zirconia-toughened alumina, made from Daichii powder,
- ZTAC-HIP, hot isostatic pressed ZTA-C,
- Si_3N_4, hot pressed silicon nitride.

Table 7.1: Material and tribological properties of the various home-made and commercially available ceramics used for practical tests; tribological properties are based on the maximum values measured. Below the line values are given obtained with laboratory measurements of a ZTA pin dry sliding against a colloidal processed ZTA disc.

Material	Density [kg/m^3]	Grain size [µm]	Counterface	Running time [hrs]	Max. k_w [mm^3/(N·m)]	Max. track depth [µm]
Y-TZP	5700	0.18	ZY-C	1120	$3 \cdot 10^{-9}$	6
ZY-C[1]	6100	0.35	ZY-C	375	$1 \cdot 10^{-7}$	13
A100[1]	3970	2	ZY-C	1095	$7 \cdot 10^{-9}$	24
Si_3N_4[1]	3300	800	ZY-C	1082	$1 \cdot 10^{-7}$	56
ZTA	4200	Al_2O_3:1.0 ZrO_2: 0.3	ZY-C	575	$4 \cdot 10^{-9}$	18
ZTA-C[1]	4120	Al_2O_3: 3.0 ZrO_2: 0.7	ZY-C	253	$1 \cdot 10^{-6}$	650
ZTA-HIP[2]	4200	Al_2O_3: 0.5 ZrO_2: 0.2	ZTAC-HIP[3]	317	$1 \cdot 10^{-9}$	0.5
ZTAC-HIP[2]	4200	Al_2O_3: 3.0 ZrO_2: 0.7	ZTAC-HIP[3]	481	$1 \cdot 10^{-9}$	0.7
ZTA-CF	4200	Al_2O_3:0.5 ZrO_2: 0.2	ZTA	140	$6 \cdot 10^{-10}$	0.08

[1] supplied by Dynamic Ceramic, Great Britain; [2] HIP performed by Dynamic Ceramic, Great Britain; [3] HIP performed by ECN, Petten, The Netherlands.

The performance under practical conditions of these materials was tested by using them for an axial bearing in a gear wheel pump and by using them as cutting materials for biological tissue. For the former application a combination is desired of high hardness and strength, whereas for the latter strength and minimisation of material break-out are of major importance. Using these demands, a choice was made for ZTA and Y-TZP for the pump application and Y-TZP only for the cutting applications because of its better toughness and smaller grain size.

7.3 Axial bearings

The axial bearings studied are used in gear wheel pumps for chemically aggressive fluid surroundings with varying viscosities. The bearings primarily act as seals, to prevent leakage of process fluids to other pump parts. Typical operating conditions are: a linear sliding velocity of 0.03 to 0.06 m/s, a temperature between 80 a 85°C and a pressure varying between 1 and 5 MPa that is created on the axial bearing through a driving spindle. This pressure depends on other properties like pressure and viscosity of the process fluids and resistance in the pipes. Pump operation is frequently interrupted during testing

and there is an acid-resistant grease present as an extra aid to avoid leakage. The conditions mentioned make that the bearing material should have sufficient wear resistance in combination with a good corrosion resistance at poorly defined tribological conditions. Engineering metals for pump parts do not meet the requirements of corrosion resistance, so that the use of ceramic materials was explored.

7.3.1 Practical tests

Before testing the average surface roughness of the materials was between 30 and 50 nm and the flatness of the opposing surfaces within 1 μm. Since the materials had little elasticity while minimal wear was expected, it was very important to obtain a system lining in the mechanical seal that was as exact as possible. After testing, the worn surfaces were inspected by surface profiling and the materials were regarded as suitable for gear wheel pump operation if the following criteria were met:

- Most important was that the wear track should not be deeper than <2 μm after 200 hrs of testing.
- Additional wear had to remain <1 μm in depth for every other 100 hrs of prolonged testing.

Since in practice the materials should last for >8000 hrs (equivalent to 1 year of operation), the criteria as mentioned correspond to a wear track of no deeper than 80 μm at the end of the operational lifetime. To obtain more systematic data for materials characterisation, the specific wear rate, k_w, was determined using the actual operating conditions:

$$k_w = \frac{V_w}{F \cdot s} \tag{7.1}$$

in which V_w is the wear volume, F the applied force and s the sliding distance. (A material is generally considered wear-resistant if $k_w < 10^{-6}$ mm^3/N·m.)

Ceramic axial bearings, made from the materials as mentioned, were mounted in a gear-wheel pump and tested for at least 150 hrs. Most of the samples were tested for longer times with commercially available ZY-C counter-face (HIPed Y-TZP) material. These tests showed that Y-TZP and ZTA, all made on lab scale, had an extremely good wear resistance with wear rates in the order of 10^{-9} mm^3/N·m. The fact that zirconia- and alumina-based material showed similar wear behaviour can be explained by the low sliding velocities that are present in the specific pump that was used for testing. If velocities larger than 0.2 m/s would be present, the zirconia material (Y-TZP) would suffer from thermally induced fracture [1] and not be suitable for this application.

The commercial material ZTA-C showed a very poor wear behaviour, but when this material was isostatic hot-pressed (ZTAC-HIP), the wear behaviour became similar to that of the pressureless sintered ZTA material. The wear behaviour of the laboratory-made ZTA material, however, was not significantly improved by the same post treatment. The poor wear resistance of ZTA-C can be explained by the less homogeneous microstructure of this material. This is particularly the case for the dispersion of the second phase (zirconia) in the main phase (alumina): large clusters of zirconia material were found to be present, resulting in easy material removal.

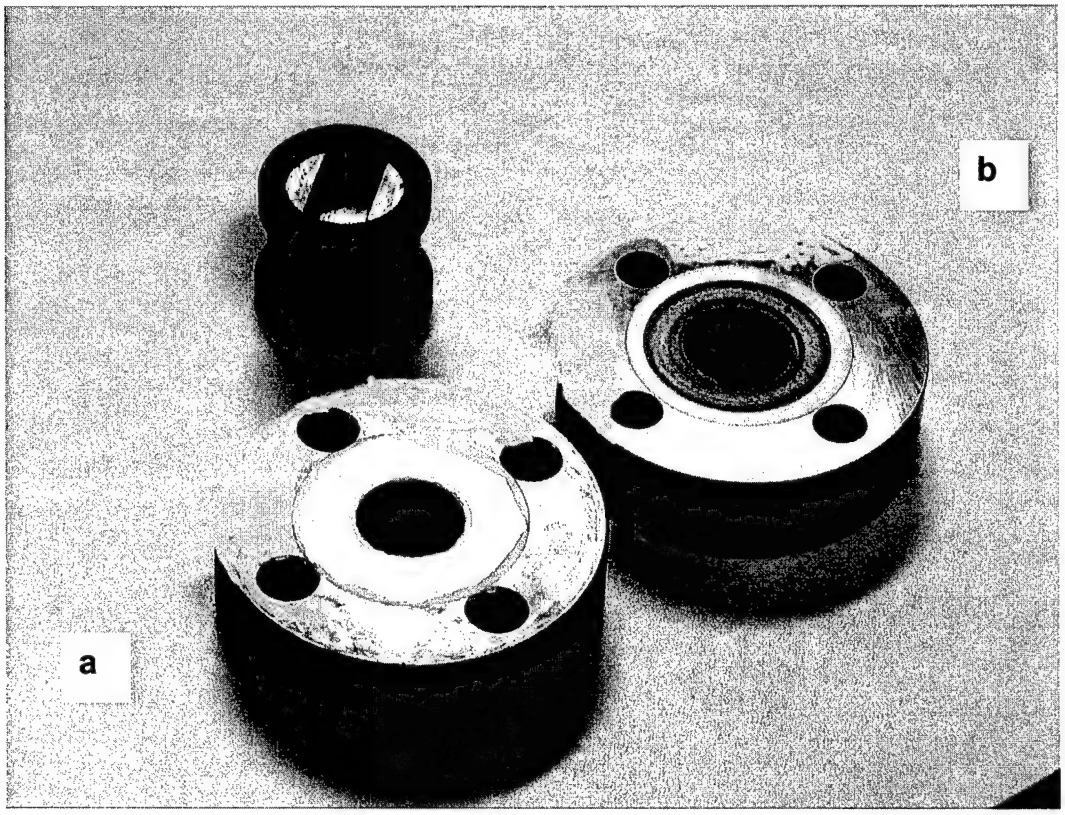

Figure 7.1: Two axial bearings showing clearly differences in wear behaviour after 575 hrs of operation. a: laboratory-made ZTA material where a wear track is hardly visible. b: commercially available ZTA-C material showing severe wear. Both materials have run against a ZY-C driving plug.

For pure alumina ceramics, a wear behaviour is found that is initially similar to that of the ZTA materials but increasing dramatically after a certain time. Besides this it should be taken into account that the materials must have a strength such that reliable designs of all kinds of pump parts can be realised. Hence ZTA materials are most suitable for this application because they have a higher toughness and strength than alumina and suffer less from fatigue processes that may initiate severe wear. Si_3N_4 ceramics were also tested against the zirconia counterfaces and showed severe wear after less than 200 hrs of testing.

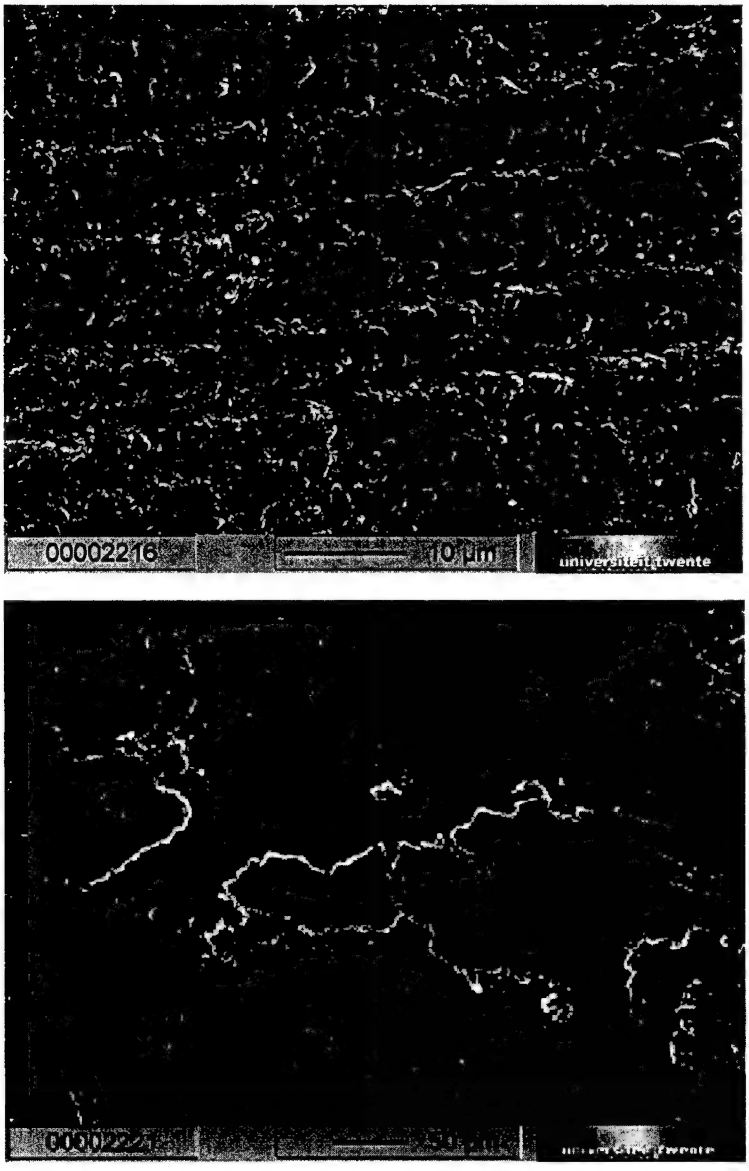

Figure 7.2: SEM details of the wear tracks of Figure 7.1. a: the laboratory-made material only shows slight grooving of the surface caused by the incorporation of broken-out alumina particles in the ZY-C counterface. b: the commercial material shows severe fracture and large portions of smeared-out debris. Note the scale difference between a and b.

The results obtained for ceramic parts were compared to those obtained with stellite-20, which is the most suitable engineering metal for the pump application considered. At the given conditions stellite-20 components all showed severe wear, with a track depth of >100 µm, after 200 hrs of testing.

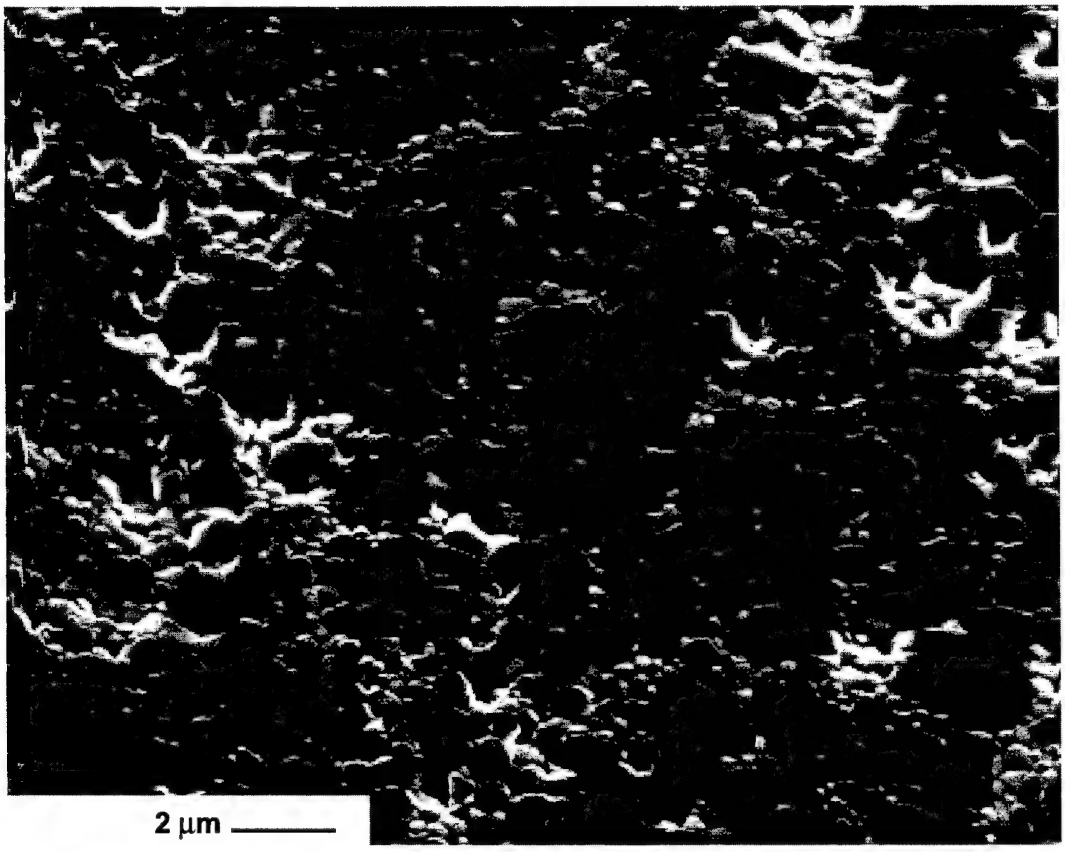

Figure 7.3: Wear track of a laboratory ZTA material. No grooving is found; the material wears by grain removal only. This micrograph shows the influence of the counterface, since the ZTA counterface does not allow incorporation of hard broken-out particles.

In a previous study, involving laboratory tests only, it was revealed that tribological systems made only from ZTA materials may show extremely low wear rates [7]. Hence a limited number of tests were conducted with a commercially available ZTA counterface of the type ZTAC-HIP. For that case, extremely good wear behaviour was found for both the commercial and the laboratory-made ZTA ceramics. Similar to what was found in the laboratory tests, wear took mainly place by polishing with some grain pull-out. Slight grooving was occasionally found and probably caused by minor deviations from the ideal system lining.

7.3.2 Laboratory tests

There is a significant spread in the experimental k_w values obtained with the practical gear-wheel pump tests. This large spread can partly be assigned to uncontrollable variations in the force that is applied to the axial bearing and to lack of control of the chemical nature of the compounds present between the counterparts. Yet it is possible to use the k_w values to obtain a qualitative ranking of the various materials operated at practical conditions. "Pin-on-disc" measurements performed in the laboratory with colloidal processed ZTA discs sliding against pins made from the same material without any lubrica-

tion revealed extremely low wear rates [7], solely taking place by polishing. If these measurements were performed under mild conditions similar to those of the gear wheel pump tests, no ZTA wear was found at all. To obtain a quantitative ranking of the materials performance, measurements were made under more extreme tribological conditions with higher initial pressures up to 1.7 GPa and sliding velocities of 0.5 m/s. At such conditions, reproducible specific wear rates could be obtained, for colloidal processed ZTA of the order of 10^{-10} $mm^3/N{\cdot}m$. Other materials like Si_3N_4, alumina and ZTA-C showed destructive failure at these extreme conditions. We did not obtain convincing support for the use of (expensive) HIP post-treatments. All this indicates that ZTA is the best choice for this application. Colloidal processed ZTA is more expensive to produce but has an even better homogeneity than the normal ZTA produced by dry pressing.

7.4 Cutting edges

Cutting applications require materials that can be machined with very sharp and well-defined cutting edges. Besides that, the cutting edge should have an extended useful lifetime and it should be able to withstand cleaning treatments such as high-temperature sterilisation for medical applications, which generally leads to deterioration of the properties of the material. The use of ceramics is then the logical choice. The major problem with ceramics, however, is that brittle fracture of the material in the cutting edge is more likely to occur.

The cutting materials used in this study were made from Y-TZP ceramics. Such ceramics are less brittle than conventional ceramics and can be easily made with a small grain size. The latter makes that cutting edges can be produced with a better definition and that break-out of single grains does not immediately have a catastrophic effect on cutting performance. Since ceramic materials for cutting applications are envisaged to replace hard metals (WC-Co), the quality of ceramic cutting edges should be comparable to hard metals. In such a comparison both initial sharpness and usable lifetime of the cutting edges are of major importance. The initial sharpness can easily be determined from optical microscopy. Pictures of the cutting edges at magnifications of 500 up to 1000 times should reveal very limited or, preferably, no break-out of the cutting edge material. The cutting properties of the ceramic materials are determined best by examining the quality of the most critical biological microtome specimens. Too much friction in the knife specimen couple will result in superficial distortion and hence the quality of the sample will not be good enough for further processing.

Ceramic cutting edges made on laboratory scale produced test samples were first examined on the quality of the cutting edges, which should at least be equal to hard metal cutting edges. For Y-TZP ceramics with small grain sizes (<0.2 μm) this was possible, even though the density of the ceramics was not 100%. In addition the quality of those cutting edges was at least equal to that of commercially available ceramics. Examination at a 500-times magnification of the cutting edges made from similar Y-TZP ceramics with >0.4 μm grains revealed the presence of "craters" The occurrence of these craters provides an indication of significant material removal at the cutting edge taking place by

break-out of a large portion of grains at once. Cutting edges with craters could no longer be used.

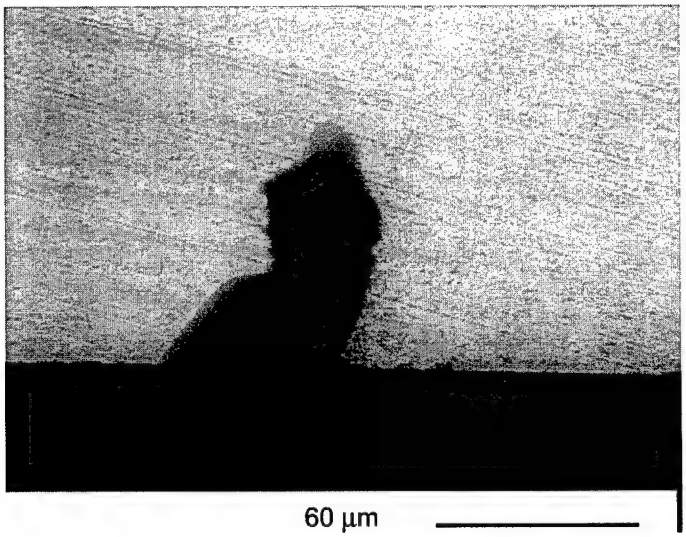

(a)

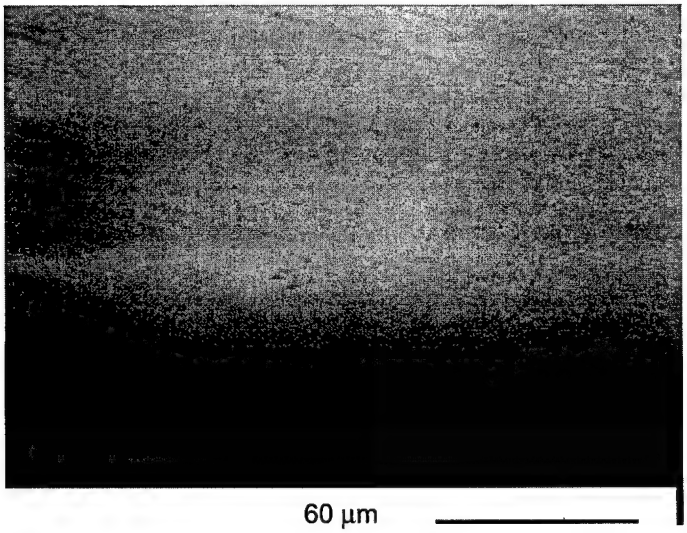

(b)

Figure 7.4: Optical micrographs of a: coarse-grained Y-TZP cutting edge of a, showing a large break-out crater; b: cutting edge of fine-grained Y-TZP material with a quality similar to that of hard metal.

Cutting experiments were performed on organic material and it was found that the quality of the specimens made with fine-grained Y-TZP ceramic cutting edges were of a quality equal to those made with a state-of-the-art hard metal knife. The long term performance of the ceramic cutting materials was superior to that of the metals. This result can be explained by the fact that corrosion and wear resistance of the ceramics were better than those of hard metal.

7.5 Conclusions

Practical tests were performed with various ZTA and Y-TZP ceramics as seal plates of an axial bearing in a gear wheel pump. These tests showed qualitatively that both ZTA and Y-TZP may have sufficient wear resistance under the specific circumstances used. A more quantitative ranking of the relevant properties of the materials used could only be made in a series of laboratory tests with standardised conditions that approached the practical situation as much as possible. In these tests a clear influence was found of microstructural homogeneity on wear resistance. Hence this aspect can be taken as a guideline for making choices between chemically similar materials. Wear rate values of 10^{-10} $mm^3/(N \cdot m)$ were measured for ZTA dry sliding against ZTA in laboratory pin-on-disc measurements, whereas similar values could be obtained in practical tests with ZTA materials sliding against materials of the same nature. The fact that ZTA is the preferable material for mechanical seals is further supported by its favourable mechanical strength. A detailed choice of the most suitable ZTA material largely depends on ultimate quality versus cost-price considerations.

Fine-grained Y-TZP ceramics (grain size <0.2 μm) can be very suitable to manufacture edges for cutting organic specimens. The ceramics studied were not yet fully optimised for this application, so further improvements may be expected, particularly in usable life-time.

7.6 References

1. H.S.C. Metselaar, A.J.A. Winnubst and D.J. Schipper, *Wear*, 225-229 (1999) 875.
2. M.Baumann and K.H. Zum Gahr, *Trib. Schmier. Techn.*, (in German), 43 [1] (1996) 23.
3. B. Kerkwijk, A.J.A. Winnubst, H. Verweij, H.S.C. Metselaar, E.J. Mulder and D.J. Schipper, *Wear*, 225-229 (1999) 1293.
4. B. Kerkwijk, A.J.A. Winnubst, E.J. Mulder and H. Verweij, J. *Am. Ceram. Soc.*, accepted for publication, (1999).
5. J.G.P. van Valkenhoef and J.W.J. Appeldoorn, *Materialen* (in Dutch), 4 (1993) 10.
6. K. Adachi, K. Kato and N. Chen, *Wear* 203-204 (1997) 291.
7. B. Kerkwijk, E.J. Mulder and H. Verweij, *Adv. Eng. Mater.*, accepted for publication, (1999).
8. M. Burström, *Proc. of the International Conference on machining of Advanced Materials*, Gaithersburg USA (1993), 1.
9. T. Sornakumar, R. Krishnamurthy and C.V. Gokularathnam, *J. Eur. Ceram. Soc.* 12 (1993) 455.

8 Evaluation

8.1 Introduction

The work described in this thesis has been carried out in the framework of the project TST.3418 "Nanoscale zirconia ceramics with extremely high wear-resistance", financed by the Dutch Technology Foundation STW. This project was preceded by the IOP-ceramics project elaborated by He [1], who performed a study on the tribological and mechanical properties of fine-grained zirconia and zirconia-alumina ceramics. The IOP-ceramics project offered perspectives for much improved tribological performance of fine-grained ceramics. This thesis presents subsequent research on the tribological behaviour of nanostructured zirconia and alumina ceramics and composites. Advanced processing routes were used to manufacture nanostructured homogeneous ceramics with extremely good wear resistance and low friction. A qualitative description of the relation between ceramic microstructure and tribological behaviour was given.

8.2 Influence of second-phase addition on wear-resistance

The results from chapter 3 showed that the addition of a second phase to either a zirconia or an alumina matrix ceramic improves the tribological properties. Addition of alumina to zirconia does not create a percolative system, since thermally induced fracture processes are still found at higher sliding velocities. In addition, the material can be tested at higher contact pressures and also higher velocities before transition to severe wear takes place. Addition of the second phase close to the percolation limit may improve the tribological behaviour, but the preparation of such a material will be more difficult, since two-phase sintering will be a problem then.

Alumina shows low specific wear rates at all test conditions. The specific wear rate, however, does increase significantly with increasing sliding velocity. The load dependence of wear transition is not necessarily accounted for in the overall specific wear rate. From on-line wear measurements it is found that after a short period of severe failure of the ball, a low specific wear rate can be achieved again. The addition of a zirconia second phase improves the wear resistance in all cases. Moreover, these zirconia toughened alumina (ZTA) materials can still be tested up to initial contact pressures of 1600 MPa, without showing significant wear. In this case, the alumina balls show failure again, but the overall specific wear rate of the ZTA discs is still below the limiting value of 10^{-6} $mm^3/(N \cdot m)$.

8.3 Influence of microstructural homogeneity on wear-resistance

He [1] showed that ceramic grain size is one of the most important microstructural properties that needs to be controlled to increase the wear-resistance of ceramics. Resulting from this understanding, mainly fine-grained ceramics were used in the work described in this thesis. One of the recommendations made by Y.J. He was that attention had to be paid to the production of dense, defect-free and homogeneous ceramics. The results from this thesis show that homogeneously structured composite ceramics of zirconia and alumina show extremely good wear behaviour indeed.

Colloidal processing of zirconia-toughened alumina (ZTA) results in defect-poor, dense composites [2]. The ceramic formed by colloidal processing and sintering, as was described in chapter 2, showed a very homogeneous phase distribution and also smaller average grain sizes than for dry-pressed ceramics, sintered from both home-made and commercial powders. The colloidal processed material sintered at 1400°C had grain sizes as low as 0.5 μm for alumina and 0.2 μm for zirconia. During sintering of colloidal-processed ceramics, considerable mutual grain-growth inhibition of alumina and zirconia grains was caused by a uniform distribution of the particles in the green compact. An option to improve the properties of these composite materials and their processing, may be the use of even finer-grained alumina powders to obtain a smaller grain size. Furthermore, the question arises if it will then still be possible to create such a homogeneous dispersion. If the particle size distribution of the alumina powder will be very "sharp", this may be a possibility.

Tribological investigations performed on these ZTA ceramics, showed mild wear under dry sliding testing conditions against alumina balls (initial contact pressure 1130 MPa (10 N), velocity 0.5 m/s). The specific wear rate was $5 \cdot 10^{-8}$ $mm^3/(N \cdot m)$ for the colloidal processed material and $2 \cdot 10^{-6}$ mm^3/Nm for the reference materials made by dry pressing, as described in chapter 3. The differences in wear rates are caused by grain pullout in regions of the reference material that were not affected by abrasive wear, whereas the colloidal-processed material shows only polishing and deformation in these regions. It can therefore be concluded that the improved microstructure of the colloidal processed material leads to an improved wear resistance compared to the more coarse-structured and irregular reference material. This improvement is mainly seen from the fact that less grain pull-out occurs during sliding. This means that the materials have a good stacking of the particles after consolidation, resulting in stronger grain boundaries and an improved grain boundary morphology.

These ZTA ceramics also have a self-mating, dry sliding specific wear rate as low as $6.3 \cdot 10^{-10}$ $mm^3/(N \cdot m)$ under extreme pressures (1.7 GPa, 14 N). These values, reported in chapter 4, are significantly lower than values reported in literature [3,4]. The use of pins of this homogeneously structured ZTA ceramic shows that no transition from mild to severe wear occurred. Compared to the use of alumina, where the transition did occur, this also shows the importance of microstructural homogeneity with respect to transition phenomena. In addition, alumina has more limitations in practical use, since its maximum applicable load before a wear transition occurs is lower than for ZTA composite ceramics.

This finding supports the use of colloidal processing routes to obtain homogeneously structured ceramic materials, in particular for composite ceramics.

8.4 Wear modelling

Considerable experimental work was done to verify the model that was initiated by Metselaar *et al.* [5]. The main basis of this model work described in chapter 5, is to create a wear map based on dimensionless numbers for the description and prediction of wear behaviour for a variety of ceramics under a wide range of operating conditions. These dimensionless numbers are representative for the mechanical severity (MS) of the sliding contact, as described by Adachi *et al.* [3], and the thermal severity (TS) of the sliding contact. The TS parameter is developed using the work of Bos [6], who describes the temperature rise in an elliptic contact with an elliptic heat source. Results from the verification experiments were divided in the categories mild ($k_w < 10^{-6}$ mm^3/(N·m)) and severe ($k_w > 10^{-6}$ mm^3/(N·m)) wear. Using the characterisation in mild and severe wear in combination with the MS and TS parameters, clearly shows the on-set of the transition from mild to severe wear for several material combinations. So far, the problem is that the model does not give a unified number for TS where the on-set of this transition occurs. For Al_2O_3 this value is 1, whereas it is 1.5 for Si_3N_4, 2 for SiC and 3 for Y-TZP. Based on the model description the prediction is that the value for TS should have the same value, regardless of the materials and test parameters used. Up to now, there is no understanding for these differences, but the model maps the transition behaviour well for the materials separately.
Further work in this subject may focus on the understanding of the influence of microstructural properties on the transition behaviour. Also the amount of materials combinations needs to be expanded to be able to explain the differences in transition values for TS. The development of the model may result in a unified wear map, where both mechanical (MS) and thermal influences on the tribological behaviour may be included.

8.5 Friction reduction

In most practical applications coefficients of friction should be below 0.2 to minimise energy loss. Since even the most wear-resistant materials found in this study showed a coefficient of friction of no less than 0.43, an experimental study was performed on materials with solid state lubricating additives [7]. The study, described in chapter 6, showed the possibility of preparation and use of alumina and Y-TZP ceramics with soft metal oxide additives intended to lower friction. Low contents of additives were used to preserve the mechanical properties of the single-phase ceramics. The addition of CuO occasionally resulted in a friction reduction of 40% in a number of experiments, indicating that the approach may be successful. In Y-TZP ceramics the additives mainly influence the properties of the grain boundaries since practically no grain pull-out was found, but only deformation of grains and some evidence of film formation. The same counts for the alumina-based materials, only here, no film formation takes place. The presence of a friction reducing distinct separate phase in both matrix materials was not proved yet.

The minimum coefficient of friction found was 0.41, a value that is still too high. Evidence was found that improvement of the dispersion homogeneity might result in even lower values for the coefficient of friction. This means that it is interesting to use methods like colloidal filtration. As was shown in chapter 2 and 4, colloidal processed composite materials revealed improved tribological behaviour (low wear and friction), because of the improved microstructural homogeneity. Since all results up to now were obtained from dry-pressed materials, colloidal filtration can be used to obtain a better homogeneity of the ceramic microstructure, e.g. a better dispersion of the additive through the ceramic matrix. With a better dispersion of the lubricating phase it may also be possible to introduce larger or smaller amounts of additives while still retaining the favourable mechanical properties of the matrix. The preparation by this method, of more complicated systems (non-oxides, graphite) may be considered as well, but such a preparation may be more complicated. The characterisation of the materials microstructure needs to be performed with other techniques like TEM or AES. This is necessary since the small amounts of additive are very difficult to trace in the bulk. This may contribute to a better understanding of the operative wear and friction reducing mechanisms as well.

8.6 Practical relevance

To demonstrate the use of the nanostructured zirconia and alumina ceramics and composites, practical tests were performed with various ZTA and Y-TZP ceramics. Tests performed on ceramic seal plates of an axial bearing in a gear wheel pump, showed qualitatively that both ZTA and Y-TZP may have sufficient wear resistance under the specific circumstances used. Hence, this similarity between laboratory and practice results can be taken as a guideline for making choices between chemically similar materials. As mentioned, specific wear rates of 10^{-10} $mm^3/(N \cdot m)$ were measured for ZTA dry sliding against ZTA in laboratory pin-on-disc measurements, whereas similar values could be obtained in practical tests with ZTA materials sliding against materials of the same nature. The fact that ZTA is the preferable material for mechanical seals is further supported by its favourable mechanical strength. A detailed choice of the most suitable ZTA material largely depends on ultimate quality versus cost-price considerations.

Fine-grained Y-TZP ceramics (grain size <0.2 μm) were found to be suitable to manufacture edges for cutting organic specimens. The ceramics studied were not yet fully optimised for this application, so that we may expect further improvements, particularly in usable lifetime. It is expected that further development of nanostructured Y-TZP ceramics will result in even better defined ceramic cutting edges, because of extremely small grain sizes. The resulting homogeneity of the microstructure may improve the lifetime, because of diminished grain removal.

To increase the number of future applications, it may be necessary to translate the properties of the bulk ceramic materials to applied coatings of these materials. It should be possible to apply such coatings on "cheap" substrates as engineering polymers or metals. This means that these could coatings should be sintered dense at extremely low temperatures (max. 600°C). Resulting from this demand, nanometer-sized particles should be made for these coatings. This may be possible by the use of emulsion-

precipitation techniques. When the same homogeneity of, for instance, the ZTA ceramics made by colloidal filtration, can be reached with extremely small grains, it may be possible to obtain wear-resistant, low friction coatings, made from relatively cheap material.

8.7 References

1. Y.J. He, *Tribological and mechanical properties of fine-grained zirconia and zirconia-alumina ceramics*, PhD. thesis, University of Twente (1995) ISBN 90-90086242.
2. B. Velamakanni and F.F. Lange, *Effect of interparticle potentials and sedimentation on particle packing density of bimodal distributions during pressure filtration*, J. Am. Ceram. Soc., 75 [**10**] (1991) 166-172.
3. K. Adachi, K. Kato and N. Chen, *Wear maps of ceramics*, Wear, 203-204 (1997) 291-301.
4. H. Czichos, D. Klaffke, E. Santner and M. Woydt, *Advances in tribology: the materials point of view*, Wear, 190 (1995) 155-161.
5. H.S.C. Metselaar, A.J.A. Winnubst and D.J. Schipper, *Thermally induced wear of ceramics*, Wear, 225-229 (1999) 856-861.
6. J. Bos, *Frictional heating of tribological contacts*, PhD. thesis., University of Twente, The Netherlands (1995) ISBN 90-90089209.
7. A. Gagyopadhyan, S. Jahanmir and M.B. Peterson, in "Friction and wear of ceramics" ed. S. Jahanmir, Marcel Dekker, New York (1994), 163.

Summary

The work described in this thesis is about wear and friction of zirconia and alumina ceramics and composites of zirconia and alumina. Tribological properties are system properties that can only be studied for given combinations of materials and operating conditions. The tribological properties of ceramics, however, are particularly influenced by the homogeneity of the ceramic microstructure. Important parameters of that are porosity, grain size and possibly phase dispersion homogeneity of composites.

In this thesis mainly attention was paid to the preparation of ceramic systems, as homogeneous as possible and the influence of homogeneity on tribological properties.

The preparation of homogeneously structured composite material was mostly done by conventional processing but occasionally extreme homogeneity was achieved by colloidal processing. The preparation of dense homogeneous zirconia-toughened alumina (ZTA) with high dry sliding wear resistance is described in *chapter 2*. These ZTA ceramics were sintered for 2 hours at 1400°C and consists of a homogeneous distribution of zirconia grains in an alumina matrix with grain sizes of 0.2 and 0.5 μm, respectively. Tribological measurements revealed for these materials a very low specific wear rate (app. 10^{-9} mm^3/Nm) and a coefficient of friction of 0.5 with alumina as the counter material. It is shown that, in this case, wear is dominated by abrasion and polishing.

The influence of the second phase of alumina or zirconia on the tribological properties of zirconia and alumina, respectively, is dealt with in *chapter 3*. It was shown that, with initial Hertzian contact pressures up to 1 GPa and sliding velocities up to 0.5 m/s, the specific wear rate was the highest for Y-TZP, 10^{-6} $mm^3/(N{\cdot}m)$, and the lowest for ZTA, 10^{-9} $mm^3/(N{\cdot}m)$. For both single-phase zirconia and alumina ceramics it was found that addition of a harder (alumina) or a tougher (zirconia) phase, respectively, leads to an improved wear resistance. Depending on the test conditions the wear mechanisms are abrasion, delamination and polishing. The main conclusion of this work is that ZTA composites manufactured and tested in this study have a superior wear resistance and a relatively low coefficient of friction under dry sliding conditions.

The results of measurements on some exceptionally wear-resistant materials are given in *chapter 4*. ZTA ceramics, prepared by colloidal processing, show an improvement in wear resistance of >3 orders of magnitude in dry-sliding self-mating tests compared to less homogeneous ZTA, prepared by conventional processing of commercial powders. The composite ceramics also show superior tribological behaviour compared to self-mating α-alumina and yttria-stabilised zirconia couples.

Modelling of the tribological results is described in *chapter 5*. The objective of this study is to introduce a wear map of ceramics which shows the different regimes of dominant wear modes observed for a wide range of material properties and operational conditions. For this purpose, friction and wear tests are carried out with tetragonal zirconia discs sliding against various pin materials under various contact pressures and sliding

velocities. The sliding wear phenomena observed in all tests can be classified into two types: "mild wear" and "severe wear". If the specific wear rate exceeds the value of $3 \cdot 10^{-6}$ $mm^3/(N \cdot m)$, wear is indicated as "severe". The critical condition for transition from mild to severe wear is obtained with an intergranular fracture model that considers both mechanical and thermal properties. A wear map of ceramics, in which the mild and severe wear regimes can be distinguished, is introduced using two dimensionless parameters, namely an existing mechanical severity of contact (*MS*) and a newly developed thermal severity of contact (*TS*). The availability of the wear map constructed by this method is proven by the experimental results observed for a wide range of test material properties and operational conditions.

Chapter 6 describes the preparation and frictional properties of alumina and Y-TZP ceramic composites with small amounts of soft oxide additives. The concentration of additive was kept low to preserve the mechanical properties of the matrix ceramics. Various single oxide additives (ZnO, MgO, CuO, B_2O_3 and MnO_2) were used to establish which oxides could result in a significant friction reduction in dry sliding pin-on-disc experiments against alumina or Y-TZP balls. All additives resulted in medium friction (app. 0.5) for dry sliding of ceramics with alumina and high friction (> 0.65) for ceramics with Y-TZP. The addition of CuO in alumina or Y-TZP reduced the coefficient of friction from 0.65 to 0.45.

In *chapter 7*, the relation is described between ceramic wear in practice and laboratory test results. The practical case study focuses on mechanical seals in a cogwheel pump. Besides tribological issues, manufacturing and engineering issues are addressed as well. The results show that a good prediction can be made of the performance of ceramic materials classes under practical conditions on basis of tribological laboratory tests. In addition it was found that practical operational conditions showed significant variation. This led to the conclusion that a materials selection narrowed down by practice test must again be followed by accurate and reproducible laboratory test again.

In *chapter 8* an evaluation of the presented work is given together with recommendations for future research, development and production. First, it is necessary to look for more applications in which the advantageous properties of ceramic materials fully justify their use. Second, the reduction of friction is should receive more attention because the use of ceramic materials in tribosystems may be further promoted when friction is low. Finally, it may be important to obtain the bulk materials with favourable tribological properties in the form of well-defined coatings on "cheap" substrates. This will significantly reduce cost-price and hence open perspectives for a wide range of applications including consumer products.